AD-A102 342 AERONAUTICAL RESEARCH ASSOCIATES OF PRINCETON INC NJ F/G 20/4
STATISTICAL CONSTRAINTS ON SCALAR VARIABLES IN TURBULENT FLOWS.(U)
FEB 81 G SANDRI, P J MANSFIELD, A K VARMA F44620-76-C-0048
UNCLASSIFIED ARAP-346 AFOSR-TR-81-0593 NL

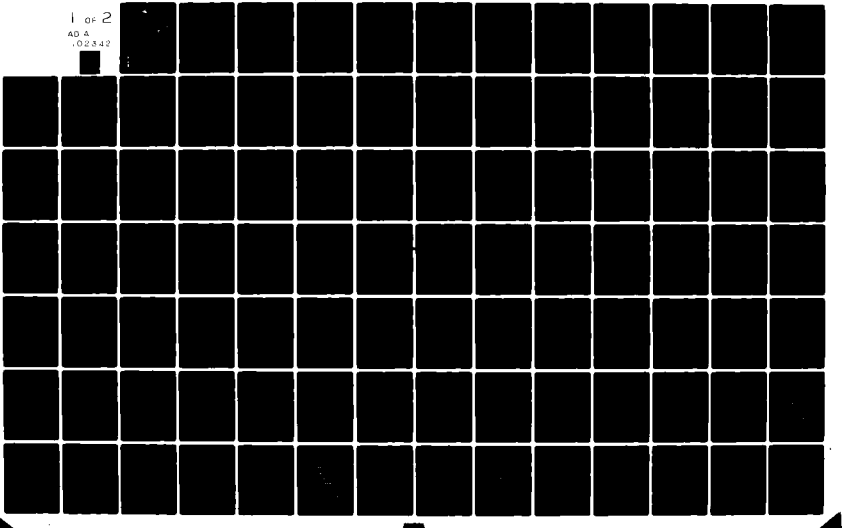

LEVEL II

A.R.A.P. Report No. 346

STATISTICAL CONSTRAINTS ON SCALAR VARIABLES IN TURBULENT FLOWS

Aeronautical Research Associates of Princeton, Inc.
50 Washington Road
P.O. Box 2229
Princeton, New Jersey 08540

February 1981

Scientific Report

The views and conclusions contained in this document are those of the authors and should not be interpreted as necessarily representing the official policies or endorsements, either expressed or implied, of the Air Force Office of Scientific Research or the U.S. Government.

Prepared for

AIR FORCE OFFICE OF SCIENTIFIC RESEARCH
Building 410
Bolling Air Force Base, DC 20332

Unclassified

SECURITY CLASSIFICATION OF THIS PAGE (When Data Entered)

REPORT DOCUMENTATION PAGE		READ INSTRUCTIONS BEFORE COMPLETING FORM
1. REPORT NUMBER AFOSR-TR-81-0593	2. GOVT ACCESSION NO. AD-A102 342	3. RECIPIENT'S CATALOG NUMBER
4. TITLE (and Subtitle) Statistical Constraints on Scalar Variables in Turbulent Flows.		5. TYPE OF REPORT & PERIOD COVERED Scientific Interim 1 Jan 78 – 31 Jul 78
		6. PERFORMING ORG. REPORT NUMBER A.R.A.P. Report No. 346
7. AUTHOR(s) Guido Sandri, Peter J. Mansfield, Ashok K. Varma and Coleman duP. Donaldson		8. CONTRACT OR GRANT NUMBER(s) F44620-76-C-0048
9. PERFORMING ORGANIZATION NAME AND ADDRESS Aeronautical Research Associates of Princeton, Inc. 50 Washington Road, P.O. Box 2229 Princeton, New Jersey 08540		10. PROGRAM ELEMENT, PROJECT, TASK AREA & WORK UNIT NUMBERS 2307A2 61102F
11. CONTROLLING OFFICE NAME AND ADDRESS Air Force Office of Scientific Research/NA Bolling Air Force Base, DC 20332		12. REPORT DATE February 1981 13. NUMBER OF PAGES 110
14. MONITORING AGENCY NAME & ADDRESS (if different from Controlling Office)		15. SECURITY CLASS. (of this report) Unclassified 15a. DECLASSIFICATION/DOWNGRADING SCHEDULE

16. DISTRIBUTION STATEMENT (of this Report)

Approved for public release; distribution unlimited

17. DISTRIBUTION STATEMENT (of the abstract entered in Block 20, if different from Report)

DTIC ELECTE AUG 3 1981

18. SUPPLEMENTARY NOTES

C

19. KEY WORDS (Continue on reverse side if necessary and identify by block number)

Turbulence
Statistical fluctuations
Mixing layer
Turbulent chemical reactions

20. ABSTRACT (Continue on reverse side if necessary and identify by block number)

We consider the statistical behavior of scalar variables in turbulent flows. The presence of chemical reactions requires statistical models for third and higher moments in order to close the rate equations. A realistic analysis should not be restricted to small fluctuations. The results presented here are completely free from such restrictions. The essential points to be demonstrated are:
1) Given $\overline{A}$ and $\overline{A'^2}$, we can obtain stringent statistical bounds on $\overline{A'^2B'}$ and related moments. These bounds are found to be of interest in discussing

DD FORM 1 JAN 73 1473

Unclassified

SECURITY CLASSIFICATION OF THIS PAGE (When Data Entered)

recent experiments.

2) Maximum and minimum third (and higher) moments can be reached only with Dirac functions (i.e., discrete distributions).

3) We can always realize a statistically acceptable choice of $\overline{A}$ and $\overline{A'^2}$ with a few Dirac functions (the minimum number is two distinct ones).

The statements given above hold true when several moments (rather than only $\overline{A}$ and $\overline{A'^2}$ are given as well as when the means of several variables are given. As one consequence, we shall see that we can find, for the purposes of modeling, a discrete distribution that represents the desired set of moments and that is statistically legitimate for all allowed values of the derived moments (box model).

TABLE OF CONTENTS

I. INTRODUCTION

We consider below the statistical behavior of scalar variables in turbulent flows. The presence of chemical reactions requires statistical models for third and higher moments (e.g., $\overline{A'^2B'}$ and $\overline{K'A'^2B'}$) in order to close the rate equations. A realistic analysis should not be restricted to small fluctuations. The results presented here are completely free from such restrictions. The essential points to be demonstrated are

1) Given $\bar{A}$ and $\overline{A'^2}$, we can obtain stringent statistical bounds on $\overline{A'^2B'}$ and related moments. These bounds are found to be of interest in discussing the CalTech experiments (e.g., as reduced by Konrad*).

2) Maximum and minimum third (and higher) moments can be reached only with Dirac functions (i.e., discrete distributions).

3) We can always realize a statistically acceptable choice of $\bar{A}$ and $\overline{A'^2}$ with a few Dirac functions (the minimum number is two distinct ones).

The statements given above hold true when several moments (rather than only $\bar{A}$ and $\overline{A'^2}$) are given as well as when the means of several variables are given (e.g., $\bar{A}$, $\overline{A'^2}$, $\bar{\alpha}$, $\overline{\alpha'^2}$). As one consequence, we shall see that we can find, for the purposes of modeling, a discrete distribution that represents the desired set of moments and that is statistically legitimate for all allowed values of the derived moments (box model).

The role of the higher moments can be illustrated with a second-order chemical reaction

$$A + B \rightarrow C$$

We have the familiar rate equation

$$\frac{dA}{dt} = \frac{dB}{dt} = -K(T)AB$$

It follows that the product, AB, satisfies

$$\frac{d}{dt}(AB) = -K(AB^2 + A^2B)$$

In terms of the Reynolds decomposition

$$A = \bar{A} + A'$$

we find, in the absence of temperature fluctuations,

*Konrad, J.H., "An Experimental Investigation of Mixing in Two-Dimensional Turbulent Shear Flows with Applications to Diffusion-Limited Chemical Reactions." Graduate Aero.Labs., California Institute of Technology, Project SQUID Tech. Report CIT-8-PU (1976)

$$\frac{d}{dt}\left(\bar{A}\bar{B} + \overline{A'B'}\right) = -K\left(\overline{AB^2} + \overline{A^2B}\right)$$

where

$$\overline{AB^2} = \left\langle (\bar{A} + A')(\bar{B} + B')^2 \right\rangle$$

$$= \bar{A}\,\bar{B}^2 + \bar{A}\,\overline{B'^2} + 2\bar{B}\,\overline{A'B} + \overline{A'B'^2}$$

We shall use below this third moment, $\overline{AB^2}$, to test the stringency of the statistical bounds derived.

When temperature fluctuations are included, a joint distribution in T, A and B need be assumed to close the rate equations. Although we do not develop temperature models in detail in this report, we note that many of the statistical (lower) bounds derived for A do apply to the temperature fluctuations; for example, the third moment of the concentration satisfies

$$\overline{A'^3} \geq \frac{\overline{A'^2}^2}{\bar{A}}\left(\overline{A'^2} - \bar{A}^2\right)$$

for any $0 \leq \bar{A} \leq 1$ and $0 \leq \overline{A'^2} \leq \bar{A}(1 - \bar{A})$; similarly, the temperature third moment satisfies

$$\overline{T'^3} \geq \frac{\overline{T'^2}^2}{\bar{T}}\left(\overline{T'^2} - \bar{T}^2\right)$$

for any $\bar{T}$ and any $\overline{T'^2}$ positive. The usefulness of the $\overline{A'^3}$ bound is shown below by ruling out the model $\overline{A'^3} = 0$ over the edges of a mixing layer.

The statistically allowed values of any set of moments can be shown (Appendix 1) to form a domain that is necessarily convex; therefore, the domain has no "holes." This property is very useful when a numerical scan is performed.

The statistical bounds that we obtain are "sharp"; that is, we can prove in each case that the equal sign is realized by a (unique) probability distribution that is discrete. It follows that the bounds obtained are "best bounds" and cannot be improved.

Although we apply here our analysis to mixtures with two species (He and N_2), the results derived for the (molar) concentration A (and its

conjugate $B \equiv 1 - A$) apply to each concentration of an n-component mixture.

We develop a model for the probability of the molar fraction by choosing a discrete distribution that realizes the mean and second moment of the molar fraction as well as the mean and second moments of the mass fraction. The model selected contains a free parameter. Since the empirical evidence is that the mean entropy of mixing is below the maximum allowed statistically (in qualitative agreement with the dominance of large scale structures in the turbulent mixing), we fix our free parameter so as to minimize the mean entropy of mixing.

II. STATISTICAL ANALYSIS

To illustrate the main features of our statistical analysis, we discuss below in detail the behavior of the second moments and we give results for the third and fourth moments.

We introduce the analysis with a useful diagram, the "box" diagram which gives a concise representation of a (one-dimensional) probability distribution.

Given a $P(A) \geq 0$, the quantity

$$\tau(A_o) = \int_0^{A_o} P(A)\, dA \tag{1}$$

is the fraction of time during which $A \leq A_o$. The graph of the inverse of the map $\tau(A)$ is the box diagram. For example,

$$P(A) = \bar{A}\delta(A-1) + (1-\bar{A})\delta(A) \tag{2}$$

gives $\tau(A) = (1-\bar{A})H(A) + \bar{A}H(1-A)$ where the heaviside function is

$$H(A) = \begin{cases} 1 & A > 0 \\ 0 & A < 0 \end{cases}$$

and then,

$$A(\tau) = \begin{cases} 0 & 0 \leq \tau \leq 1-\bar{A} \\ 1 & 1-\bar{A} \leq \tau \leq 1 \end{cases} \tag{3}$$

(see Fig. 1).

We will now consider the bounds on the second moment for a given value of $\bar{A}$. We first observe that

$$0 \leq A \leq 1 \tag{4}$$

implies the two inequalities

$$0 \leq AP(A) \; ; \; AP(A) \leq P(A) \tag{5}$$

because $P(A) \geq 0$. Integrating both between 0 and 1,

$$0 \leq \bar{A} \leq 1 \tag{6}$$

By a similar reasoning, we can prove

$$\bar{A}^2 \leq \overline{A^2} \leq \bar{A} \tag{7}$$

To prove the upper bound, we have successively

$$\begin{aligned} A &\leq 1 && \text{by (4U), i.e., the upper bound} \\ A^2 &\leq A && \text{by (4L), i.e., the lower bound} \\ \overline{A^2} &\leq \bar{A} && \text{because } P \geq 0, \text{ q.e.d.} \end{aligned} \tag{8}$$

To prove the lower bounds, we use Reynolds' decomposition

$$A = \bar{A} + A' \tag{9}$$

Thus,

$$\overline{A^2} = \left\langle (\bar{A} + A')^2 \right\rangle = \bar{A}^2 + \overline{A'^2} \geq \bar{A}^2 \quad \text{because } \overline{A'^2} \geq 0, \text{ q.e.d.}$$

The bounds on the second moment have been obtained by elementary methods. We can similarly show that the bounds ($\overline{A^2} = \bar{A}$ and $\bar{A}^2 = \overline{A^2}$) are realized by unique discrete distribution.

For the upper bound, we have successively

$$\bar{A} = \overline{A^2}$$

$$\bar{A} - \overline{A^2} = 0$$

and

$$\int_0^1 (A - A^2) P(A)\, dA = 0$$

However, the integrand is positive (or zero) by Eq. (8) and hence the integrand must vanish:

$$(A - A^2) P(A) = 0 \tag{10}$$

If P is to be nonzero, we must have $A = 0$ or $A = 1$ and, therefore,

$$P(A) = (1 - \varepsilon)\delta(A) + \varepsilon\delta(A - 1) \tag{11}$$

Since $\bar{A}$ is given, ϵ is determined. In fact, by direct computation, $\bar{A} = \epsilon$ and

$$P(A) = (1 - \bar{A})\delta(A) + \bar{A}\delta(A - 1) \tag{12}$$

which is the distribution given in Eq. (2) above. We note that the $P(A)$ that realizes the upper bound of $\overline{A^2}$, Eq. (12), is uniquely determined by $\bar{A}$. We can view relation (12) as a consequence of (10) and of L. Schwartz' theorem $x\delta(A) = 0$.

The lower bound is also realized by a unique distribution. We have from (7L)

$$\overline{A^2} = \bar{A}^2$$

or

$$\int_0^1 (A^2 - \bar{A}^2)P(A)\, dA = \int_0^1 (A - \bar{A})^2 P(A)\, dA = \int_0^1 A'^2 P(A)\, dA$$

As for the upper bound, the integrand is positive or zero and, therefore,

$$A'^2 P(A) = 0$$

or

$$(A - \bar{A})^2 P(A) = 0$$

It follows that $A = \bar{A}$ if $P \neq 0$, or

$$P(A) = \delta(A - \bar{A}) \tag{13}$$

This distribution can be represented by a box diagram as

$\delta(A - \bar{A}) =$ 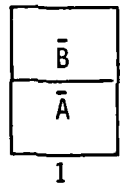

(14)

This result completes the proof that both extreme values of $\overline{A^2}$ are realized, for given $\bar{A}$, by unique, discrete, probability densities.

A summary of the relations obtained so far is obtained in describing the statically allowed values of $\bar{A}$ and $\overline{A^2}$ as a domain in a plane with

coordinates $\bar{A}$, $\overline{A^2}$. The domain of moments $M_{12}(\bar{A}, \overline{A^2})$ is shown in Figure 2 that represents

$$M_{12} = \left\{ 0 \leq \bar{A} \leq 1 \; ; \; \bar{A}^2 \leq \overline{A^2} \leq \bar{A} \right\} \tag{15}$$

We note that the maximum width of the domain occurs at $\bar{A} = 1/2$ and is $W_{12} = 1/4 = .25$. Clearly the maximum width of the statistically allowed domain should be large compared with the experimental error if a statistically significant experiment is contemplated. We show below that the Cal Tech experiments amply fulfill this requirement.

We recast our result in terms of the centered moment $\overline{A'^2}$ by means of the identity

$$\overline{A'^2} = \overline{A^2} - \bar{A}^2 \tag{16}$$

The domain of statistically allowed $(\bar{A}, \overline{A'^2})$ pairs is readily shown to be, from Eq. (15)

$$M'_{12} = \left\{ 0 \leq \bar{A} \leq 1 \; ; \; 0 \leq \overline{A'^2} \leq \bar{A}(1 - \bar{A}) \right\} \tag{17}$$

In Figure 3, we show a diagram of M'_{12} . We illustrate our theoretical bounds with the Konrad data in Figure 4. In this and similar following figures of this section

$$B = N_2 \text{ concentration} \tag{18}$$

$$\frac{y}{x - x_0} = \text{similarity variable across the flow} \tag{19}$$

$$\Delta = 1 - \frac{M_{(He)}}{M_{N_2}} = 0 \quad \begin{array}{l}\text{(The He is premixed with A to} \\ \text{achieve molecular mass equality)}\end{array} \tag{20}$$

$s = 1$ = Konrad's mass ratio parameter

$r = .38$ = velocity ratio (He is faster)

In view of the fact that $\bar{B}$ is monotonic in the similarity variable $y/(x - x_0)$, we may plot the experimental data on the diagram of Figure 2 using the $\bar{B}$ axis as a "stretched" similarity variable. The resulting diagrams, Figures 4 and 5, show two alternative (and equivalent) representations of the second moment of the N_2 concentration $\overline{B^2}$ and of its

statistical bounds as dictated by the corresponding values of $\bar{B}$. Konrad gives plots of both the Gaussian measure for the second moment $\sqrt{\overline{B'^2}}$ and of the (second order) mixedness parameter

$$\frac{|\overline{A'B'}|}{\bar{A}\,\bar{B}} = \frac{\overline{A'^2}}{\bar{A}(1-\bar{A})} = \frac{\overline{A^2} - \bar{A}^2}{\bar{A}(1-\bar{A})} \tag{21}$$

Readings of the reproducibility of the similarity profiles and comparison of values obtained for the moment $\bar{B}$ and $\overline{B^2}$ from the distribution functions vs those obtained from the Konrad plots indicate an "experimental error bar" (or uncertainty) of ± 0.01 on the scales indicated. Sensitivity of the bounds to errors in $\bar{B}$ is estimated by setting $\bar{B} = \bar{B}_0 \pm 0.01$. Then at $y/(x - x_0) = 0$ (center of flow),

$$\delta L_2 \cong \pm 0.011 \tag{22}$$

$$\delta U_2 \cong \pm 0.010 \tag{23}$$

$$\delta W_2 \cong \mp 0.001 \tag{24}$$

where

$$W_2 = U_2 - L_2 \leq 0.25 \tag{25}$$

We see that the width of the statistical bounds is less sensitive to error than the lower and upper bounds themselves. The equivalent shift in the similarity variable near $y/(x - x_0) \approx 0$ is estimated to be $\delta(y/(x - x_0)) \approx -0.004$.

In conclusion, statistical analysis of the second moment indicates that the experiment is clearly statistically significant and that the second-order fluctuations are on the low side in the central portions of the flow.

As a final point in the statistical analysis of the second moment, we give a constructive procedure whereby, given any allowed value of the pair $(\bar{A}, \overline{A^2})$ (or alternatively of $(\bar{A}, \overline{A'^2})$), a discrete distribution is found that realizes the given values. The construction is based on the results obtained on the realizability of the extreme values of the moments. In particular, we have demonstrated that maximal fluctuations are achieved by discrete distributions. Exploiting the convexity of the domain of values

of $(\bar{A}, \overline{A^2})$ proven in App. 1, we proceed as follows (Fig. 6). At points a and b we must have

$$P_a = \varepsilon\delta(A) + (1 - \varepsilon)\delta(A - 1) \tag{26}$$

$$P_b = \delta(A - A_o) \tag{27}$$

We now form the (convex) combination

$$P = \lambda P_a + (1 - \lambda)P_b \tag{28}$$

where $$0 \leq \lambda \leq 1 \tag{29}$$

The resulting distribution is given by the box diagram, Figure 7. Straightforward calculation (best carried out with the general method of the characteristic equation given in Section IV) yields

$$\begin{aligned} \varepsilon_1 &= \frac{\overline{A^2} - \bar{A}A_3}{1 - A_3} \\ \varepsilon_2 &= 1 - \bar{A} - \frac{\bar{A} - \overline{A^2}}{1 - \bar{A}} \\ \varepsilon_3 &= \frac{\bar{A} - \overline{A^2}}{A_3(1 - A_3)} \end{aligned} \tag{30}$$

where A_3 is bounded above and below from the requirements, respectively, that ε_1 be positive and ε_2 be positive

$$\frac{\overline{AB}}{\bar{B}} \leq A_3 \leq \frac{\overline{A^2}}{\bar{A}} \tag{31}$$

Three special cases are particularly interesting since they correspond respectively to: (1) maximal A moments; (2) minimal A moments; and (3) symmetric A and B moments. The three special cases are given in full in Figure 8. The corresponding cells are obtained from Figure 6.

To discuss moments higher than the second, we need some additional tools. These are incorporated in the following inequalities:

1. Hölder's inequality. f and g are arbitrary and P is positive.

Then,

$$\left[\int_0^1 f^p(\alpha)P(\alpha)\,d\alpha\right]^{1/p} \cdot \left[\int_0^1 g^q(\alpha)P(\alpha)\,d\alpha\right]^{1/q} \geq \int_0^1 f(\alpha)g(\alpha)P(\alpha)\,d\alpha \tag{32}$$

provided

$$1/p + 1/q = 1 \tag{33}$$

or

$$\overline{f^p}^{1/p} \cdot \overline{g^q}^{1/q} \geq \overline{fg} \tag{34}$$

Equality holds if, and only if,

$$f^p = \lambda\, g^q \tag{35}$$

Furthermore, the Cauchy-Schwarz inequality corresponds to $p = q = 2$; that is

$$\overline{f^2} \cdot \overline{g^2} \geq \overline{fg}^2 \tag{36}$$

with equality at

$$f = \lambda g \tag{37}$$

The conditions for equality are essential in our analysis since they allow us to determine the realizations of the extreme values of the moments.

2. Jensen's inequality. If $\phi(\alpha)$ is convex (i.e., $\phi'' > 0$ throughout the domain of interest ($0 \leq \alpha \leq 1$)), then

$$\overline{\phi(\alpha)} \geq \phi(\bar{\alpha}) \tag{38}$$

3. Tchebytcheff's inequality. If f and g are similar (both increase or both decrease in the interval $0 \leq \alpha \leq 1$), then

$$\overline{fg} \geq \bar{f}\bar{g} \tag{39}$$

Utilizing these inequalities, we find the lower and upper bound on the

third moments, given $\bar{A}$ and $\overline{A^2}$,

$$\frac{\overline{A^2}^2}{\bar{A}} \leq \overline{A^3} \leq \overline{A^2} - \frac{(\bar{A} - \overline{A^2})^2}{1 - \bar{A}} \tag{40}$$

We confine our discussion to the lower bound since the upper bound can be treated by similar methods. To establish the bound, we use the Cauchy-Schwarz inequality, Eq. (36), with

$$f = A^{3/2} \quad , \quad g = A^{1/2} \tag{41}$$

The realization of the lower bound is obtained from Eq. (37)

$$A^{3/2} = \lambda A^{1/2} \tag{42}$$

whose roots are

$$A = 0 \quad \text{and} \quad A = \lambda \tag{43}$$

Therefore, the minimum of $\overline{A^3}$ is realized by the probability density

$$P(A) = w\delta(A) + (1 - w)\delta(A - \lambda) \tag{44}$$

From the given moments,

$$\bar{A} = (1 - w)\lambda \tag{45}$$

and

$$\overline{A^2} = (1 - w)\lambda^2 = \bar{A} \cdot \lambda \tag{46}$$

Hence,

$$\lambda = \frac{\overline{A^2}}{\bar{A}} \tag{47}$$

Substituting Eq. (47) into (45)

$$1 - w = \frac{\bar{A}}{\lambda} = \frac{\bar{A}^2}{\overline{A^2}} \tag{48}$$

which completes the determination of $P(A)$. Using Eq. (44),

$$P(A) = \frac{\overline{A^2} - \bar{A}^2}{\overline{A^2}} \delta(A) + \frac{\bar{A}^2}{\overline{A^2}} \delta\left(A - \frac{\overline{A^2}}{\bar{A}}\right) \tag{49}$$

In terms of the box diagram, we can symbolize this distribution as in Figure 8.

An entirely analogous discussion of the upper bound is obtained with

$$f = A B^{1/2} \quad , \quad g = B^{1/2} \tag{50}$$

The resulting extremal distribution is P_1 of Figure 8.

The statistical bounds established in Eq. (40) are sufficiently stringent to give information on the experimental values of $\overline{B^3}$ that can be obtained from Konrad's paper. In Figure 9, we show the successive restrictions obtained by statistical considerations when we use the information that $\bar{B}$ is given and when we use both $\bar{B}$ and $\overline{B^2}$. Our estimated experimental error is the one discussed in the context of $\overline{B^2}$. The maximum width of 1/16 is the maximum of the difference between upper and lower bounds in Eq. (40). The sensitivity of the bounds to errors in $\overline{B^2}$ and $\bar{B}$ is readily estimated. For $\overline{B^2} = B_0^2 \pm 0.01$, at $y/(x - x_0) = 0$, is

$$\delta L_3 \cong \pm 0.013$$

$$\delta U_3 \cong \pm 0.010$$

$$\delta W_3 \cong \mp 0.003 \ , \ W_3 \cong 0.039$$

If both $\bar{B}$ and $\overline{B^2}$ are varied as

$$\bar{B} = \overline{B_0} \pm 0.01$$

$$\overline{B^2} = \overline{B_0^2} \pm 0.01$$

we find comparable variations in the bounds.

It is of interest to restate the bounds of Eq. (40) in terms of the centered moment $\overline{A'^3}$. From the relationship

$$\overline{A^3} = \bar{A}^3 + 3\bar{A}\,\overline{A'^2} + \overline{A'^3} \tag{51}$$

we obtain

$$\frac{\overline{A'^2}}{\bar{A}}\left(\overline{A'^2} - \bar{A}^2\right) \leq \overline{A'^3} \leq \overline{A'^2}\ \frac{(1 - \bar{A})^2 - \overline{A'^2}}{1 - \bar{A}} \tag{52}$$

An immediate corollary of these bounds is the determination of the allowed domains of positive (negative) skewness. These are shown in Figure 10.

A third-order mixedness, R_3, is introduced by analogy with Eq. (21)

$$R_3 = \frac{\frac{\overline{A'B'^2} - \overline{A'^2B'}}{2} - L_3'}{U_3' - L_3'} = \frac{\overline{A^3} - L_3}{U_3 - L_3} \tag{53}$$

Clearly, $0 \leq R_3 \leq 1$. A plot is shown in Figures 11a,b for two of Konrad's flows in terms of mass fractions. R_3 appears to be systematically asymmetric.

A discussion of the fourth moment can be carried out somewhat analogously to our previous discussion of the third moment.

The statistical bounds can be summarized in the following results (the bounds are proven in Section IV).

1. For given $\bar{A}$ we have the broad bounds

$$\bar{A}^4 \leq \overline{A^4} \leq \bar{A} \tag{54}$$

2. For given $\bar{A}$ and $\overline{A^2}$ we have

$$\overline{A^4} \geq \frac{\overline{A^2}^3}{\bar{A}^2} \tag{55}$$

$$\overline{A^4} \leq \frac{\overline{A^2}\left[1 - \overline{A^2} + \bar{A}^2 + (\bar{A} - \overline{A^2})^2\right] - \bar{A}^2}{(1 - \bar{A})^2} \tag{56}$$

3. If the three moments, $\bar{A}$, $\overline{A^2}$ and $\overline{A^3}$, are all given, then

$$\overline{A^4} \geq \overline{A^2}^2 + \frac{(\overline{A^3} - \bar{A}\,\overline{A^2})^2}{\overline{A^2} - \bar{A}^2} \tag{57}$$

$$\overline{A^4} \leq \overline{A^3} - \frac{(\overline{A^2} - \overline{A^3})^2}{\bar{A} - \overline{A^2}} \tag{58}$$

A plot of the successively shrinking ranges of the upper and lower bounds on $\overline{B^4}$ obtained from Konrad's data is shown in Figure 12.

The sensitivity of the stringent bounds on variations of the lower moments is approximately the same as for $\overline{B^2}$ and $\overline{B^3}$.

The relation between the total moment $\overline{B^4}$ and the Kurtosis is obtained through the Reynolds decomposition which yields

$$\overline{B^4} = \bar{B}^4 + 6\bar{B}^2\,\overline{B'^2} + 4\bar{B}\,\overline{B'^3} + \overline{B'^4} \tag{59}$$

Upon use of (51), we find

$$\text{Kurtosis} \equiv \frac{\overline{B'^4}}{\overline{B'^2}^2} = \frac{\overline{B^4} = 3\bar{B}^4 - 4\bar{B}\,\overline{B^3} + 6\bar{B}^2\,\overline{B^2}}{\left(\overline{B^2} - \bar{B}^2\right)^2} \tag{60}$$

A plot of the Kurtosis across the flow is shown in Figure 13. The Gaussian value of 3 is nearly achieved at the center.

III. INCOMPRESSIBLE FLOW WITH VARIABLE DENSITY

In this section, we characterize the state of an incompressible flow with variable density by means of appropriate state functions. In particular, the (mass) density and the entropy of mixing are calculated as functions of the mass fractions, and the relations among molar and mass variables are given.

To establish our notation, we recall that for a single component gas two measures of density are useful: the mass density ρ and the molar density $\mathcal{N}$. They are related through the number of molecules per unit volume, n (number density)

$$\rho = m\, n = M\mathcal{N} \tag{61}$$

where m = mass of one molecule

$$M = m \times \text{Arogadro's number} = \text{mass of one mole} \tag{62}$$

The gas constants are related by

$$R_m = \frac{\mathcal{R}}{M} = \frac{k}{m} \tag{63}$$

where k is Boltzmann's constant. The equation of state of our ideal gas thus acquires two possible forms in terms of molar and mass densities:

$$p = nkT = \mathcal{N}\mathcal{R}T = \rho R_m T \tag{64}$$

Correspondingly, for a binary mixture, we have two measures of concentration:

1. Mass fractions

$$\alpha = \frac{\rho_1}{\rho_1 + \rho_2}\ , \quad \beta = \frac{\rho_2}{\rho_1 + \rho_2} \tag{65}$$

with

$$\alpha + \beta = 1 \tag{66}$$

and

$$0 \leq \alpha \leq 1\ , \quad 0 \leq \beta \leq 1 \tag{67}$$

2. Molar fractions

$$A = \frac{\mathcal{N}_1}{\mathcal{N}_1 + \mathcal{N}_2} \quad , \quad B = \frac{\mathcal{N}_2}{\mathcal{N}_1 + \mathcal{N}_2} \tag{68}$$

with

$$A + B = 1 \tag{69}$$

and

$$0 \leq A \leq 1 \quad , \quad 0 \leq B \leq 1 \tag{70}$$

We adopt by convention the correspondences

$$1 \longleftrightarrow \alpha \longleftrightarrow A \longleftrightarrow \text{heavier}$$

$$2 \longleftrightarrow \beta \longleftrightarrow B \longleftrightarrow \text{lighter}$$

The equation of state for a mixture of two ideal gases can be written, assuming Dalton's law of partial pressures,

$$\begin{aligned} p &= p_1 + p_2 \\ &= \mathcal{N} \mathcal{R} T = (\mathcal{N}_1 + \mathcal{N}_2) \mathcal{R} T \qquad \text{(molar form)} \\ &= \rho \mathcal{R} T = \rho \left(\frac{\alpha}{M_\alpha} + \frac{\beta}{M_\beta} \right) \mathcal{R} T \qquad \text{(mass fraction form)} \end{aligned} \tag{71}$$

An incompressible flow with variable density is characterized by the assumptions

$$\begin{aligned} p &= \bar{p} = \text{constant across the flow} \\ T &= \bar{T} = \text{constant across the flow} \end{aligned} \tag{72}$$

We then see that in molar variables

$$\mathcal{N} = \mathcal{N}_1 + \mathcal{N}_2 = \bar{\mathcal{N}} = \text{constant across the flow} \tag{73}$$

while in mass fraction variables

$$\rho = \frac{\text{constant}}{\left(\frac{\alpha}{M_\alpha} \right) + \left(\frac{\beta}{M_\beta} \right)} \neq \text{constant} \tag{74}$$

We introduce the normalized density

$$\rho_* = \frac{\rho}{\rho_{light}} = \frac{1}{1 - \Delta\alpha} = \frac{\Delta}{1 - \Delta} A + 1 \tag{75}$$

where

$$\rho_{light} = \frac{M_\beta \bar{p}}{\mathcal{R}\bar{T}} \tag{76}$$

$$\Delta = 1 - \frac{M_\beta}{M_\alpha} \tag{77}$$

We can choose without loss of generality, $0 \leq \Delta \leq 1$. Thus for an He - N_2 mixture, $\Delta = 6/7 \approx 0.86$ and for an H_2 - O_2 mixture, $\Delta = 15/16 \approx 0.94$.

We observe that ρ_* is a rather steep function of α for $\Delta \sim 1$ and thus $\bar{\rho}_*$ is statistically independent from $\bar{\alpha}$ except for very weak turbulence. In contrast, ρ_* is linear in A and thus ρ_* and A are equivalent statistical variables. The relationship between the molar and mass fractions is therefore nonlinear. We have, in fact,

$$A = (1 - \Delta) \frac{\alpha}{1 - \Delta\alpha} \approx A(\alpha) \tag{78}$$

$$B = \frac{1 - \alpha}{1 - \Delta\alpha} \tag{79}$$

and the inverse relations

$$\alpha = \frac{A}{1 - \Delta(1 - A)} \tag{80}$$

$$\beta = (1 - \Delta) \frac{1 - A}{1 - \Delta(1 - A)}$$

A graph of the relation $A(\alpha)$ is shown in Figure 14 to show the increasing statistical independence between A and α with increasing Δ .

Another nonlinear state function of the mass fraction is the entropy of mixing. The experimentally observed pure N_2 and pure He probability shows that mixing is very slow on the time scale of turbulence variations (~ integral scale/root mean square turbulent velocity). Further, the probability profile of pure He is approximately 2-3 times thicker than the

probability profile of pure N_2 in qualitative agreement with the concept that a pocket of pure N_2 folded by a large scale eddy into the He-rich region should be mixed by molecular diffusion about 2.6 times faster than a pocket of pure He folded into N_2 ($v_{He}/v_{N_2} = \sqrt{m_{N_2}/m_{He}} = \sqrt{7} \approx 2.65$). We show below that choosing a probability distribution with low entropy of mixing is in rather good agreement with experimental evidence. In this section we calculate the entropy of mixing and give some of its properties.

For a single ideal gas we can write, for the specific entropy,

$$S = C_{v_m} \ell n(T/T_{ref}) - R_m \ell n(\rho/\rho_{ref}) \tag{82}$$

where R_m is given by Eq. (63). For a binary mixture, we have

$$S_{(mixture)} = \alpha S_\alpha + \beta S_\beta \tag{83}$$

The entropy density is obtained as $\rho S_{specific}$. Substituting (82) into (83)

$$S_{mixt} = \alpha C_{v_\alpha} \ell n \frac{T}{T_{ref}} + \beta C_{v_\beta} \ell n \frac{T}{T_{ref}} +$$

$$- \alpha R_\alpha \ell n \frac{\rho_\alpha}{\rho_{ref}} - \beta R_\beta \ell n \frac{\rho_\beta}{\rho_{ref}} \tag{84}$$

We choose for the variable density, incompressible flows that we analyze

$$T_{ref} = T_{exp} = \text{constant} \tag{85}$$

$$\rho_{ref} = \rho_{light(\alpha)} = \frac{\bar{p} M_\beta}{\mathcal{R} \bar{T}} \tag{86}$$

The resulting expression for the specific entropy is

$$S_{mixt} = - \mathcal{R} \left[\frac{\alpha}{M_\alpha} \ell n(\alpha \rho_*) + \frac{\beta}{M_\beta} \ell n(\beta \rho_*) \right] \tag{87}$$

which, using Eq. (75), reduces to

$$S_{mixt} \frac{M_\alpha}{\mathcal{R}} = - \left[\alpha \ell n \alpha + \frac{(1-\alpha)\ell n(1-\alpha)}{1-\Delta} + \frac{1-\Delta\alpha}{1-\Delta} \ell n \frac{1}{1-\Delta\alpha} \right] \tag{88}$$

The normalized entropy density is given by

$$\rho_* S_{mixt} \frac{M_\alpha}{\mathcal{R}} = - \frac{1}{1 - \Delta\alpha}\left[\alpha \ln \alpha + \frac{(1 - \alpha) \ln (1 - \alpha)}{1 - \Delta} - \frac{1 - \Delta\alpha}{1 - \Delta} \ln (1 - \Delta\alpha)\right] \tag{89}$$

The nonlinear behavior of the specific entropy is shown in Figures 15 and 16 for physically interesting values of Δ. In Figure 17 we see how the entropy density combines the nonlinear features of ρ_* and of S_{mixt}.

As a simple example of the behavior of the mean entropy of mixing, we observe that for $\Delta = 0$ ($\rho_* = 1$) we have from (88)

$$\frac{SM_\alpha}{\mathcal{R}} = - (A \ln A + B \ln B) \tag{90}$$

Thus a simple computation shows that the mean entropy associated with the "nonoverlapping" probability of Figure 1 is exactly zero.

$$\bar{S}_{mix} \left(\boxed{A \mid B} \right) = 0 \tag{91}$$

while the entropy of mixing for the distribution of Figure 14 is

$$\bar{S}_{mix} \left(\begin{array}{|c|} \hline \bar{B} \\ \hline \bar{A} \\ \hline \end{array} \right) = - \frac{\mathcal{R}}{M_\alpha} (\bar{A} \ln \bar{A} + \bar{B} \ln \bar{B}) \tag{92}$$

It is not difficult to show that (91) is minimal for given $\bar{A}$ while (92) is maximal for given $\bar{A}$.

We shall use below the distribution given by Figure 7. In this case,

$$\bar{S}_{mix} = - \frac{\mathcal{R}}{M_\alpha} (\bar{A} - \overline{A^2}) \left[\frac{\ln A_3}{1 - A_3} + \frac{\ln(1 - A_3)}{A_3} \right] \tag{93}$$

Thus for the distribution of Figure 7, $\bar{S}_{mix}/(\bar{A} - \overline{A^2})$ is a function of the single parameter A_3 and can be minimized analytically.

IV. GENERAL METHOD FOR THE DETERMINATION OF STATISTICAL BOUNDS

In this section, we first outline a general technique to obtain statistical bounds that are sharp (i.e., "best bounds") and to establish the domain of moments for which they are realized. We then give several families of useful bounds.

The essence of the method is the close relation between the equality condition in the Cauchy-Schwarz theorem and the characteristic equation for a discrete probability distribution.

Consider a discrete probability distribution of general form

$$P(A) = \sum_{i=1}^{n} \varepsilon_i \delta(A - A_i) \tag{94}$$

Using Dirac's identity

$$(A - A_i)\delta(A - A_i) = 0 \tag{95}$$

we see that

$$\prod_{i=1}^{n} (A - A_i)P(A) = 0 \tag{96}$$

so that the algebraic equation

$$\phi(A) = \prod_{i=1}^{n} (A - A_i) = 0 \tag{97}$$

determines the locations of the masses of $P(A)$. We call $\phi = 0$ the characteristic equation for (94). We can actually determine the A_i's as functions of the moments as follows. Multiply (96) by any function $F(A)$ and integrate from 0 to 1, obtaining

$$\left\langle F(A) \prod_{i=1}^{n} (A - A_i) \right\rangle = 0 \tag{98}$$

If we choose, in particular, $F = A^0=1, A, A^2, \ldots, A^{n-1}$, we obtain n linear equations for the invariants of the matrix

$$L_{ij} = A_{(i)}\delta_{ij} \qquad \text{(no sum on } i\text{)} \tag{99}$$

For example, for $n = 3$, the linear equations are

$$\overline{A^3} - \overline{A^2}I_1 + \bar{A}I_2 - I_3 = 0 \tag{100}$$

$$\overline{A^4} - \overline{A^3}I_1 + \overline{A^2}I_2 - \bar{A}I_3 = 0 \tag{101}$$

$$\overline{A^5} - \overline{A^4}I_1 + \overline{A^3}I_2 - \overline{A^2}I_3 = 0 \tag{102}$$

where

$$I_1 = A_1 + A_2 + A_3 \tag{103}$$

$$I_2 = A_1A_2 + A_1A_3 + A_2A_3 \tag{104}$$

$$I_3 = A_1A_2A_3 \tag{105}$$

By writing Eqs. (100)-(102) as a matrix equation

$$\begin{bmatrix} \overline{A^2} - \bar{A} & 1 \\ \overline{A^3} - \overline{A^2} & \bar{A} \\ \overline{A^4} - \overline{A^3} & \overline{A^2} \end{bmatrix} \begin{bmatrix} I_1 \\ I_2 \\ I_3 \end{bmatrix} = \begin{bmatrix} \overline{A^3} \\ \overline{A^4} \\ \overline{A^5} \end{bmatrix} \tag{106}$$

we can obtain the I_k's in terms of the Cramer determinants of (106). Thus, with obvious notation

$$I_k = \frac{N_k}{N_o} \tag{107}$$

It follows then quite generally from Eq. (97) that the A_i's are the n roots of an n'th order polynomial whose coefficients follow from (107)

$$N_oA^n - A^{n-1}N_1 + \ldots + (-1)^nN_n = 0 \tag{108}$$

The locations A_i of the masses are then determined by establishing that $N_i > 0$ and $N_n < N_o$. N_o is always positive by Hankel's inequality. This is established as follows:

$$\sum_{i=0}^{n}\sum_{j=0}^{n}\langle x_i A^{i+j} x_j\rangle = \left\langle\left(\sum_{i=0}^{n} x_i A^i\right)\left(\sum_{j=0}^{n} x_j A^j\right)\right\rangle \geq 0 \tag{109}$$

for any choice of real x_i . Thus $\overline{A^{i+j}}$ is positive definite and has a positive determinant.

The weights ε_i are also readily characterized through Eq. (97). Multiplying (94) by $\prod_{i=1}^{n=1}(A - A_i)$, we have in fact, after integration,

$$\left\langle \prod_{i=1}^{n=1}(A - A_i)\right\rangle = \varepsilon_n \prod_{i=1}^{n-1}(A_n - A_i) \tag{110}$$

To obtain the lower bound on $\overline{A^{2n}}$, we write the Cauchy-Schwarz inequality

$$\overline{f^2}\,\overline{g^2} > \overline{fg}^2 \tag{111}$$

with the choice

$$g = (-1)^{n+1}\prod_{i=1}^{n} A_i \tag{112}$$

$$f = \phi + g \tag{113}$$

Substitution of Eqs. (112) and (113) into (111) yields

$$\overline{A^{2n}} \geq L\left(\overline{A^0}, \overline{A^1}, \ldots, \overline{A^{2n-1}}\right)$$

To obtain the lower bound on $\overline{A^{2n+1}}$, the upper bound on $\overline{A^{2n+1}}$, and the upper bound on $\overline{A^{2n+2}}$, we multiply (112) and (113) successively by $A^{\frac{1}{2}}$, $B^{\frac{1}{2}}$, $(AB)^{\frac{1}{2}}$. For the lower bound on $\overline{A^{2n+2}}$, we return to the forms (112) and (113).

As a simple example of the method, we establish the least upper bound on $\overline{A^4}$ for given $\bar{A}$, $\overline{A^2}$, and $\overline{A^3}$. Since we require the upper bound on an even moment, we consider the distribution of Figure 18. The characteristic equation is

$$A(A - 1)(A - A_3) = 0 \tag{114}$$

averaging

$$\langle A(A - 1)A\rangle - A_3\langle A(A - 1)\rangle = 0 \tag{115}$$

Thus,

$$A_3 = \frac{\overline{A^3} - \overline{A^2}}{\overline{A^2} - \bar{A}} \tag{116}$$

To show that $A_3 \leq 1$, we observe that $\left\langle A(A^2 + 1 - 2A) \right\rangle \geq 0$. The location of the "middle" mass is thus determined without knowledge of the weights. To find ε we note that

$$\overline{A(A - 1)} = \varepsilon A_3(A_3 - 1) \tag{117}$$

Thus,

$$\varepsilon = \frac{(\overline{A^2} - \bar{A})^3}{(\overline{A^3} - \overline{A^2})\,(\overline{A^3} - 2\overline{A^2} + \bar{A})} \tag{118}$$

the proof that $\varepsilon < 1$ is analogous to the one for $A_3 < 1$. Having established the realizability of the limit, we construct the Cauchy-Schwarz inequality with

$$f = A^{\frac{1}{2}}(1 - A)^{\frac{1}{2}}A \tag{119}$$

$$g = A^{\frac{1}{2}}(1 - A)^{\frac{1}{2}} \tag{120}$$

and find after simplifications that

$$\overline{A^4} \leq \overline{A^3} - \frac{(\overline{A^2} - \overline{A^3})^2}{\bar{A} - \overline{A^2}} \tag{121}$$

We note that the proof given establishes Eq. (121) as the "best bound" for $\overline{A^4}$ in the following sense. The right-hand side of (121) is the least upper bound on $\overline{A^4}$ for all probability distributions of given $\bar{A}$, $\overline{A^2}$, and $\overline{A^3}$.

An important shortcut for the odd moments is obtained from the "renormalization theorem." Given that we have established

$$\int_0^1 f^2(A)D_1(A)\,d\alpha \int_0^1 g^2(A)D_1(A)\,dA \geq \left[\int_0^1 fgD_1\,dA\right]^2 \tag{122}$$

it follows that

$$\int_0^1 Af^2 D_1 \, dA \cdot \int_0^1 Ag^2 D_1 \, dA \geq \left(\int_0^1 AfgD_1 \, dA \right)^2 \tag{123}$$

The proof is simple. Since (122) holds for all D_1, we can choose D_1 of the special form αD_2 for any D_2. (The passage from (123) to (122) is not legitimate, in general.)

We now consider several important families of inequalities. First, consider a variable α, $0 \leq \alpha \leq 1$, and its conjugate, $\beta = 1 - \alpha$, i.e., either a mass or a mole fraction. Applying Cauchy-Schwarz to

$$f = \alpha \quad , \quad g = 1 \tag{124}$$

we obtain

$$\bar{1}\,\overline{\alpha^2} \geq \overline{\alpha}^2 \tag{125}$$

where $\bar{1} \equiv \int_0^1 D(\alpha)\, d\alpha$. If D is a probability density, $\bar{1} = 1$. The presence of the $\bar{1}$ allows application of the renormalization procedure. The Cauchy-Schwarz limit for (125) is $\alpha = \lambda$, i.e., a single mixed cell

$$P(\alpha) = \delta(\alpha - \bar{\alpha}) \tag{126}$$

Renormalizing (125) by α we find

$$\overline{\alpha^3} \geq \frac{\overline{\alpha^2}^2}{\bar{\alpha}} \tag{127}$$

The Cauchy-Schwarz limit is $\alpha^{3/2} = \lambda\alpha^{1/2}$, i.e., $\alpha = 0$, $\alpha = \lambda = \dfrac{\overline{\alpha^2}}{\bar{\alpha}}$. Therefore, at equality,

$$P(\alpha) = \frac{\bar{\alpha}^2}{\overline{\alpha^2}}\,\delta\left(\alpha - \frac{\overline{\alpha^2}}{\bar{\alpha}}\right) + \frac{\overline{\alpha^2} - \bar{\alpha}^2}{\overline{\alpha^2}}\,\delta(\alpha) \tag{128}$$

Renormalizing Eq. (125) by β, we find

$$\overline{\alpha\beta}^2 \leq \overline{\alpha^2\beta} \cdot \bar{\beta} \tag{129}$$

or, eliminating β ,

$$\overline{\alpha^3} \leq \overline{\alpha^2} - \frac{(\bar{\alpha} - \overline{\alpha^2})^2}{1 - \bar{\alpha}} \tag{130}$$

The Cauchy-Schwarz limit for Eq. (127) is

$$\alpha\beta^{\frac{1}{2}} = \lambda\beta^{\frac{1}{2}} \tag{131}$$

with roots

$$\beta = 0 \ , \quad \alpha = \lambda = \frac{\overline{\alpha\beta}}{\bar{\beta}} \tag{132}$$

i.e., a pure α and a mixed cell. Therefore, at equality

$$P(\alpha) = \frac{(1 - \bar{\alpha})^2}{1 - 2\bar{\alpha} + \overline{\alpha^2}} \, \delta\left(\alpha - \frac{\bar{\alpha} - \overline{\alpha^2}}{1 - \bar{\alpha}}\right) + \frac{\overline{\alpha^2} - \bar{\alpha}^2}{1 - 2\bar{\alpha} + \overline{\alpha^2}} \, \delta(\alpha) \tag{133}$$

Renormalizing (125) by $\alpha\beta$, we find

$$\overline{\alpha^2\beta}^2 \leq \overline{\alpha^3\beta} \cdot \overline{\alpha\beta} \tag{134}$$

or, eliminating β ,

$$\overline{\alpha^4} \leq \overline{\alpha^3} - \frac{(\overline{\alpha^2} - \overline{\alpha^3})^2}{\bar{\alpha} - \overline{\alpha^2}} \tag{135}$$

The Cauchy-Schwarz limit was discussed following Eq. (114).

The lower bound on $\overline{\alpha^4}$ requires two mixed cells. We find

$$\overline{\alpha^4} \geq \overline{\alpha^2}^2 + \frac{(\overline{\alpha^3} - \bar{\alpha}\overline{\alpha^2})^2}{\overline{\alpha^2} - \bar{\alpha}^2} \tag{136}$$

The α inequalities and some of the higher ones are summarized in the trees, Figures 18 and 19. For all cases, the equality corresponds to a unique discrete distribution. This situation persists when we include "skips." These are most readily derived from a generalization of Eq. (125) which is obtained from Hölder's inequality

$$\bar{1}^{n-2} \cdot \overline{\alpha^{n-1}} \geq \bar{\alpha}^{n-1} \tag{137}$$

We observe that for $n = 3$, Eq. (137) becomes (125). We readily find, following the tree of Figure 20, the bounds on $\overline{\alpha^3}$ given only $\bar{\alpha}$, i.e.,

$$\bar{\alpha}^3 \leq \overline{\alpha^3} \leq \bar{\alpha} \tag{138}$$

The equal sign of the lower bound is realized by (126) just like the lower bound on $\overline{\alpha^2}$. Similarly, the bounds on $\overline{\alpha^4}$ given $\bar{\alpha}$ and $\overline{\alpha^2}$ are

$$\frac{\overline{\alpha^2}^3}{\bar{\alpha}^2} \leq \overline{\alpha^4} \leq \overline{\alpha^3} - \frac{(\bar{\alpha} - \overline{\alpha^2})^3}{(1 - \bar{\alpha})^4} \tag{139}$$

and they are realized, respectively, by (128) and (133). In Appendix 3 we prove a strong version of this result.

The inequalities for $\overline{\rho_\star \alpha}$ are most readily obtained by observing that renormalizing Eq. (125) by the (positive) quantity $\rho_\star$ gives us

$$\overline{\rho_\star} \cdot \overline{\rho_\star \alpha^2} \geq \overline{\rho_\star \alpha}^2 \tag{140}$$

Using the equation of state and the relations given in Appendix 4, we can recast (140) either as a lower bound on $\overline{\rho_\star}$ (given $\bar{\alpha}$)

$$\bar{\rho}_\star > \frac{\bar{1}^2}{1 - \Delta\bar{\alpha}} \tag{141}$$

or as a lower bound on $\overline{\rho_\star \alpha}$ (given $\bar{\alpha}$)

$$\overline{\rho_\star \alpha} \geq \frac{1}{\Delta}\left[\frac{\bar{1}^2}{1 - \Delta\bar{\alpha}} - \bar{1}\right] \tag{142}$$

Following the tree of Figure 21 or the (simpler but less obvious) alternative tree of Figure 22 and using the equation of state, we readily obtain the lower and upper bounds on $\overline{\rho_\star \alpha}$ for given $\bar{\alpha}$ and $\overline{\alpha^2}$ as well as the upper bound on $\overline{\rho_\star \alpha}$ for given $\bar{\alpha}$ $\overline{\alpha^2}$ and $\overline{\alpha^3}$. The lower bound on $\overline{\rho_\star \alpha}$ for given $\bar{\alpha}$, $\overline{\alpha^2}$ and $\overline{\alpha^3}$ initiates a new tree and is relatively difficult. We thus give it in detail. We show, in fact, that given

$$\bar{1}\ ,\ \bar{\alpha}\ ,\ \overline{\alpha^2}\ ,\ \overline{\rho_\star \alpha} \tag{143}$$

we have the upper bound on $\overline{\alpha^3}$

$$\overline{\alpha^3} \leq \alpha_\star^3 \tag{144}$$

where

$$\overline{\alpha_\star^3} \equiv \frac{\overline{\rho_\star\alpha}\left[\overline{\alpha^2}(1 - \Delta^2\overline{\alpha^2}) - \bar{\alpha}(\bar{\alpha} - \Delta\overline{\alpha^2})\right] - \bar{\alpha}\,\overline{\alpha^2} - \Delta\overline{\alpha^2}^2 + \overline{\alpha^3}}{\Delta\left[\overline{\rho_\star\alpha}\,(1 - \Delta\bar{\alpha}) - \bar{\alpha}\right]}$$

Clearly the (least) upper bound on $\overline{\alpha^3}$ is equivalent to the (greatest) lower bound on $\overline{\rho_\star\alpha}$ (given $\bar{\alpha}, \overline{\alpha^2}$ and $\overline{\alpha^3}$).

We choose

$$f = \rho_\star^{\frac{1}{2}}(\alpha^2 + c) \tag{145}$$

$$g = \rho_\star^{\frac{1}{2}}\alpha \tag{146}$$

To obtain the Cauchy-Schwarz inequality, we square f and g, obtain the product fg, and average. The result is

$$\left[\overline{\rho_\star\alpha^4}\cdot\overline{\rho_\star\alpha^2} - \overline{\rho_\star\alpha^3}^2\right] + 2c\left[\overline{\rho_\star\alpha^2}^2 - \overline{\rho_\star\alpha}\cdot\overline{\rho_\star\alpha^3}\right] + c^2\left[(1 + \Delta\overline{\rho_\star\alpha})\overline{\rho_\star\alpha^2} - \overline{\rho_\star\alpha^2}^2\right] \geq 0 \tag{147}$$

The terms have been arranged as coefficients of c^n to facilitate cancellations.

Using the equation of state relations of Appendix 3, we obtain from (147) after several cancellations, an inequality which is linear both in $\overline{\rho_\star\alpha}$ and $\overline{\alpha^3}$. (The slight variant in the choice of f and g was designed to achieve this goal):

$$\left[\frac{\rho_\star\alpha}{\Delta^2}\left(-\overline{\alpha^3} + \frac{\overline{\alpha^2}}{\Delta}\right) + \frac{\bar{\alpha}\,\overline{\alpha^3}}{\Delta^2} - \frac{\overline{\alpha^2}^2}{\Delta^2} - \frac{\bar{\alpha}\,\overline{\alpha^2}}{\Delta^3}\right] + 2c\left[\frac{\overline{\rho_\star\alpha}}{\Delta}\left(-\frac{\bar{\alpha}}{\Delta} + \overline{\alpha^2}\right) + \frac{\bar{\alpha}^2}{\alpha^2}\right] + c^2\left[\overline{\rho_\star\alpha}\left(\frac{1}{\Delta} - \bar{\alpha}\right) - \frac{\bar{\alpha}}{\Delta}\right] \geq 0 \tag{148}$$

To ensure that the inequality yields the least upper bound on $\overline{\alpha^3}$ (over the probability densities of given $\bar{1}$, $\bar{\alpha}$, $\overline{\alpha^2}$, and $\overline{\rho_\star\alpha}$), we rewrite (148) as

$$F(c) \geq \frac{\overline{\alpha^3}\;\overline{\rho_*\alpha} - \bar{\alpha}}{\Delta^2} \tag{149}$$

and minimize F with respect to c. We have

$$F(c) = \left[\frac{\overline{\rho_*\alpha}}{\Delta^2}\frac{\overline{\alpha^2}}{\Delta} \quad \frac{\overline{\alpha^2}^2}{\Delta^2} \quad \frac{\bar{\alpha}\,\overline{\alpha^2}}{\Delta^3}\right] + 2c\left[\frac{\overline{\rho_*\alpha}}{\Delta}\left(-\frac{\bar{\alpha}}{\Delta} + \overline{\alpha^2}\right) + \frac{\bar{\alpha}^2}{\Delta^2}\right]$$

$$+ c^2\left[\overline{\rho_*\alpha}\left(\frac{1}{\Delta} - \bar{\alpha}\right) - \frac{\bar{\alpha}}{\Delta}\right] \tag{150}$$

The curvature of F is positive by virtue of (142) and the first derivative vanishes at $c = c_o$

$$c_o = \frac{1}{\Delta}\,\frac{\overline{\rho_*\alpha}\,(\bar{\alpha} - \Delta\overline{\alpha^2}) - \bar{\alpha}^2}{\overline{\rho_*\alpha}\,(1 - \Delta\bar{\alpha}) - \bar{\alpha}} \tag{151}$$

Substituting this value of c into (149) we obtain, after some algebra, $\overline{\alpha^3} \leq \alpha_*^3$ as given in (144).

We now examine the equal sign condition, i.e.,

$$f = \lambda g \tag{152}$$

Using (145) and (146), we have

$$\rho_*^{\frac{1}{2}}\,(\alpha^2 + c) = \lambda\rho_*^{\frac{1}{2}}\alpha \tag{153}$$

Since ρ_* has no zero for α between 0 and 1, Eq. (153) gives

$$\alpha^2 - \alpha\lambda + c = 0 \tag{154}$$

We now determine λ and c by averaging the characteristic equation (154) and also multiplying by α and averaging:

$$\overline{\alpha^2} - \bar{\alpha}\lambda + c = 0 \tag{155}$$

$$\overline{\alpha^3} - \overline{\alpha^2}\lambda + \bar{\alpha}c = 0 \tag{156}$$

We have as solutions of (155) and (156):

$$\lambda = \frac{\overline{\alpha^3} - \bar{\alpha}\,\overline{\alpha^3}}{\overline{\alpha^2} - \bar{\alpha}^2} \tag{157}$$

$$c = \frac{\bar{\alpha}\,\overline{\alpha^3} - \overline{\alpha^2}^2}{\overline{\alpha^2} - \bar{\alpha}^2} \tag{158}$$

It is clear from (154) that the probability density that realized the equality is the two-mixed cells distribution:

$$P(\alpha) = \varepsilon_1 \delta(\alpha - \alpha_1) + \varepsilon_2 \delta(\alpha - \alpha_2) \tag{159}$$

where

$$\alpha_1 + \alpha_2 = \lambda \tag{160}$$

$$\alpha_1 \alpha_2 = c \tag{161}$$

as given by Eqs. (157) and (158). In order to complete the realizability proof of the equal sign, we must show that (159) has all four parameters, ε_1 , ε_2 , α_1 and α_2 between 0 and 1.

We first discuss the locations and prove that

$$\alpha_1 + \alpha_2 \geq 0 \tag{162}$$

$$\alpha_1 \alpha_2 \geq 0 \tag{163}$$

and

$$\alpha_1 \alpha_2 \leq 1 \tag{164}$$

Clearly, Eqs. (162), (163) and (164) imply that α_1 and α_2 are between zero and one. To prove these inequalities, we multiply the characteristic equation for (159) by an arbitrary function F assumed similar to α . We have

$$\overline{F\alpha^2} - \overline{F\alpha}(\alpha_1 + \alpha_2) + \overline{F}\alpha_1 \alpha_2 = 0 \tag{165}$$

and (F = 1)

$$\overline{\alpha^2} - \bar{\alpha}(\alpha_1 + \alpha_2) + \alpha_1 \alpha_2 = 0 \tag{166}$$

Equations (165) and (166) determine $\alpha_1 + \alpha_2$ and $\alpha_1 \alpha_2$

$$\alpha_1 + \alpha_2 = \frac{\overline{F\alpha^2} \cdot \bar{1} - \bar{F}\,\overline{\alpha^2}}{\overline{F\alpha} \cdot \bar{1} - \bar{F} \cdot \bar{\alpha}} \tag{167}$$

and

$$\alpha_1\alpha_2 = \frac{\bar{\alpha}\,\overline{F\alpha^2} - \overline{F\alpha}\,\overline{\alpha^2}}{\overline{F\alpha} \cdot \bar{1} - \bar{F} \cdot \alpha} \tag{168}$$

By using Tchebycheff's inequality, we find

$$\overline{F\alpha} \cdot \bar{1} \geq \bar{F}\,\bar{\alpha} \tag{169}$$

because F is similar to α. Also

$$\overline{F\alpha^2} \cdot \bar{1} \geq \bar{F}\,\overline{\alpha^2} \tag{170}$$

because F is similar to α^2 and renormalizing (169) by α:

$$\overline{F\alpha^2} \cdot \bar{\alpha} \geq \overline{F\alpha} \cdot \overline{\alpha^2} \tag{171}$$

This completes the proof of Eqs. (162) and (163).

To prove that $\alpha_1\alpha_2 < 1$, we need

$$\bar{\alpha}\,\overline{F\alpha^2} - \overline{F\alpha}\,\overline{\alpha^2} \leq \overline{F\alpha} \cdot \bar{1} - \bar{F} \cdot \bar{\alpha} \tag{172}$$

We rewrite (172) as

$$\langle F\,\psi(\alpha)\rangle \geq 0 \tag{173}$$

with ψ given by

$$\psi(\alpha) = \alpha \cdot \bar{1} - \bar{\alpha} + \alpha\overline{\alpha^2} - \alpha^2\,\bar{\alpha} \tag{174}$$

But ψ is similar to α because

$$\psi'(\alpha) = \bar{1} + \overline{\alpha^2} - 2\alpha\,\bar{\alpha} \tag{175}$$

is linear in α and

$$\psi'(0) = \bar{1} + \overline{\alpha^2} > 0 \tag{176}$$

$$\psi'(1) = (1 - \bar{\alpha})^2 + \overline{\alpha'^2} > 0 \tag{177}$$

so that

$$\psi'(\alpha) > 0 \quad \text{for} \quad 0 \leq \alpha \leq 1 \tag{178}$$

We also note that

$$\bar{\psi} = 0 \tag{179}$$

Applying Tchebycheff to (173)

$$\overline{F\psi} \geq \bar{F}\,\bar{\psi} = 0 \qquad \text{q.e.d.} \tag{180}$$

We have completed the proof that α_1 and α_2 are between 0 and 1.

We note that $\alpha_1 + \alpha_2$ and $\alpha_1\alpha_2$ can be expressed either in terms of $\overline{\alpha^3}$ or in terms of $\overline{\rho_\star\alpha}$. This shows that the two-mixed cells distribution realizes either $(\bar{1}, \bar{\alpha}, \overline{\alpha^2}, \overline{\alpha^3})$ or $(\bar{1}, \bar{\alpha}, \overline{\alpha^2}, \overline{\rho_\star\alpha})$.

We now prove that the weights ε_1 and ε_2 of Eq. (159) are between zero and one. By introducing

$$\alpha_1 = \bar{\alpha} - \delta_1 \tag{181}$$

$$\alpha_2 = \bar{\alpha} + \delta_2 \tag{182}$$

we find that

$$\overline{\alpha^r} = 0 \tag{183}$$

$$T = 1 \tag{184}$$

imply

$$\varepsilon_1 = \frac{\delta_2}{\delta_1 + \delta_2} \quad , \quad \varepsilon_2 = \frac{\delta_1}{\delta_1 + \delta_2} \tag{185}$$

A simple calculation further shows that

$$\overline{\alpha'^2} = \delta_1\delta_2 \tag{186}$$

Since $\overline{\alpha'^2}$ is given (and positive), δ_1 and δ_2 have the same sign. It follows then from (185) that $\varepsilon_1 > 0$ and $\varepsilon_2 > 0$. Since their sum is 1, both ε_1 and ε_2 are between zero and one.

Another important family of inequalities is the one pertaining to $\overline{\rho_*^2}$. Clearly, from Cauchy-Schwarz

$$\bar{1} \cdot \overline{\rho_*^2} \geq \overline{\rho_*}^2 \tag{187}$$

This is a lower bound on $\overline{\rho_*^2}$ for given $\overline{\rho_*\alpha}$. The tree of Figure 23 yields the relevant bounds except for the lower bound on $\overline{\rho_*^2}$ for given $\bar{\alpha}$, $\overline{\alpha^2}$, $\overline{\rho_*\alpha}$. We proceed to prove this bound separately.

We choose

$$g = -\rho_{*1}\alpha_2 \tag{188}$$

$$f = \phi + g = \rho_*(\alpha - \alpha_2) - \rho_{*1}\alpha \tag{189}$$

where

$$\phi = (\rho_* - \rho_{*1})(\alpha - \alpha_2) \tag{190}$$

$$\rho_{*1} = \frac{1}{1 - \Delta\alpha_1} \tag{191}$$

Thus, Eq. (190) is the characteristic equation for two mixed cells with one of the singularities expressed in terms of ρ. We use the equation of state relations of Appendix 3 to eliminate products of ρ_* and α (to a power). After some algebra, we find

$$f^2 = \rho_*^2\left(\alpha_2 - \frac{1}{\Delta}\right)^2 + \rho_* \frac{2}{\Delta}(\rho_{*1} + 1)\left(\alpha_2 - \frac{1}{\Delta}\right) + \\ + \alpha^2\rho_{*1}^2 + \frac{2}{\Delta}\alpha\rho_{1*} + \left(\frac{1}{\Delta^2} + \frac{2\rho_{*1}}{\Delta} - \frac{2\rho_{*1}\alpha_2}{\Delta}\right) \tag{192}$$

$$g^2 = (\rho_{*1}\alpha_2)^2 \tag{193}$$

$$fg = -(\rho_{*1}\alpha)\left[\rho_*\left(\frac{1}{\Delta} - \alpha_2\right) - \frac{1}{\Delta} - \rho_{*1}\alpha\right] \tag{194}$$

By using the Cauchy-Schwarz inequality, we find

$$\left[\overline{\rho_*^2}\left(\alpha_2-\frac{1}{\Delta}\right)^2+\overline{\rho_*}\,\frac{2}{\Delta}\,(\rho_{*1}+1)\left(\alpha_2-\frac{1}{\Delta}\right)+\overline{\alpha^2}\rho_{*1}^2+\bar{\alpha}\,\frac{2}{\Delta}\,\rho_{*1}+\left(\frac{1}{\Delta^2}+\frac{2\rho_{*1}}{\Delta^2}-\frac{2\rho_{*1}\alpha_2}{\Delta}\right)\right]\geq$$

$$\geq\left[\overline{\rho_*}\left(\frac{1}{\Delta}-\alpha_2\right)-\bar{\alpha}\rho_{*1}-\frac{1}{\Delta}\right]^2 \qquad (195)$$

The fact that the inequality represents a lower bound on $\overline{\rho_*^2}$ follows from the fact that its coefficient on the large side is positive. The fact that the bound is the greatest lower bound for given $\bar{\alpha}$, $\overline{\alpha^2}$, and $\overline{\rho_*\alpha}$ follows from the realizability of the two-mixed cells distribution which was obtained above, Eqs. (152) through (186).

The last family of inequalities that we consider are bounds on the mass fraction, given the mole fraction. From the tree of Figure 24, several follow.

V. MODEL SELECTION

In this section, we first describe our process for selecting a model probability density. Having chosen a model with a free parameter that is adjusted to minimize the average entropy (density), we compare several features of the model against the data reduced and presented by Konrad.

In selecting the model, we find

1) At the edges of the mixing region, the experimental probability distribution is sufficiently skewed to rule out symmetric models.

2) The experimental probability for finding pure N_2 and pure He is sufficiently large to rule out models that do not have strong spikes at molar fractions close to one or zero.

3) We find that the third moment is rather insensitive to the selection of a model providing the model is statistically correct.

We conclude that the most satisfactory model distribution is one for which the average entropy density is minimized.

With regard to the skewness factor, we consider first a square hat in A (Figure 25). The probability density has three parameters and it is thus fully specified by $\bar{1}$, $\bar{A}$, $\overline{A^2}$. The moment equations are

$$\bar{1} = \int_0^1 P(A)\, dA = H(R - L) \tag{196}$$

$$\bar{A} = \frac{R + L}{2} \tag{197}$$

$$\overline{A^2} = \frac{1}{3}(R^2 + RL + L^2) \tag{198}$$

with solutions for the edge locations

$$R = \bar{A} + \delta_1 \tag{199}$$

$$L = \bar{A} - \delta_1 \tag{200}$$

where

$$\delta_1 = \sqrt{3\,\overline{A'^2}} \tag{201}$$

and finally for the height

$$H = \frac{1}{2\sqrt{3\,\overline{A'^2}}} \tag{202}$$

The fit to Konrad's equal mass flow is shown in Figure 26. Unacceptably large probabilities are found for negative molar fractions. The origin of the difficulty is the large skewness of the edge-flow distributions. The point is illustrated in Figure 27 by a simple triangle distribution that cannot be fitted by a legitimate square hat. The region of moments, $\bar{A}$, $\overline{A'^2}$, for which a square hat is statistically acceptable is readily obtained from $R < 1$ and $L > 0$. This region is shown in Figure 28, together with the region allowed by the less restrictive but still symmetric model

$$\overline{A'^3} = 0 \tag{203}$$

The various boundary curves are given by the following functions of $\bar{A}$:

$$\begin{aligned} 1 &: \quad \bar{A}^2/3 \\ 2 &: \quad \bar{B}^2/3 \\ 3 &: \quad 2\bar{A}^2 \\ 4 &: \quad 2\bar{B}^2 \\ 5 &: \quad \bar{A}(1 - \bar{A}) = \bar{A}\bar{B} \end{aligned} \tag{204}$$

In Figure 29, we show the value of the ratio

$$\Gamma = \frac{Q_{\text{model}}}{Q_{\text{experiment}}} \tag{205}$$

where

$$Q = \overline{AB^2} \tag{206}$$

The value of Q_U corresponds to the upper bound for Q given $\bar{A}$ and $\overline{A'^2}$; similarly Q_L corresponds to the lower bound for Q, given $\bar{A}$ and $\overline{A^2}$. The graph emphasizes the fact that towards the edges of the mixing region any symmetric model would be in disagreement with experiment.

A model with much less symmetry and some promise of describing a flow with low mixing is defined by

$$0 = (AB)' = \bar{A}B' + A'\bar{B} + A'B' - \overline{A'B'} \tag{207}$$

Equation (207) is a quadratic for A' once B' is eliminated ($B' = -A'$) and the resulting probability density is given by

$$P(A) = \varepsilon_1 \delta(A - A_1) + \varepsilon_2 \delta(A - A_2) \tag{208}$$

where

$$A_1 = \frac{1 - D}{2} \quad , \quad A_2 = \frac{1 + D}{2} \tag{209}$$

$$\varepsilon_1 = \frac{1}{D}\left(\frac{1 + D}{2} - \bar{A}\right) \tag{210}$$

$$\varepsilon_2 = \frac{1}{D}\left(\bar{A} - \frac{1 - D}{2}\right) \tag{211}$$

and

$$D = \sqrt{1 - 4\overline{AB}} \tag{212}$$

We note that for this model

$$A_2 = B_1 \ , \quad A_1 = B_2 \tag{213}$$

Furthermore, Eq. (207) is exactly equivalent to the requirement

$$\overline{A^2 B^2} = \min \text{ (for fixed } \bar{A}, \overline{A^2}\text{)} \tag{214}$$

In Figure 30, the values of ε_1 and of ε_2 are superimposed on Konrad probability densities and are seen to follow the patterns reasonably well. The model is not acceptable in view of the experimental values for pure He (Fig. 31) and pure N_2 (Fig. 32). The model given by (208) yields zero values for both probabilities.

In view of the experimental probabilities for pure species, the model given by P_3 in Figure 33 offers a chance with both pure cells built in. Comparison with the probability density is shown in Figure 32 and is tolerable. Comparison with the pure species data, Figures 31 and 32, shows however that the weights of the pure cells are too weak.

Since the entropy of mixing is clearly quite low in the flow, the model of Figure 7 was made determinate by minimizing the entropy (density) of mixing with respect to A_3 . The resulting model is defined as follows. The weights are those given by Eq. (30) and the bounds on A_3 are those of Eq. (31). For this model, the quantity

$$\eta = \frac{\left\langle (S\ M_\alpha)/\mathcal{R} \right\rangle}{\bar{A} - \overline{A^2}} \tag{215}$$

is sketched in Figure 34. The quantity η is even in A_3 with a minimum

of approximately 2.76 at $A_3 = 0.5$. A_3 is therefore determined as follows. We call the bounds of A_3 L and U . Then

$$L = \frac{\bar{A} - \overline{A^2}}{1 - \bar{A}} \tag{216}$$

$$U = \frac{\overline{A^2}}{\bar{A}} \tag{217}$$

Minimization occurs as follows:

$$\text{If } U < \frac{1}{2} \text{ , then } A_3 = U \tag{218}$$

$$\text{If } L < \frac{1}{2} < U \text{ , then } A_3 = \frac{1}{2} \tag{219}$$

$$\text{If } \frac{1}{2} < L \text{ , then } A_3 = L \tag{220}$$

The resulting weights are plotted in Figure 35 and show a good pattern relative to the probability densities; furthermore, the pure species plots of Figures 31 and 32 are in reasonable agreement with experiment. The fact that the model distribution is somewhat He rich is in qualitative agreement with the low mixing allowed by large-scale transport and with the data on pure species.

By way of contrast on this point, in Figure 36 we show the entropy maximized for the same cell structure. It is in poor agreement with the pure species probabilities.

In Figure 37, we give the Γ ratio of Eq. (205) for the minimum entropy model. Although the agreement with experiment on this point is low (~50%), the opposite extreme of maximal entropy is roughly as good on this count. Statistical consistency seems to be all that is needed to obtain a reasonable Γ . This point will be taken up again later in connection with the flows with large mass differences.

In Figures 38, 39 and 40 we give the average entropy density, its fluctuations and its second moment to give an idea of the actual flow values and their model values.

We now turn to the discussion of the model chosen for large mass differences. In this case we have at our disposal both the mass fraction and the density moments (equivalently the mass and the molar fractions). We have thus chosen a four-cell distribution with one free parameter,

Figure 41. We give $T = 1$, $\bar{\alpha}$, $\overline{\alpha^2}$, $\overline{\rho_*\alpha}$ and $\overline{\rho_*^2}$. We note that for given $\bar{\alpha}$, $\overline{\alpha^2}$ and $\overline{\rho_*\alpha}$, $\overline{\rho_{*\min}^2}$ requires two mixed cells (a discrete distribution) and similarly, $\overline{\rho_{*\max}^2}$ requires two pure and one mixed cell (again a discrete distribution). The algebraic solution of the moment equations can be summarized as follows. The weights are given in terms of parameters C_i and u_i^* as follows:

$$\varepsilon_1 = C_1 \frac{u - u_1^*}{1 - u} \tag{221}$$

$$\varepsilon_2 = C_2 \frac{u_2^* - u}{u} \tag{222}$$

$$\varepsilon_3 = C_3 \frac{u_3^* - u}{u - \alpha_3} \tag{223}$$

$$\varepsilon_4 = C_4 \frac{u_4^* - u}{u(1 - u)(u - \alpha_3)} \tag{224}$$

The singularities of the denominators correspond to one of the mixed cells degenerating with a pure one or the second mixed cell.

The parameters C_i and u_i^* are in turn given by

$$C_1 = \frac{1 - \Delta}{\Delta} \frac{\bar{\alpha} - \overline{\rho_*\alpha}\,(1 - \Delta\alpha_3)}{1 - \alpha_3} \tag{225}$$

$$C_2 = \frac{\bar{\alpha} - 1 - \left[1 - \overline{\rho_*\alpha}\,(1 - \Delta)\right](1 - \Delta\alpha_3)}{\Delta\alpha_3} \tag{226}$$

$$C_3 = \frac{(1 - \Delta\alpha_3)\left[\overline{\rho_*\alpha}\,(1 - \Delta) - \bar{\alpha}\right]}{\Delta\alpha_3(1 - \alpha_3)} \tag{227}$$

$$C_4 = \bar{\alpha}\left(\frac{1}{\Delta} - 1 - \alpha_3\right) - \frac{1 - \Delta}{\Delta}(1 - \Delta\alpha_3)\,\overline{\rho_*\alpha} + \overline{\alpha^2} \tag{228}$$

and

$$u_1^* = \frac{\overline{\alpha^2} - \frac{1 - \Delta\alpha_3}{\Delta}(\overline{\rho_*\alpha} - \bar{\alpha})}{\bar{\alpha} - (1 - \Delta\alpha_3)\,\overline{\rho_*\alpha}} \tag{229}$$

$$u_2^* = \frac{2\bar{\alpha} - 1 - \overline{\alpha^2} - \frac{1 - \Delta\alpha_3}{\Delta}\left[\bar{\alpha} - \overline{\rho_*\alpha}\,(1 - \Delta)\right]}{1 - \bar{\alpha} - (1 - \Delta\alpha_3)(1 - \overline{\rho_*\alpha}\,[1 - \Delta])} \tag{230}$$

$$u_3^* = \frac{\overline{\alpha^2} - \frac{1 - \Delta}{\Delta}\,(\overline{\rho_*\alpha} - \bar{\alpha})}{\bar{\alpha} - (1 - \Delta)\,\overline{\rho_*\alpha}} \tag{231}$$

$$u_4^* = \frac{1}{\Delta} \tag{232}$$

The concentrations are related by the following formula which is derived using two s cells and two α cells in the characteristic equation

$$u = \frac{\left\langle \alpha^2\left(\rho_*^2 - \rho_*\left[1 + \frac{1}{1-\Delta}\right] + \frac{1}{1-\Delta}\right)\right\rangle - \alpha_3\left\langle \alpha\left(\rho_*^2 - \rho_*\left[1 + \frac{1}{1-\Delta}\right] + \frac{1}{1-\Delta}\right)\right\rangle}{\left\langle \alpha\left(\rho_*^2 - \rho_*\left[1 + \frac{1}{1-\Delta}\right] + \frac{1}{1-\Delta}\right)\right\rangle - \alpha_3\left\langle \rho_*^2 - \rho_*\left[1 + \frac{1}{1-\Delta}\right] + \frac{1}{1-\Delta}\right\rangle} \tag{233}$$

The minimim of the mean entropy occurs when $\varepsilon_1 = 0$ leaving a "helium rich" model. If we set

$$u = u_1^* \tag{234}$$

using Eqs. (233) and (229), we obtain a quadratic equation for α_3. Its two roots correspond to the presence of two mixed cells and the interchangeability of cell 3 with cell 4. The model is thus fully determinate.

We now compare the model with the two flows of $\Delta \neq 0$ given by Konrad. We give

1) the ratio Γ of Eq. (205) (Figs. 42 and 43),
2) the probabilities of pure species (Figs. 44 and 45),
3) the locations and strengths of the Dirac functions superimposed on the Konrad densities (Figs. 46 and 47).

On all three grounds, the chosen model fares quite well. By contrast, we show in Figure 48 a maximal entropy model. As was the case for $\Delta = 0$, the resulting model is substantially worse than the minimum entropy model.

As a final indication of the stringency of our statistical bounds, we give in Figures 49 and 48 the bounds on the (mass fraction) moment ratio

with $Q = \overline{\alpha\beta^2}$. The bounds are of the same order of magnitude as those given in the molar plots. The successive tightening of the bounds, given 2, 3 and 4 moments, is clearly indicated. The bounds on $\overline{\alpha^3}$ that were used in the plot were not fully included in the theoretical discussion. They are recorded below for completeness.

$$L \leq \overline{\alpha^3} \leq U \tag{235}$$

For given $\bar{\alpha}$, $\overline{\alpha^2}$, $\overline{\rho_*\alpha}$

$$L = \overline{\alpha^2} - \frac{(\bar{\alpha} - \overline{\alpha^2}) \left[\frac{\bar{\alpha}}{\Delta} - \overline{\rho_*\alpha} \frac{1 - \Delta}{\Delta} - \bar{\alpha} + \overline{\alpha^2} \right]}{\bar{\alpha} - \overline{\rho_*\alpha} (1 - \Delta)} \tag{237}$$

$$U = \frac{\overline{\rho_*\alpha} \left[\overline{\alpha^2}(1 - \Delta^2 \overline{\alpha^2} - \bar{\alpha}(\bar{\alpha} - \Delta\overline{\alpha^2}) \right] - \bar{\alpha}\,\overline{\alpha^2} - \Delta\overline{\alpha^2}^2 + \bar{\alpha}^3}{\Delta[\,\overline{\rho_*\alpha}\,(1 - \Delta\bar{\alpha}) - \bar{\alpha}\,]} \tag{237}$$

APPENDIX 1. CONVEXITY OF MOMENT DOMAINS

Proof. Let $\vec{m}_1 , \vec{m}_2 \in M_n$ be given.

For $\lambda \in (0,1)$ we show that

$$\vec{m} \equiv \lambda\vec{m}_1 + (1 - \lambda)\vec{m}_2 \in M_n \tag{1.1}$$

Write $\vec{m}_1$ and $\vec{m}_2$ as

$$\vec{m}_1 = (c_0 , c_1 , \ldots , c_{n-1}) \tag{1.2}$$

$$\vec{m}_2 = (d_0 , d_1 , \ldots , d_{n-1}) \tag{1.3}$$

Then by computation (i.e., substitute (1.2) and (1.3) into (1.1))

$$\vec{m} = \lambda c_0 + (1 - \lambda)d_0 , \lambda c_1 + (1 - \lambda)d_1 , \ldots , \lambda c_{n-1} + (1 - \lambda)d_{n-1}$$

Since $\vec{m}_1 \in M_n$, there is a non-negative measure, P_1 , whose moments are the components of $\vec{m}_1$:

$$\vec{m}_1 = (c_0 , c_1 ,\ldots,c_{n-1}) = ({}^1\bar{1} , {}^1\bar{\alpha} ,\ldots,{}^1\overline{\alpha^{n-1}})$$

where

$${}^1\overline{\alpha^n} = \int_0^1 \alpha^n P_1(\alpha)\, d\alpha$$

Similarly there is a $P_2(\alpha)$ such that

$$\vec{m}_2 = (d_0 , d_1 ,\ldots,d_{n-1}) = ({}^2\bar{1} , {}^2\bar{\alpha} ,\ldots {}^2\overline{\alpha^{n-1}})$$

Consider a new non-negative measure:

$$P = \lambda P_1 + (1 - \lambda)P_2$$

Then,

$$(\bar{1},\ \bar{\alpha},\ \ldots,\ \overline{\alpha^{n-1}}) =$$

$$= \left(\lambda^{1}\bar{1} + (1-\lambda)^{2}\bar{1}\ ,\ \lambda^{1}\bar{\alpha} + (1-\lambda)^{2}\bar{\alpha}\ ,\ \ldots,\ \lambda^{1}\overline{\alpha^{n-1}} + (1-\lambda)^{2}\overline{\alpha^{n-1}}\right)$$

$$= \left(\lambda c_0 + (1-\lambda)d_0\ ,\ \lambda c_1 + (1-\lambda)d_1\ ,\ \ldots,\ \lambda c_{n-1} + (1-\lambda)d_{n-1}\right) = \vec{m}$$

Therefore, the point $\vec{m}$ is realized precisely by the measure P; that is, $\vec{m} \in M_n$.

APPENDIX 2. STANDARD PDF's ($s \equiv \rho_*$ of Eq. (75))

1. $\bar{1} = 1$ given, $\bar{\alpha} = 1$

$$\overline{\alpha^2} = 1 \ , \quad \bar{s} = \frac{1}{1 - \Delta} \ , \quad \overline{s\alpha} = \frac{1}{1 - \Delta} \ , \quad \overline{s^2} = \frac{1}{(1 - \Delta)^2}$$

2. $\bar{1} = 1$ given, $\bar{\alpha} = 0$

$$\overline{\alpha^2} = 0 \ , \quad \bar{s} = 1 \ , \quad \overline{s\alpha} = 0 \ , \quad \overline{s^2} = 1$$

3. $\bar{\alpha}$ given, $\overline{\alpha^2} = \bar{\alpha}$

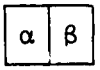

$$\bar{s} = \bar{\alpha} \frac{\Delta}{1 - \Delta} + 1$$

$$\overline{s\alpha} = \frac{\bar{\alpha}}{1 - \Delta}$$

$$\overline{s^2} = \frac{\bar{\alpha}}{(1 - \Delta)^2} + 1 - \bar{\alpha} = 1 + \bar{\alpha} \frac{\Delta(2 - \Delta)}{(1 - \Delta)^2}$$

4. $\bar{\alpha}$ given, $\overline{\alpha^2} = \bar{\alpha}^2$

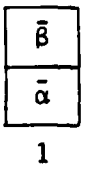

$$\bar{s} = \frac{1}{1 - \Delta\bar{\alpha}}$$

$$\overline{s\alpha} = \frac{\bar{\alpha}}{1 - \Delta\bar{\alpha}}$$

$$\overline{s^2} = \frac{1}{(1 - \Delta\bar{\alpha})^2}$$

5. $\bar{\alpha}$, $\overline{\alpha^2}$ given, $\overline{s\alpha} = \dfrac{\bar{\alpha}^2}{\bar{\alpha} - \Delta\overline{\alpha^2}} = \min$

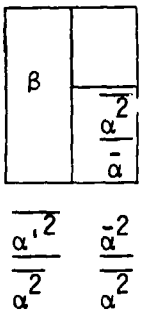

$$\bar{s} = 1 + \Delta\overline{s\alpha}$$

$$\overline{s^2} = \frac{\overline{\alpha^2} - \bar{\alpha}^2}{\overline{\alpha^2}} + \frac{\bar{\alpha}^4}{\overline{\alpha^2}\left[\bar{\alpha} - \Delta\overline{\alpha^2}\right]^2}$$

6. $\bar{\alpha}$, $\overline{\alpha^2}$ given , Auxiliary $\bar{\beta} = 1 - \bar{\alpha}$

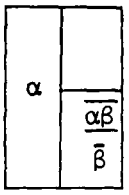

$$\overline{\beta^2} = 1 - 2\bar{\alpha} + \overline{\alpha^2}$$

$$\overline{\alpha\beta} = \bar{\alpha} - \overline{\alpha^2}$$

$$\overline{s\alpha} = \frac{\bar{\alpha}\bar{\beta} - \Delta(\bar{\alpha} - \overline{\alpha^2})}{(1 - \Delta)\left(1 - \bar{\alpha} - \Delta\left[\bar{\alpha} - \overline{\alpha^2}\right]\right)} = \max$$

$$\bar{s} = 1 + \Delta\overline{s\alpha}$$

$$\overline{s^2} = \frac{\overline{\beta^2} - \bar{\beta}^2}{\overline{\beta^2}}\left(\frac{1}{1 - \Delta}\right)^2 + \frac{\bar{\beta}^2}{\overline{\beta^2}}\frac{1}{\left[1 - \Delta\dfrac{\overline{\alpha\beta}}{\bar{\beta}}\right]^2}$$

7. $\bar{\alpha}$, $\overline{\alpha^2}$, $\overline{s\alpha}$ given, $\overline{s^2}$ is maximal

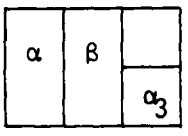

(a) $$\alpha_3 = \frac{\overline{\alpha^2} - \dfrac{1 - \Delta}{\Delta}\,\overline{s\alpha} - \bar{\alpha}}{\bar{\alpha} - (1 - \Delta)\overline{s\alpha}}$$

(b) $$\varepsilon_1 = \frac{\overline{\alpha^2} - \bar{\alpha}\alpha_3}{1 - \alpha_3}\,,\quad \varepsilon_2 = 1 - \bar{\alpha} - \frac{\bar{\alpha} - \overline{\alpha^2}}{\alpha_3}\,,\quad \varepsilon_3 = \frac{\bar{\alpha} - \overline{\alpha^2}}{\alpha_3(1 - \alpha_3)}$$

(c) $$\bar{s} = 1 + \Delta\overline{s\alpha}$$

(d) $$\overline{s^2} = \sum_{i=1}^{3} \frac{\varepsilon_i}{(1 - \Delta\alpha_i)^2}$$

8. $\bar{\alpha}$, $\overline{\alpha^2}$, $\overline{s\alpha}$ given, $\overline{s^2}$ is minimal

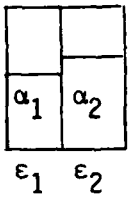

(a) $\bar{s} = 1 + \Delta\overline{s\alpha}$

(b) $x\ (= \delta_1 - \delta_2) = \dfrac{(1 - \Delta\bar{\alpha})\left[\bar{s}(1 - \Delta\bar{\alpha}) - 1\right] - \bar{s}(\overline{\alpha^2} - \bar{\alpha}^2)\Delta^2}{\Delta\left[\bar{s}(1 - \Delta\bar{\alpha}) - 1\right]}$

$$y^2\left(= \delta_1 + \delta_2)^2\right) = \left[\frac{1 - \Delta\bar{\alpha}}{\Delta} - \frac{\bar{s}(\overline{\alpha^2} - \bar{\alpha}^2)\Delta}{\bar{s}(1 - \Delta\bar{\alpha}) - 1}\right]^2 + 4(\overline{\alpha^2} - \bar{\alpha}^2)$$

(take pos ✓)

(c) $\delta_1 = \dfrac{x + y}{2}$, $\delta_2 = \dfrac{y - x}{2}$ $\qquad (\delta_1 , \delta_2 > 0)$

(d) $\varepsilon_1 = \dfrac{\delta_2}{\delta_1 + \delta_2}$, $\varepsilon_2 = \dfrac{\delta_1}{\delta_1 + \delta_2}$

$\alpha_1 = \bar{\alpha} + \delta_1$, $\alpha_2 = \bar{\alpha} - \delta_2$

(e) $\overline{s^2} = \dfrac{\varepsilon_1}{(1 - \Delta\alpha_1)^2} + \dfrac{\varepsilon_2}{(1 - \Delta\alpha_2)^2}$

APPENDIX 3. RELATIONS IMPLIED BY THE EQUATION OF STATE (REDUCTION FORMULAE)

The following relations are given as instantaneous; they also hold as averages.

1. $$\rho_* - \Delta\rho_*\alpha = 1$$

2. $$\rho_*\alpha^2 = \frac{1}{\Delta}\rho_*\alpha - \frac{1}{\Delta}\alpha = \frac{1}{\Delta^2}\rho_* - \frac{1}{\Delta}\alpha - \frac{1}{\Delta^2}$$

3. $$\rho_*\alpha^3 = \frac{1}{\Delta^2}\rho_*\alpha - \frac{1}{\Delta^2}\alpha - \frac{1}{\Delta}\alpha^2 = \frac{\rho_*}{\Delta^3} - \frac{\alpha}{\Delta^2} - \frac{\alpha^2}{\Delta} - \frac{1}{\Delta^3}$$

4. $$\rho_*\alpha^4 = \frac{1}{\Delta^3}\rho_*\alpha - \frac{\alpha}{\Delta^3} - \frac{1}{\Delta^2}\alpha^2 - \frac{1}{\Delta}\alpha^3$$

$$= \frac{1}{\Delta^4}\rho_* - \frac{1}{\Delta^3}\alpha - \frac{1}{\Delta^2}\alpha^2 - \frac{1}{\Delta}\alpha^3 - \frac{1}{\Delta^4}$$

5. $$\rho_*^2\alpha = \frac{1}{\Delta}\rho_*^2 - \frac{1}{\Delta}\rho_*$$

$$\rho_*^2\alpha^2 = \frac{1}{\Delta^2}(\rho_* - 1)^2$$

$$\rho_*^2\alpha^3 = \frac{1}{\Delta^3}(\rho_* - 1)^2 - \frac{1}{\Delta^2}(\rho_* - 1) + \frac{1}{\Delta^2}\alpha$$

$$\rho_*^2\alpha^4 = \frac{1}{\Delta^4}(\rho_* - 1)^2 - \frac{2}{\Delta^4}(\rho_* - 1) + \frac{2}{\Delta^3}\alpha + \frac{\alpha^2}{\Delta^2}$$

APPENDIX 4. APPLICATION OF INSTANTANEOUS BOUNDS TO ENSURE CORRECT STATISTICS FOR SOLUTIONS OF THE RATE EQUATIONS

We consider a simple example of second-order chemistry in which only two species participate (although the reaction collision requires three bodies as dictated by energy and momentum balance). The reaction chosen is

$$O + O_2 \rightarrow 3O \tag{4.1}$$

which idealizes the result of embedding a trace of molecular oxygen in a bath of hot atomic oxygen (the dominant reaction is dissociation).

The rate equations are

$$\frac{dn_{O2}}{dt} = -K_f\, n_O\, n_{O2} \tag{4.2}$$

$$\frac{dn_O}{dt} = +2K_f\, n_O\, n_{O2} \tag{4.3}$$

which have the conservation law

$$n_O + 2n_{O2} = c = \text{const.} > 0 \tag{4.4}$$

corresponding to the conservation of the total number of oxygen atoms, free and bound in pairs. Equation (4.3) can be rewritten as

$$\frac{dn_O}{dt} = 2K_f n_O n_{O2} = K_f n_O (c - n_O) \tag{4.5}$$

Introduce the number fractions

$$B = \frac{n_O}{c} \quad , \quad A = \frac{2n_{O2}}{c} \tag{4.6}$$

Then, (4.4) implies

$$A + B = 1 \tag{4.7}$$

and, since A and B are positive,

$$0 \leq A \leq 1 \ , \ 0 \leq B \leq 1 \tag{4.8}$$

We rescale for simplicity the time by $K_f c$ and obtain from (4.5)

$$\frac{dA}{dt} = -AB = -A + A^2 \tag{4.9}$$

The last equality follows from (4.7). From (4.9) we find the equivalent pairs:

$$\dot{\bar{A}} = -\bar{A} + \overline{A^2} \tag{4.10a}$$

$$\dot{\overline{A^2}} = -2\overline{A^2} + 2\overline{A^3} \tag{4.10b}$$

and

$$\dot{\bar{B}} = +\bar{B} - \overline{B^2} \tag{4.11a}$$

$$\dot{\overline{B^2}} = 2\overline{B^2} - 2\overline{B^3} \tag{4.11b}$$

First-order closure consists in using (4.10a) together with a model

$$\overline{A^2} = F(\bar{A}) \tag{4.12}$$

We apply the bounds on $\overline{A^2}$ derived in the text (Section II)

$$\bar{A}^2 \leq \overline{A^2} \leq \bar{A} \tag{4.13}$$

and prove the following.

(I) Given $\bar{A}(0)$, the solution of any model

$$\dot{\bar{A}} = -\bar{A} + F(\bar{A}) \tag{4.14}$$

where F satisfies the bounds of Eq. (4.13), is bounded above by the solution of

$$\dot{\bar{A}} = -\bar{A} + \bar{A} = 0 \tag{4.15}$$

and bounded below by the solution of

$$\dot{\bar{A}} = -\bar{A} + \bar{A}^2 \tag{4.16}$$

(II) Equation (4.15) gives the exact solution of (4.9) with the initial probability density

$$P(A_o) = (1 - \bar{A}_o)\delta(A_o) + \bar{A}_o\delta(A_o - 1) \tag{4.17}$$

and Eq. (4.16) gives the exact solution of (4.9) with initial density

$$P(A_o) = \delta(A_o - \bar{A}_o) \tag{4.18}$$

Subscript is used to denote the time at which the variable is considered.

(III) There exists a nonextremal choice of F which does not yield the exact solution of (4.9) for the corresponding density. The exact solution of (4.9) is

$$A_t = \frac{A_o\, e^{-t}}{1 - A_o + A_o\, e^{-t}} = \phi^{-1}(A_o) \tag{4.19}$$

The initial value of A, A_o is conveniently expressed in terms of the value of A at t by inverting (4.19)

$$A_o = \frac{A_t\, e^{+t}}{1 - A_t + A_t\, e^{+t}} = \phi(A_t) \tag{4.20}$$

which can also be obtained by time reversal of (4.9).

We now consider the above points successively. We write the general solution of (4.14) as

$$\bar{A}_t = e^{-t}\,\bar{A}_o + \int_0^t e^{-(t-\lambda)}\,\overline{A^2}(\lambda)\,d\lambda \tag{4.21}$$

where $\overline{A^2}$ is understood to be a function of $\bar{A}$. Since

$$e^{-(t-\lambda)} > 0 \quad \text{for all } \lambda \tag{4.22}$$

we have from (4.13U)

$$\int_0^t e^{-(t-\lambda)}\left[\overline{A^2}(\lambda) - \bar{A}(\lambda)\right] d\lambda \leq 0 \tag{4.23}$$

and from (4.13L)

$$\int_0^t e^{-(t-\lambda)}\left[\overline{A^2}(\lambda) - \bar{A}^2(\lambda)\right] d\lambda \geq 0 \tag{4.24}$$

Hence,

$$\int_0^t e^{-(t-\lambda)}\bar{A}^2(\lambda)\,d\lambda \leq \int_0^t e^{-(t-\lambda)}\overline{A^2}(\lambda)\,d\lambda \leq \int_0^t e^{-(t-\lambda)}\bar{A}(\lambda)\,d\lambda \qquad (4.25)$$

If we add $e^{-t}\bar{A}_o$ to each term of the double inequality, we find

$$e^{-t}\bar{A}_o + \int_0^t e^{-(t-\lambda)}\bar{A}^2(\lambda)\,d\lambda \leq$$

$$\leq e^{-t}\bar{A}_o + \int_0^t e^{-(t-\lambda)}\overline{A^2}(\lambda)\,d\lambda \leq$$

$$\leq e^{-t}\bar{A}_o + \int_0^t e^{-(t-\lambda)}\bar{A}(\lambda)\,d\lambda \qquad (4.26)$$

which proves our first proposition; i.e., the solutions of the extreme models are the bounds of the solution of any (statistically allowed) model. Furthermore, the exact solution (4.19) when averaged with (4.17) gives

$$\bar{A}_t = \bar{A}_o \qquad (4.27)$$

which is indeed the solution of (4.15). Also, (4.19) when averaged with (4.18) gives

$$\bar{A}_t = \frac{\bar{A}_o\, e^{-t}}{1 - \bar{A}_o + \bar{A}_o\, e^{-t}} \qquad (4.28)$$

which can be readily verified to be the solution of (4.16). We have thus proven our proposition II and thus demonstrated that the extreme models represent exact solutions. Therefore, combining I and II, we conclude that any statistically correct choice for the model $F(\bar{A})$ will remain statistically correct.

A simple example of III is the following. Model $F(\bar{A})$ by the mean

$$\overline{A^2} \overset{\text{Mod}}{=} \frac{1}{2}\bar{A}^2 + \frac{1}{2}\bar{A} \qquad (4.29)$$

A corresponding density is

$$P(A_o) = \frac{1}{2}\,\delta(A_o - \bar{A}_o) + \frac{1}{2}\left[(1 - \bar{A}_o)\,\delta(A_o) + \bar{A}_o\,\delta(A_o - 1)\right] \tag{4.30}$$

A short calculation shows that the solution of the model equation

$$\dot{\bar{A}} = -\bar{A} + \left[\frac{1}{2}\,\bar{A}^2 + \frac{1}{2}\,\bar{A}\right] \tag{4.31}$$

is

$$\bar{A}_t = \frac{\bar{A}_o\, e^{-t/2}}{1 - \bar{A}_o + \bar{A}_o\, e^{-t/2}} \tag{4.32}$$

while the average of (4.19) with $P(A_o)$ given by (4.30) is

$$\bar{A}_t = \int_0^1 \frac{A_o\, e^{-t}}{1 - A_o + A_o\, e^{-t}}\; P(A_o)\, dA_o = \frac{\bar{A}_o}{2}\left[1 + \frac{e^{-t}}{1 - \bar{A}_o + \bar{A}_o\, e^{-t}}\right] \tag{4.33}$$

which does not coincide with (4.32) although (4.32) is properly bounded as discussed above.

The bounds obtained on $\bar{A}_t$ *from* first-order closure (i.e., given $\bar{A}_o$ only) are loose bounds. We can, however, proceed to second-order closure and tighten them by giving $\bar{A}_o$ and $\overline{A_o^2}$. The statistical bounds on $\overline{A^3}$ (from Section II) are

$$\frac{\overline{A^2}^2}{\bar{A}} \le \overline{A^3} \le \overline{A^2} - \frac{(\bar{A} - \overline{A^2})^2}{1 - \bar{A}} \tag{4.34}$$

The equations for $\dot{\bar{A}}$ and $\dot{\overline{A^2}}$ are given in (4.10a) and (4.10b). Second-order closure corresponds to choosing a model for $\overline{A^3}$

$$\overline{A^3} = G(\bar{A}, \overline{A^2}) \tag{4.35}$$

which we assume subject to the bounds (4.34). We choose G to correspond to the lower and upper bounds in (4.34). For the lower bound, we find that the quantity

$$K_L = \frac{\bar{A}^2}{\overline{A^2}} \tag{4.36}$$

is a constant of the motion. Integration then yields ($\bar{A}_o$ and $\overline{A_o^2}$ given)

$$\bar{A}_t = \frac{\bar{A}_o^2 \, e^{-t}}{\bar{A}_o - \overline{A_o^2} + \overline{A_o^2} \, e^{-t}} \tag{4.37}$$

The density corresponding to (4.34L) is (from Section II)

$$P(A_o) = \frac{\overline{A'^2_o}}{\bar{A}_o^2} \delta(A_o) + \frac{\bar{A}_o^2}{\overline{A_o^2}} \delta\left(A_o - \frac{\overline{A_o^2}}{\bar{A}_o}\right) \tag{4.38}$$

A simple calculation shows that the exact (4.19) averaged with (4.38) gives (4.37).

The upper bound is treated conveniently in terms of 4.11a) and (4.11b). In this case, the constant of the motion is

$$K_U = \frac{\bar{B}^2}{\overline{B^2}} = \frac{1 - 2\bar{A} + \bar{A}^2}{1 - 2\bar{A} + \overline{A^2}} \tag{4.39}$$

The corresponding density is

$$P(A_o) = \frac{\overline{B'^2_o}}{\overline{B_o^2}} \delta(A_0 - 1) + \frac{\bar{B}_o^2}{\overline{B_o^2}} \delta\left(A_o - \frac{\overline{AB}_o}{\bar{B}_o}\right) \tag{4.40}$$

and the model solution coincides with the average of (4.19) over (4.40) as

$$\bar{B}_t = \frac{\bar{B}_o^2 \, e^{+t}}{\bar{B}_o - \overline{B_o^2} + \overline{B_o^2} \, e^{+t}} \tag{4.41}$$

which can be written as

$$\bar{A}_t = \frac{\overline{A_o^2} - \bar{A}_o^2 + (\bar{A}_o - \overline{A_o^2}) \, e^{-t}}{1 - 2\bar{A}_o + \overline{A_o^2} + (\bar{A}_o - \overline{A_o^2}) \, e^{-t}} \tag{4.42}$$

The bounds given by (4.37) and (4.42) are substantially more stringent than those given by first-order closure.

As an example of nonextremal choice of second-order closure, we consider

$$\overline{A^3} = (1 + \bar{A})(\overline{A^2} - \bar{A}^2) + \bar{A}^3 \tag{4.43}$$

corresponding to the density (frozen $\bar{A}$ model of Section II)

$$P(A_o) = \frac{\overline{A'^2_o}}{\bar{B}_o}\,\delta(A_o - 1) + \frac{\overline{A'^2_o}}{\bar{A}_o}\,\delta(A_o) + \left[1 - \frac{\overline{A'^2_o}}{\bar{A}_o\bar{B}_o}\right]\delta(A_o - \bar{A}_o) \tag{4.44}$$

The solution of the model equation is obtained by exploiting the integral resulting from

$$\frac{\overline{d\alpha^2}}{d\bar{\alpha}} = 2\bar{\alpha} \tag{4.45}$$

and is

$$\bar{A}_t = \frac{1}{2} - \sqrt{\frac{1}{4} - \overline{A_o^2} + \bar{A}_o^2}\ \times$$

$$\times\ \frac{\bar{A}_o - \frac{1}{2} - \sqrt{\frac{1}{4} - \overline{A_o^2} + \bar{A}_o^2} + e^{-2t}\left(\bar{A}_o - \frac{1}{2} + \sqrt{\frac{1}{4} - \overline{A_o^2} + \bar{A}_o^2}\right)}{\bar{A}_o - \frac{1}{2} - \sqrt{\frac{1}{4} - \overline{A_o^2} + \bar{A}_o^2} - e^{-2t}\left(\bar{A}_o - \frac{1}{2} + \sqrt{\frac{1}{4} - \overline{A_o^2} + \bar{A}_o^2}\right)} \tag{4.46}$$

while the exact solution (4.19) averaged over (4.44) yields

$$\bar{A}_t = \frac{\overline{A'^2_o}}{\bar{B}_o} + \left(1 - \frac{\overline{A'^2_o}}{\bar{A}_o\bar{B}_o}\right)\frac{\bar{A}_o\, e^{-t}}{1 - \bar{A}_o + \bar{A}_o\, e^{-t}} \tag{4.47}$$

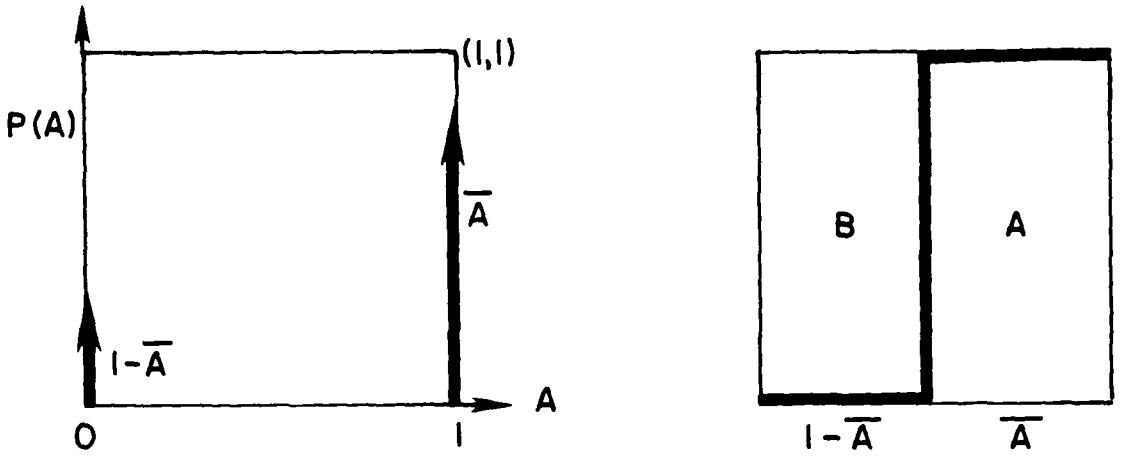

Figure 1. Example of P(A) and of its box diagram

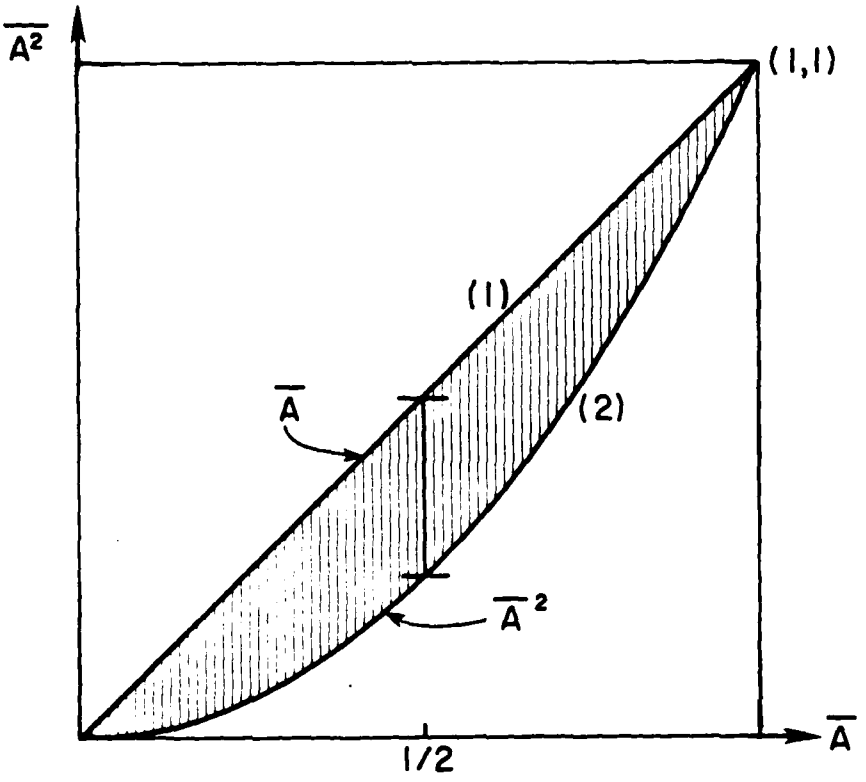

Figure 2. Statistically allowed values of the first two total moments

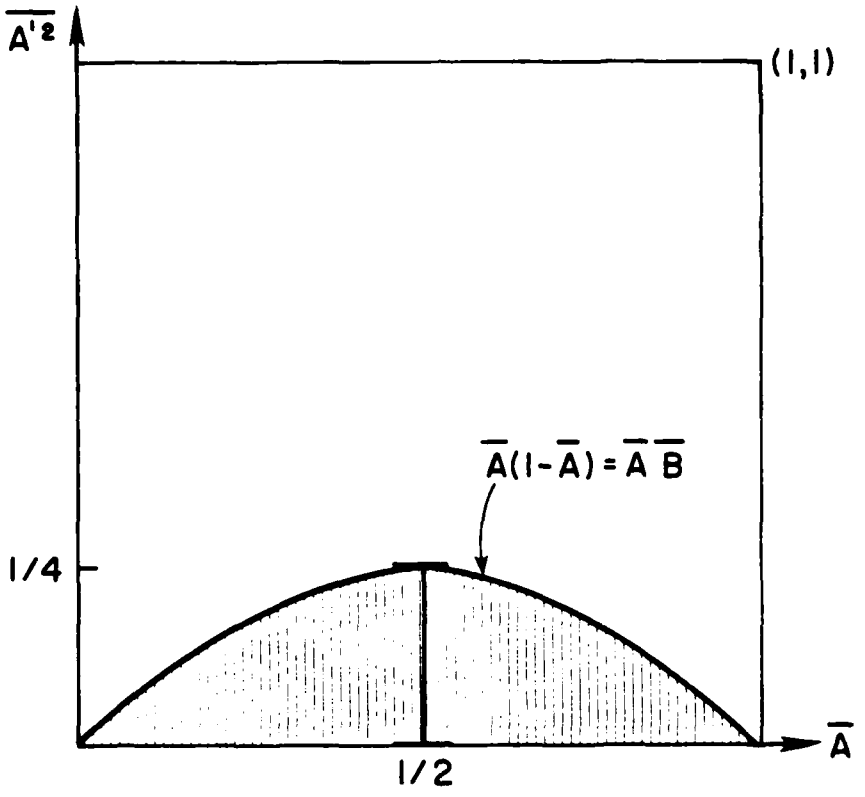

Figure 3. Statistically allowed values of the first two centered moments

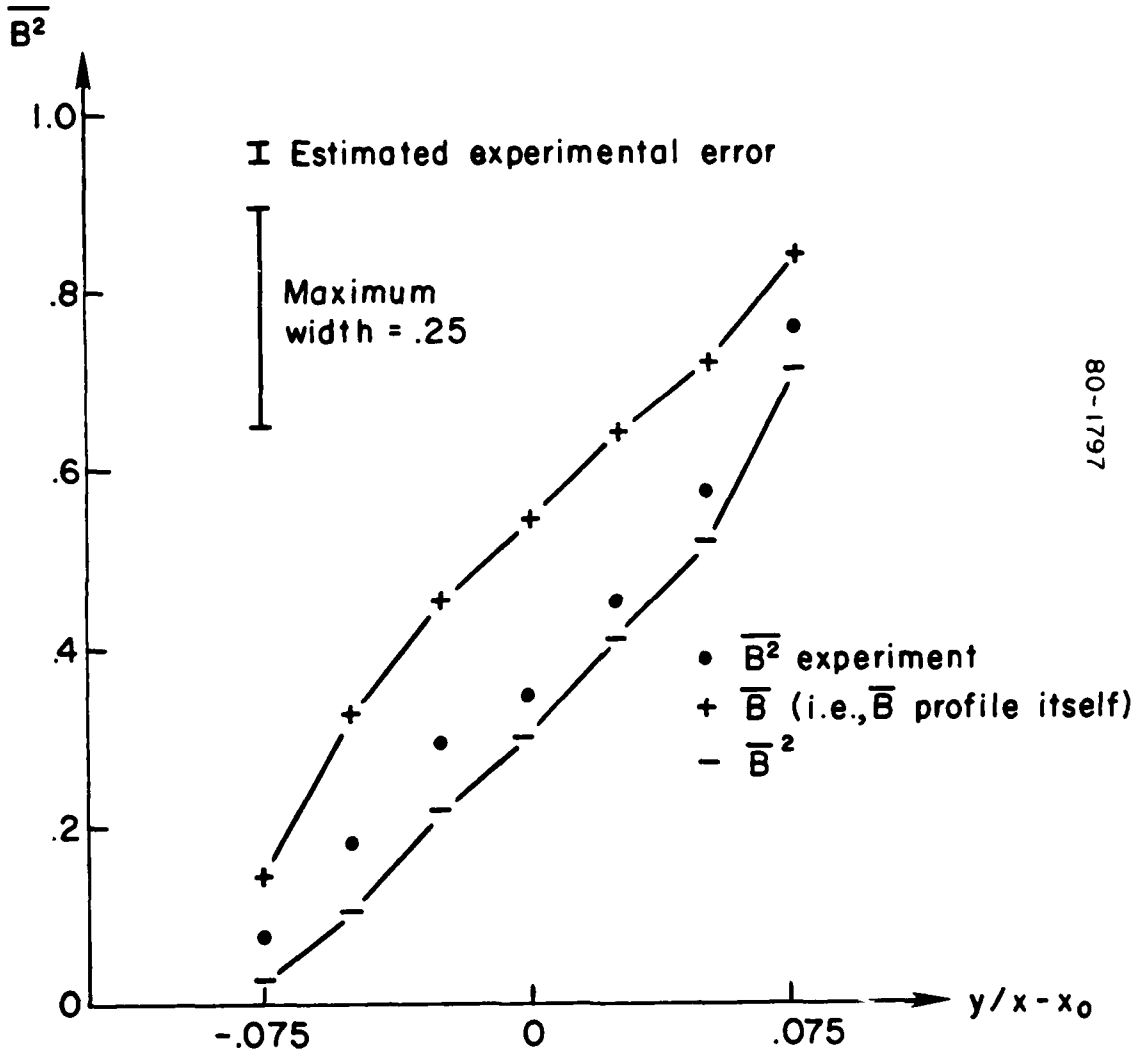

Figure 4. Experimental values of the second total moment and its theoretical bounds

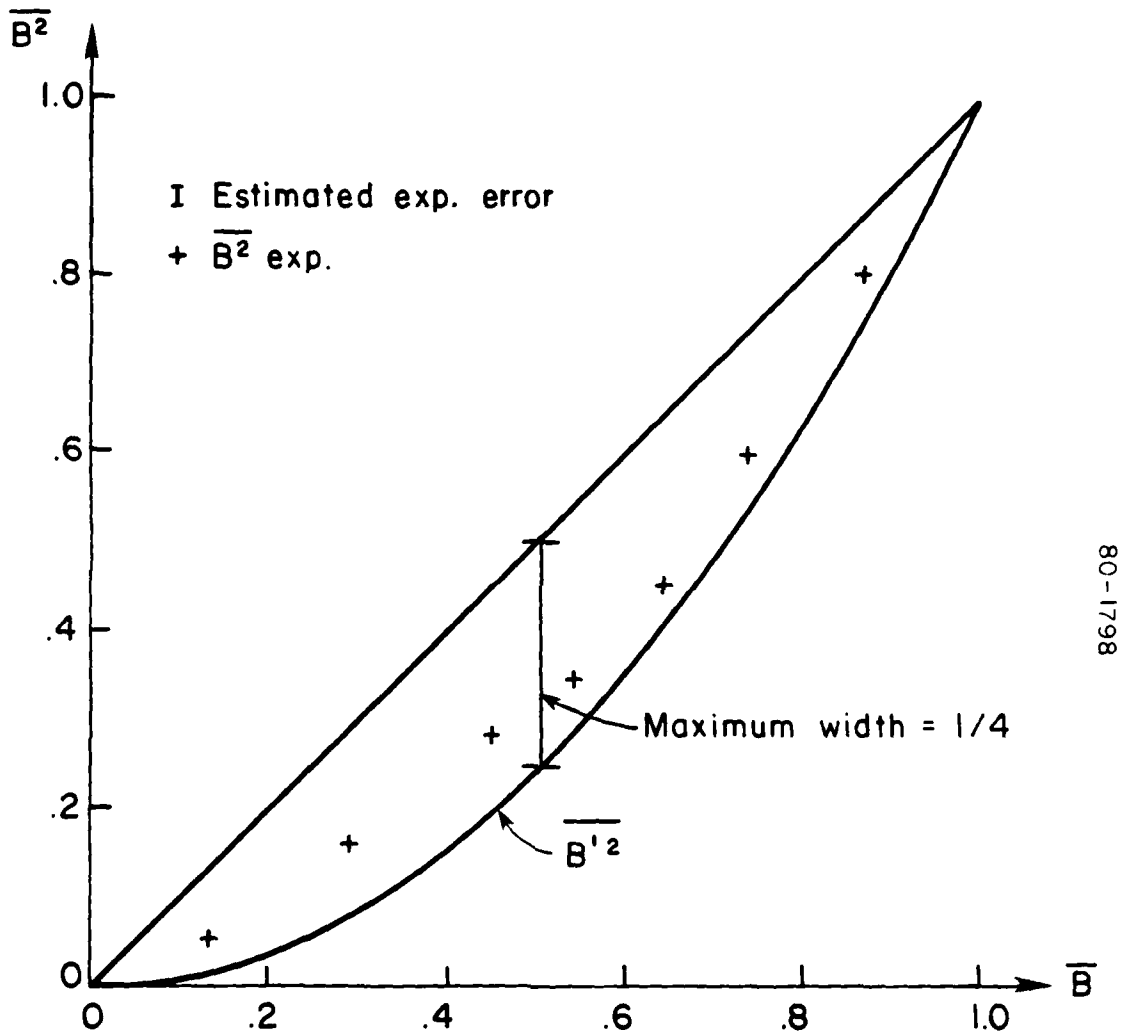

Figure 5. Interpretation of $\bar{B}$ axis on a stretched $y/(x - x_0)$ axis. This interpretation eliminates $y(x - x_0)$.

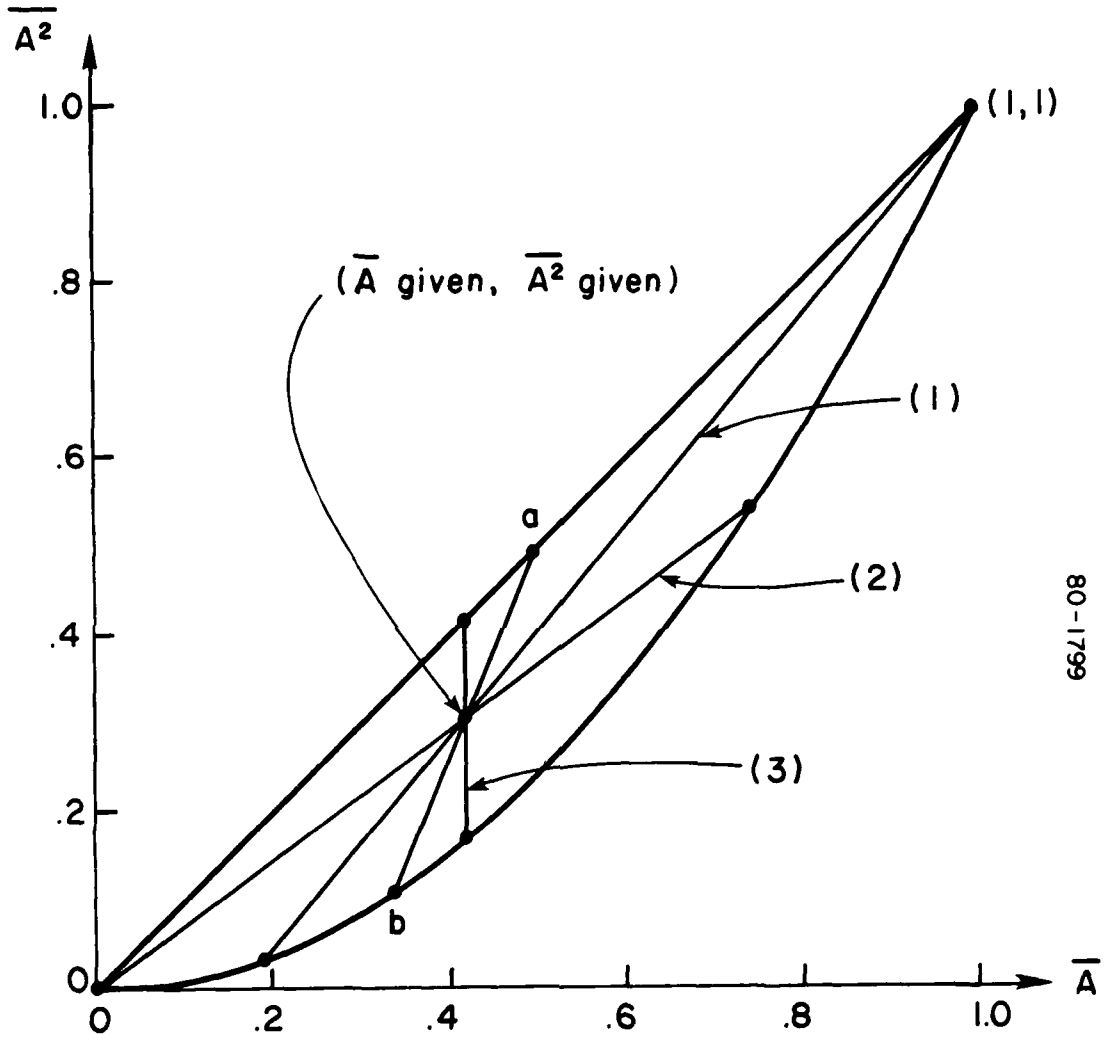

Figure 6. Representation of an arbitrary ($\bar{A}$, $\overline{A^2}$) by extreme distributions

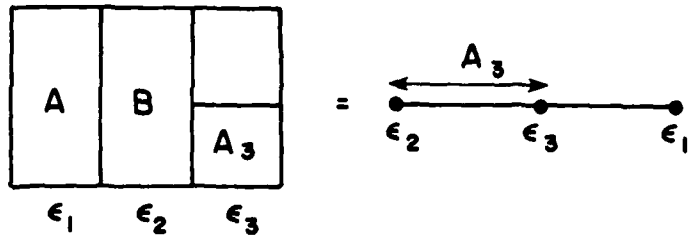

Figure 7. Generic box diagram for given $\bar{1} = 1, \bar{A}, \overline{A^2}$

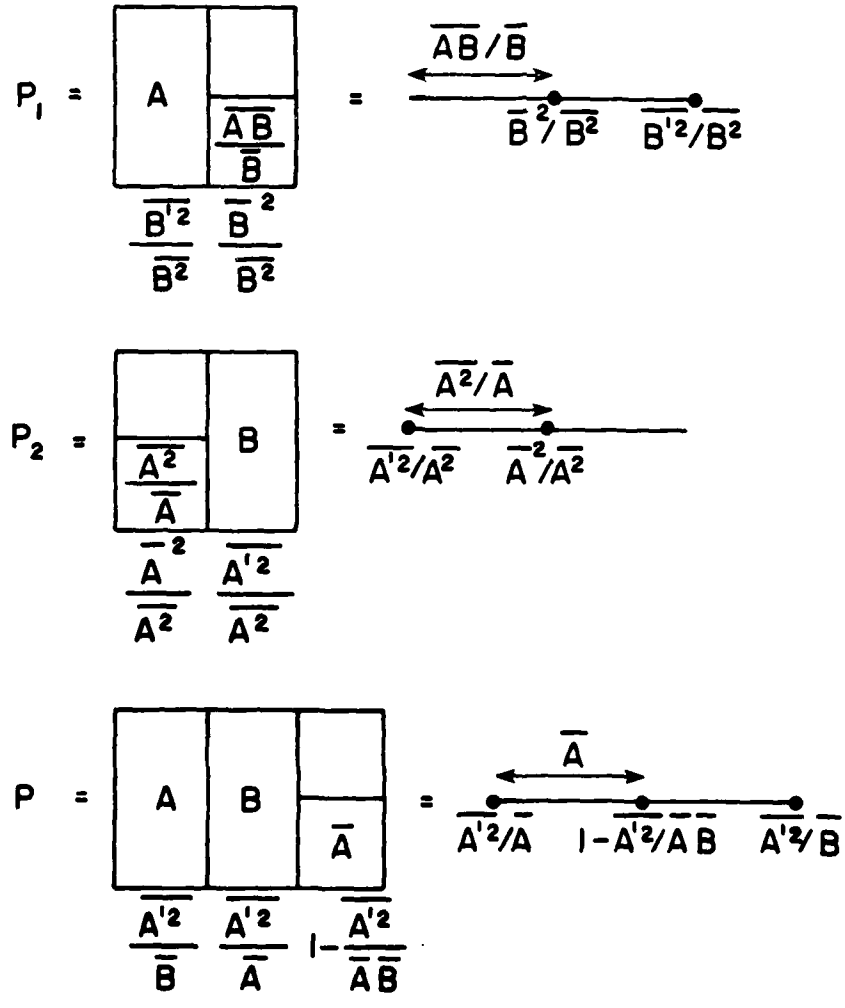

Figure 8. Three important special cases of Figure 7

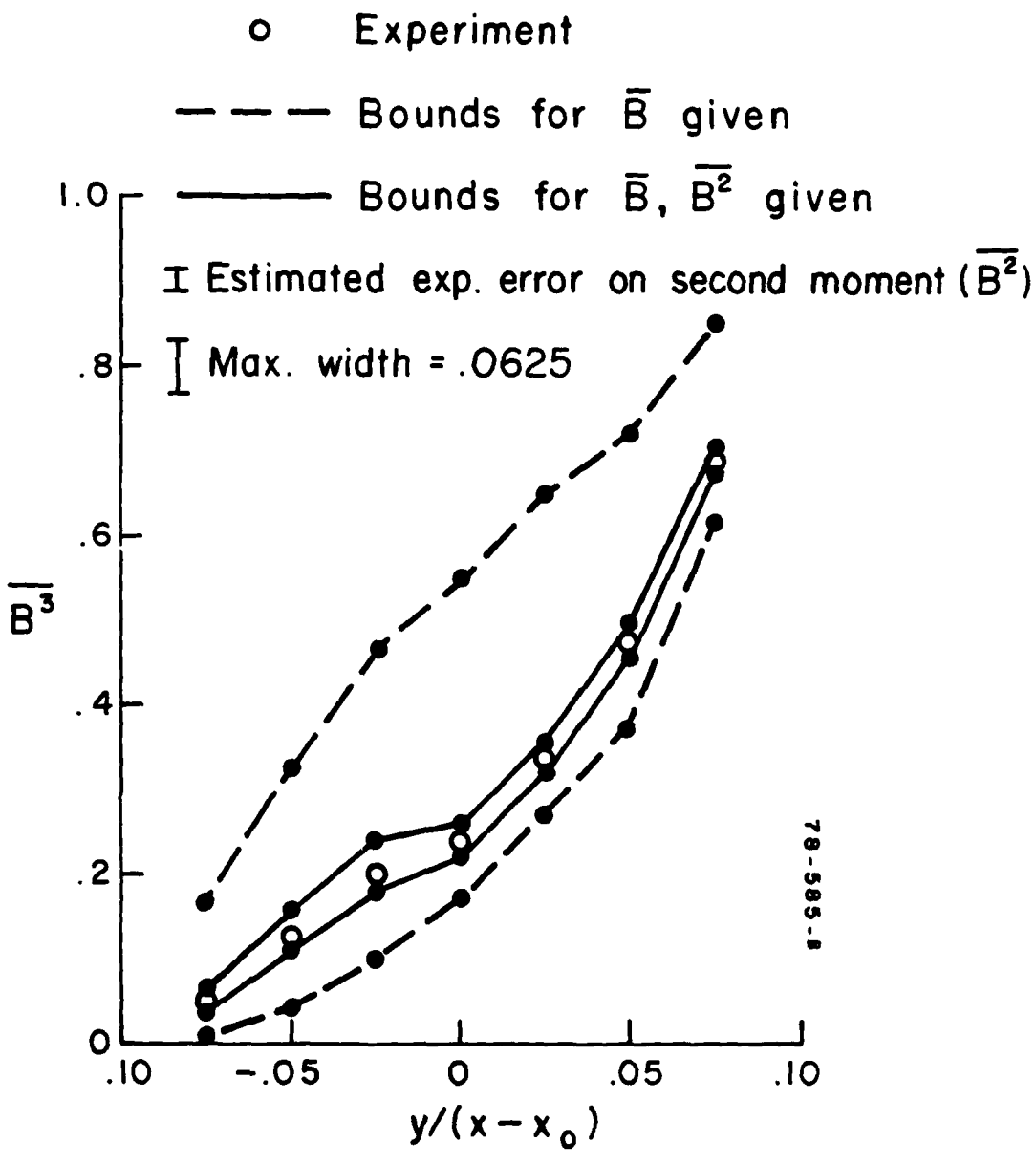

Figure 9. Experimental values of $\overline{B^3}$ and its theoretical bounds ($r = 0.38$, $S = 1.0$)

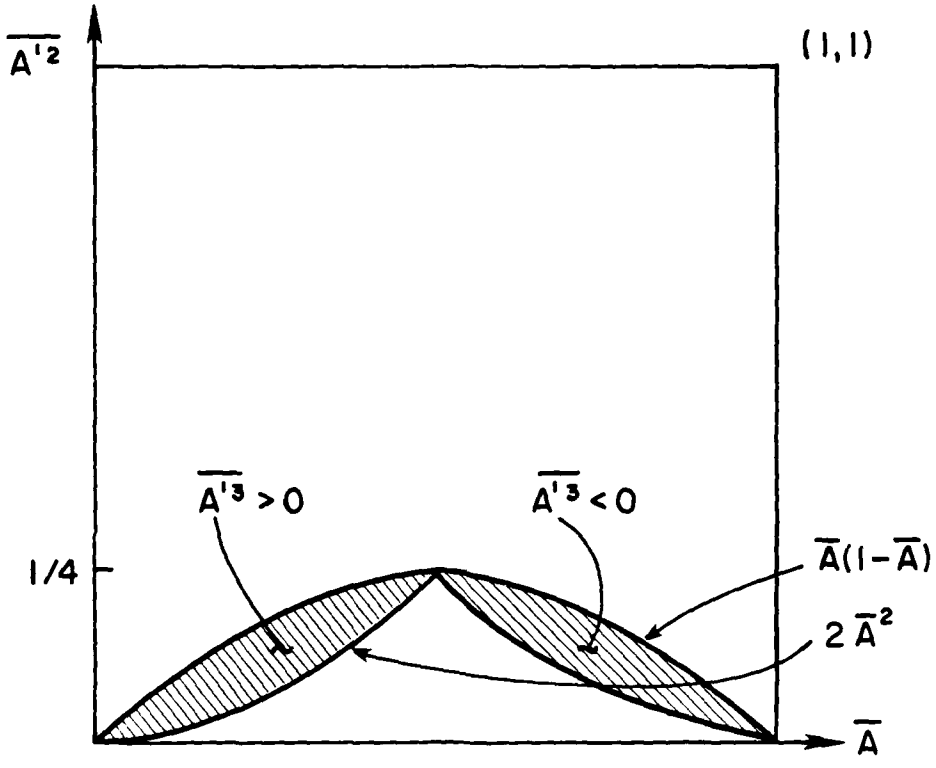

Figure 10. The domain for positive (negative) skewness for given $\bar{A}$ and $\overline{A'^2}$. The presence of experimental points in the hatched domain rules out the $\overline{A'^3} = 0$ model.

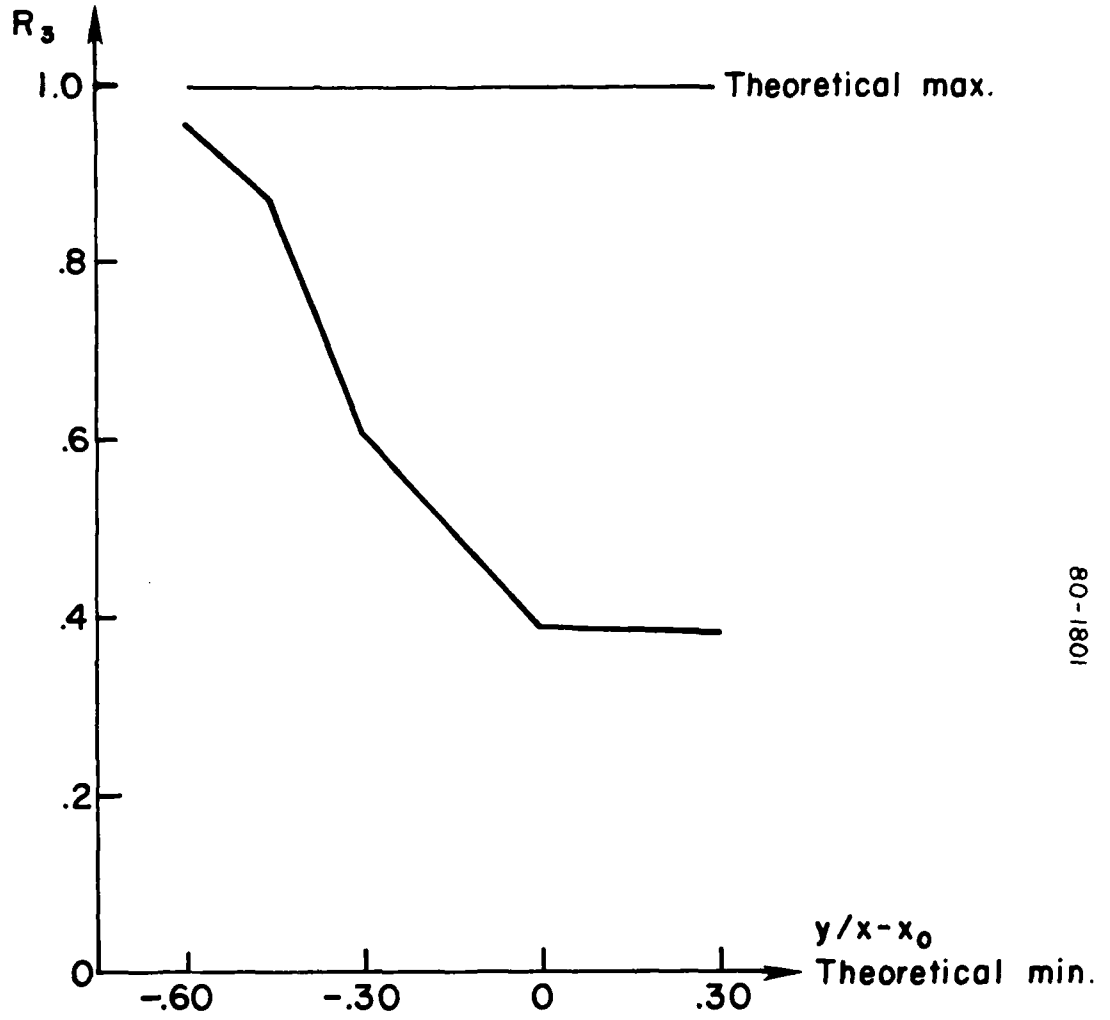

Figure 11a. Third-order mixedness (S = 7, r = 1)

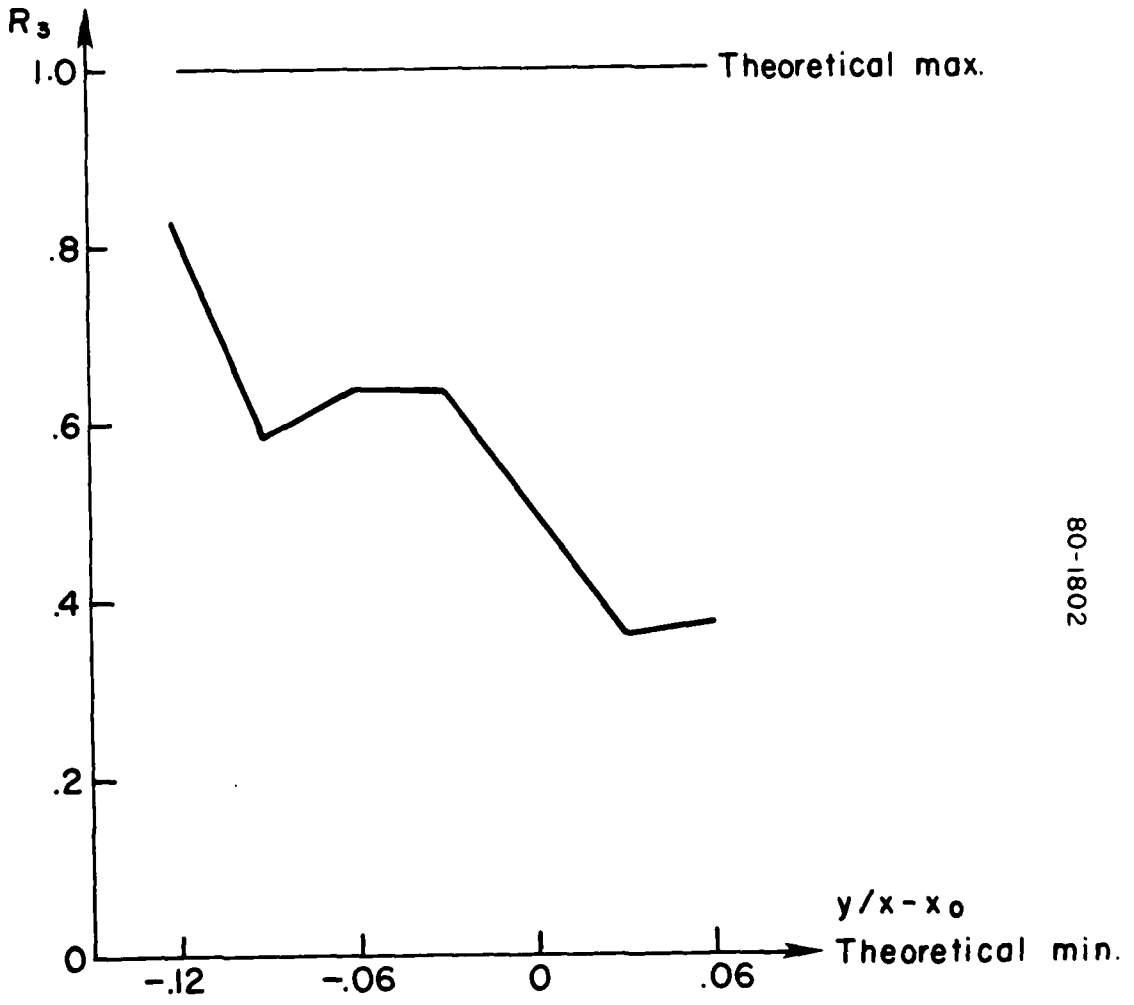

Figure 11b. Third-order mixedness (S = 7, r = 0.38)

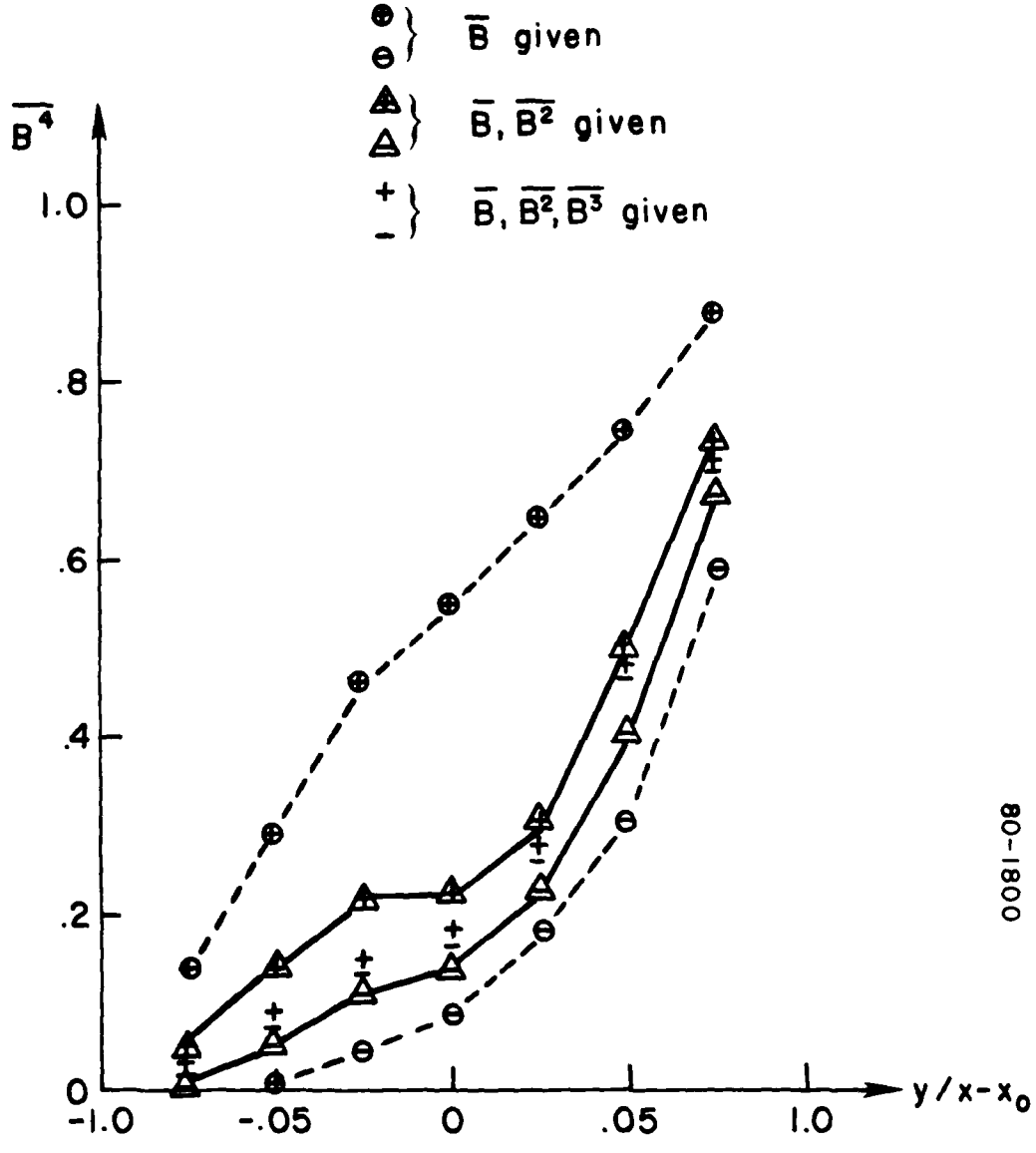

Figure 12. Experimental fourth moment and its theoretical bounds ($\Delta = 0$)

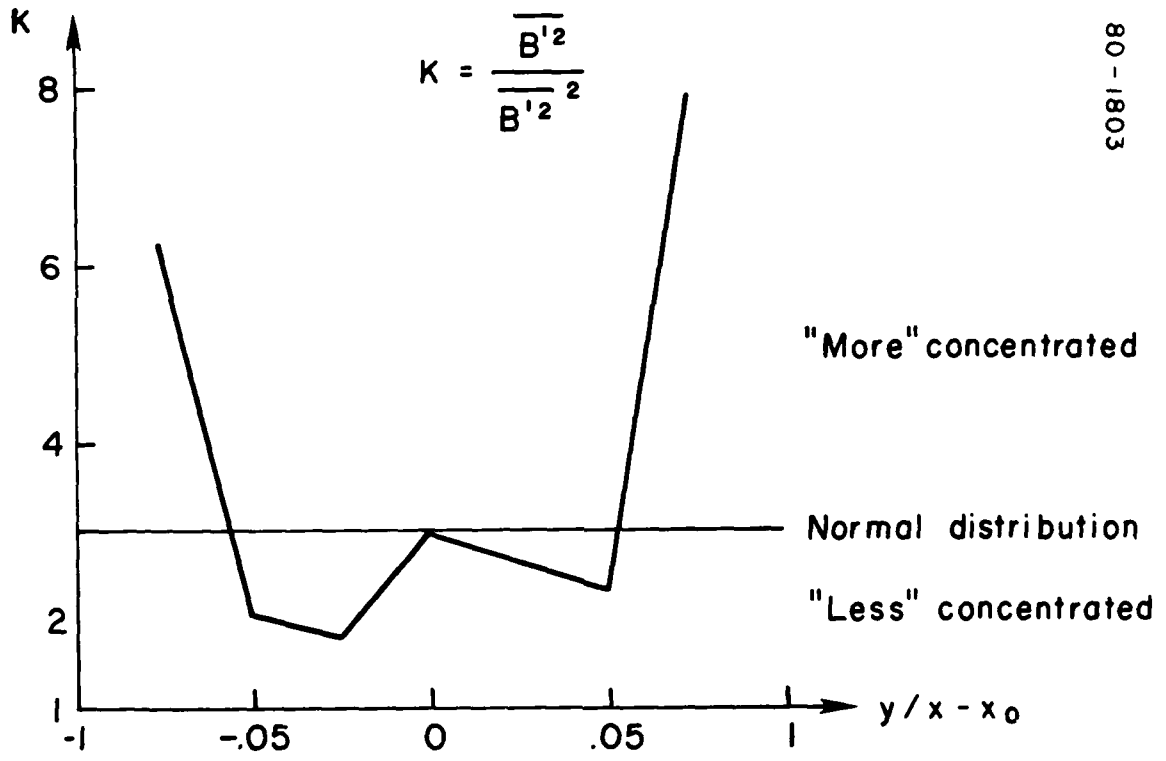

Figure 13. Kurtosis for $\Delta = 0$ (K = 3 for normal distribution)

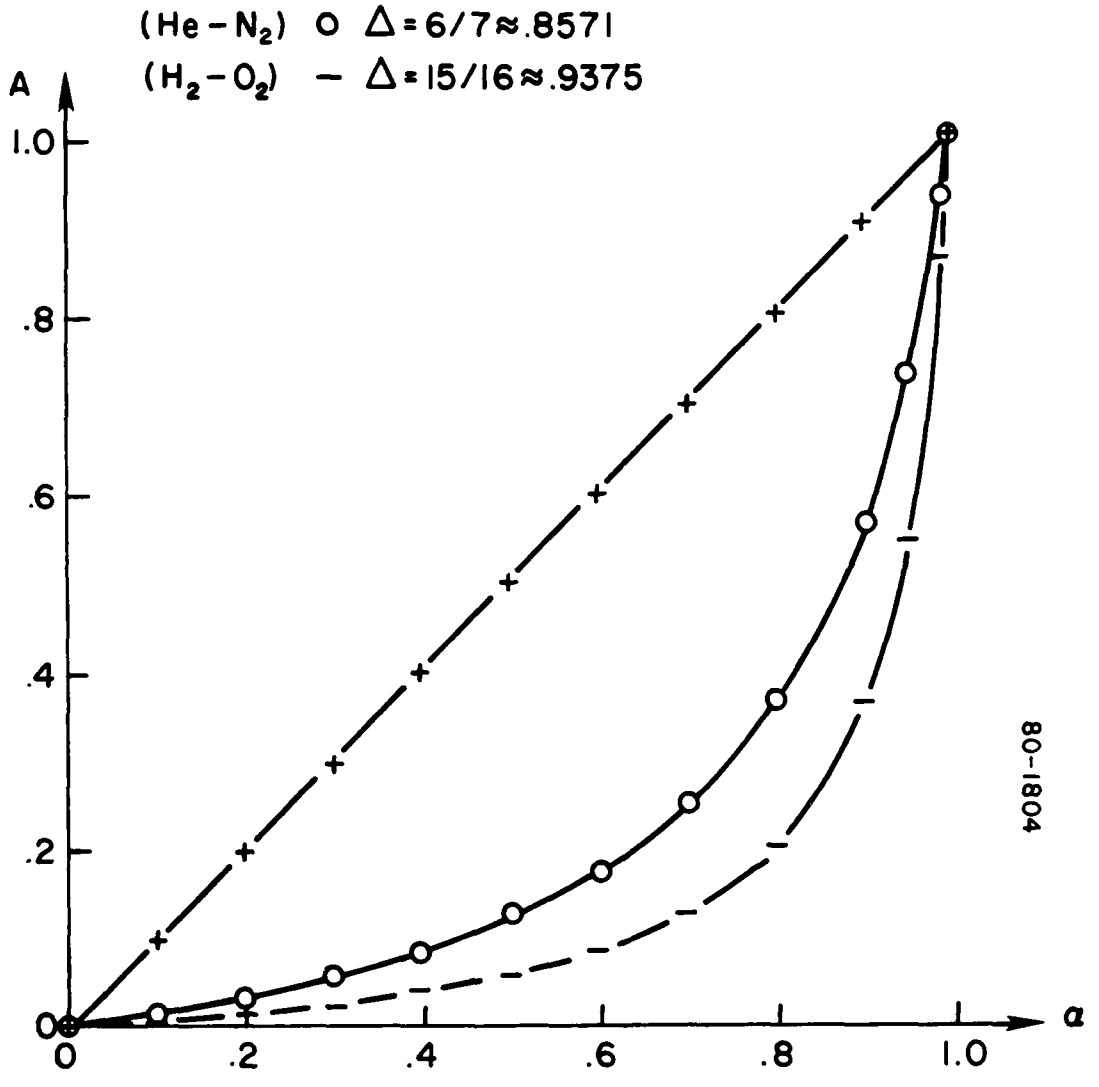

Figure 14. Relation between molar and mass fractions

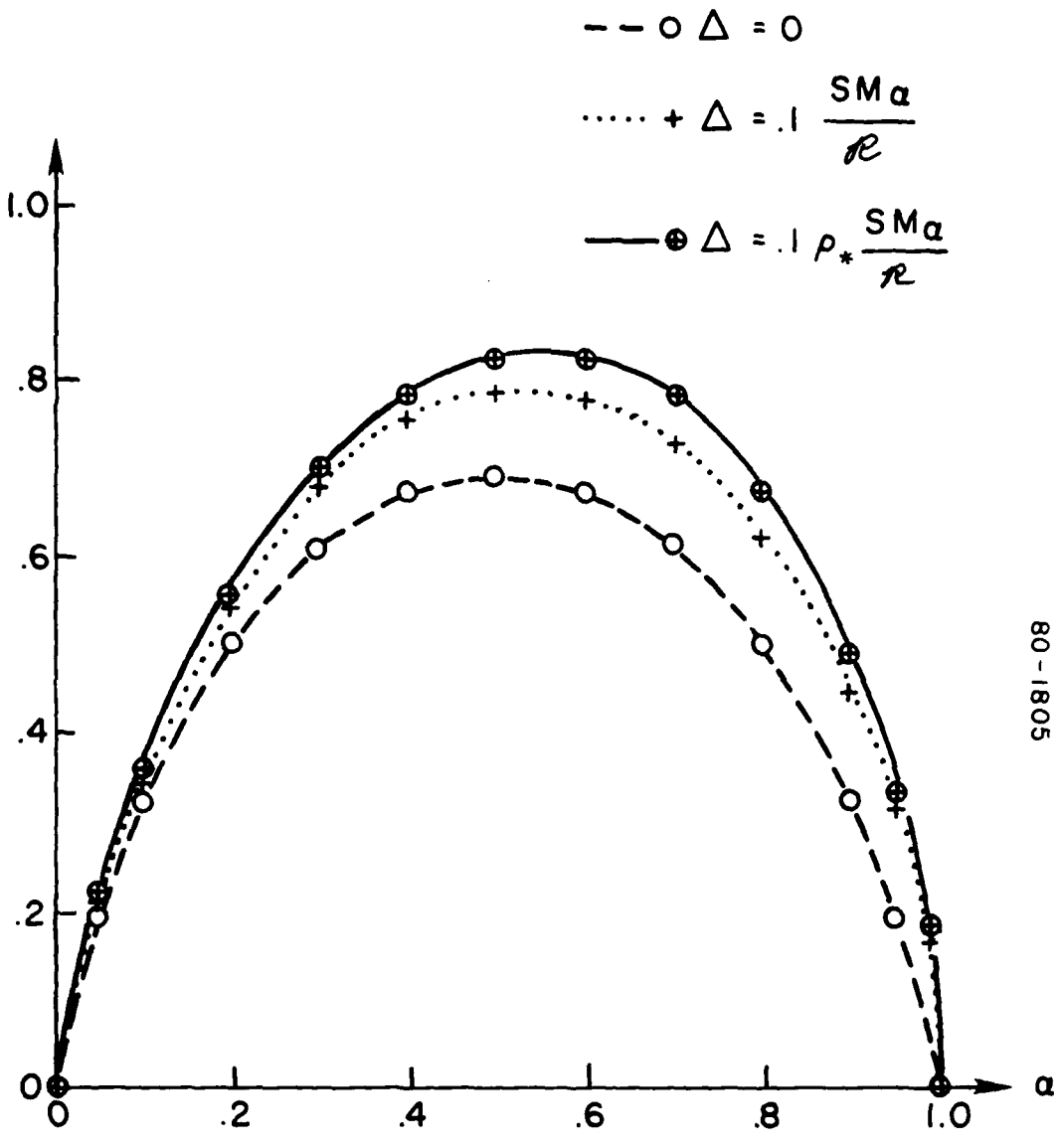

Figure 15. Entropy of mixing

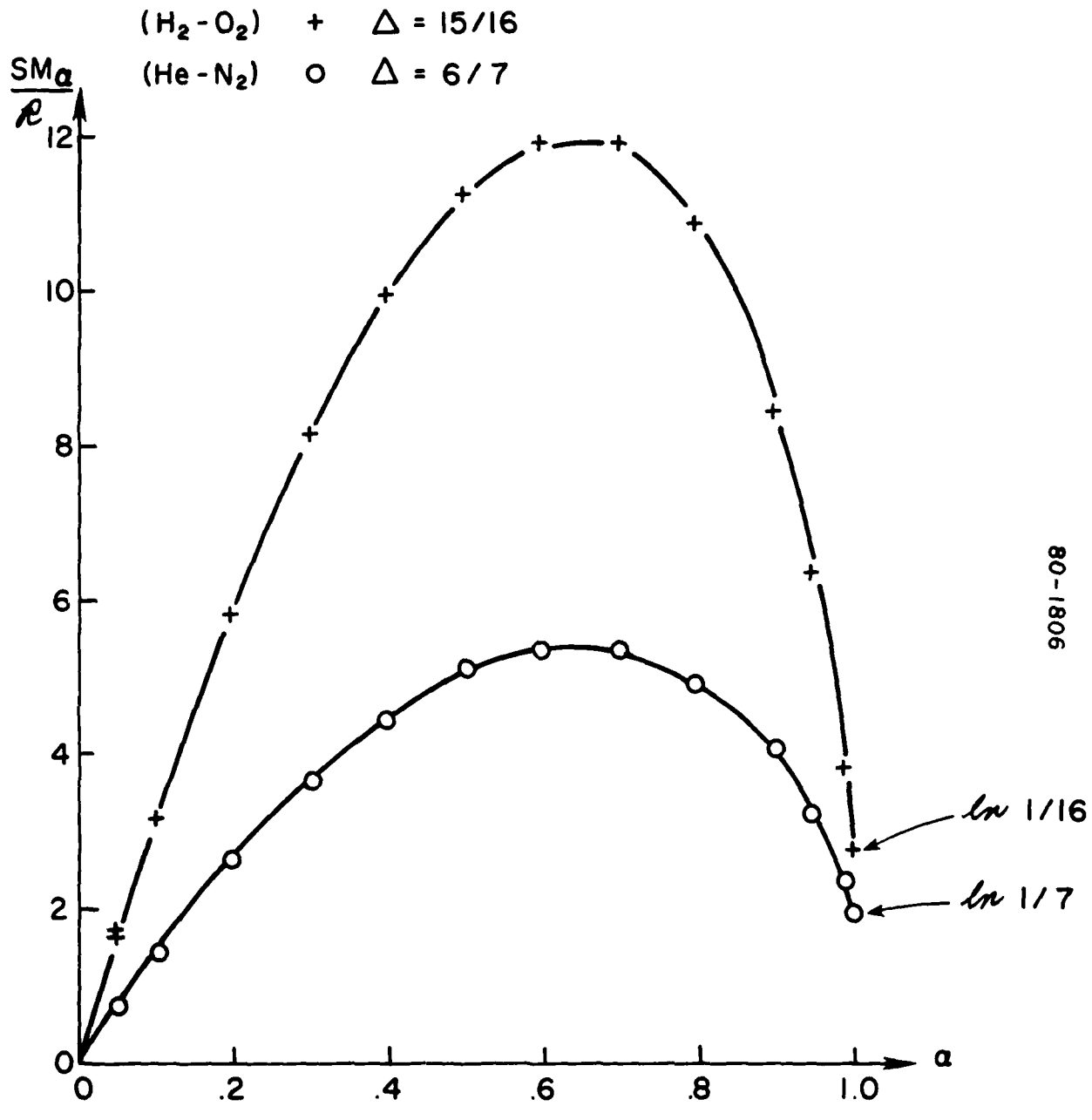

Figure 16. Specific entropy of mixing

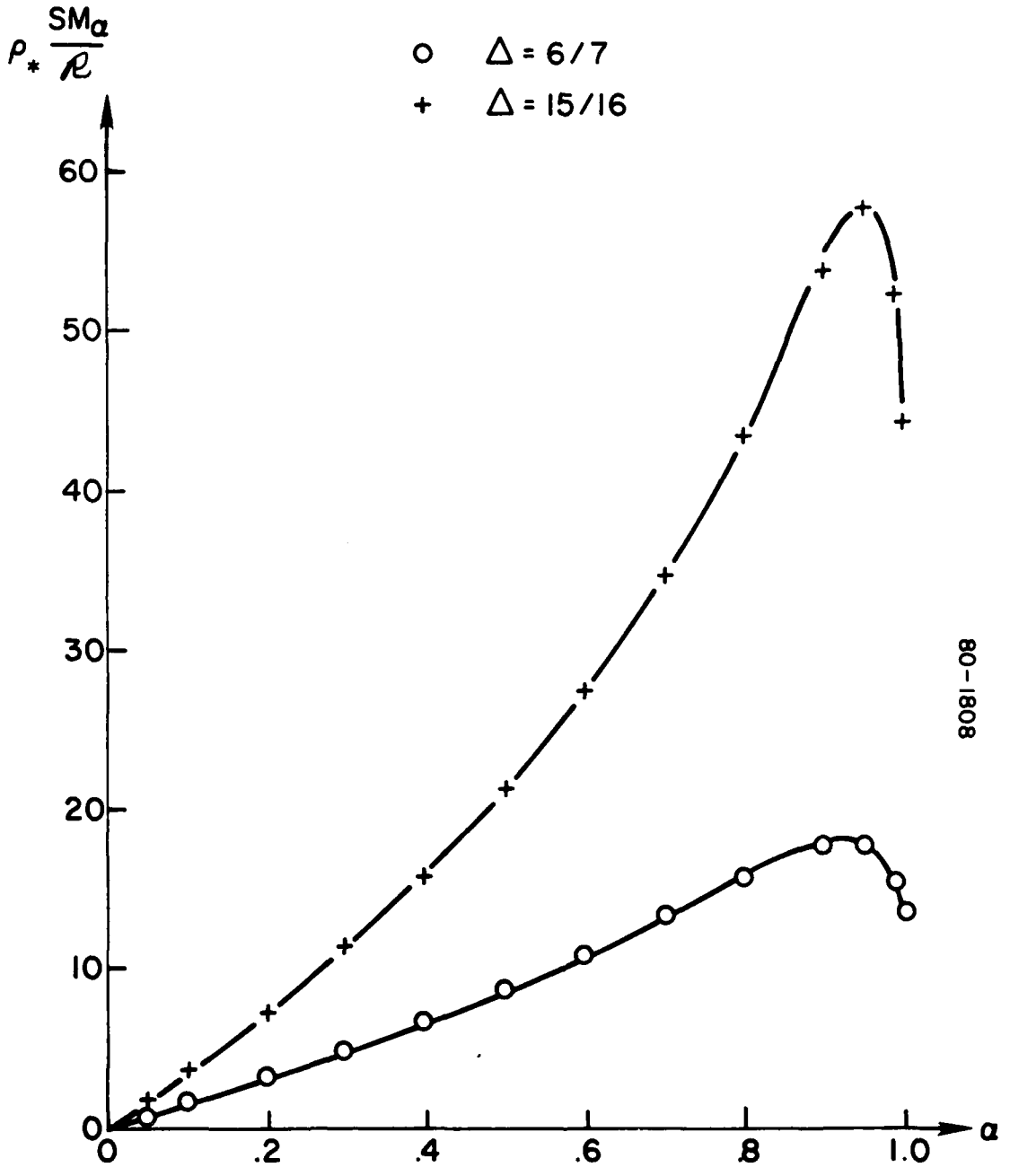

Figure 17. Mixing entropy density

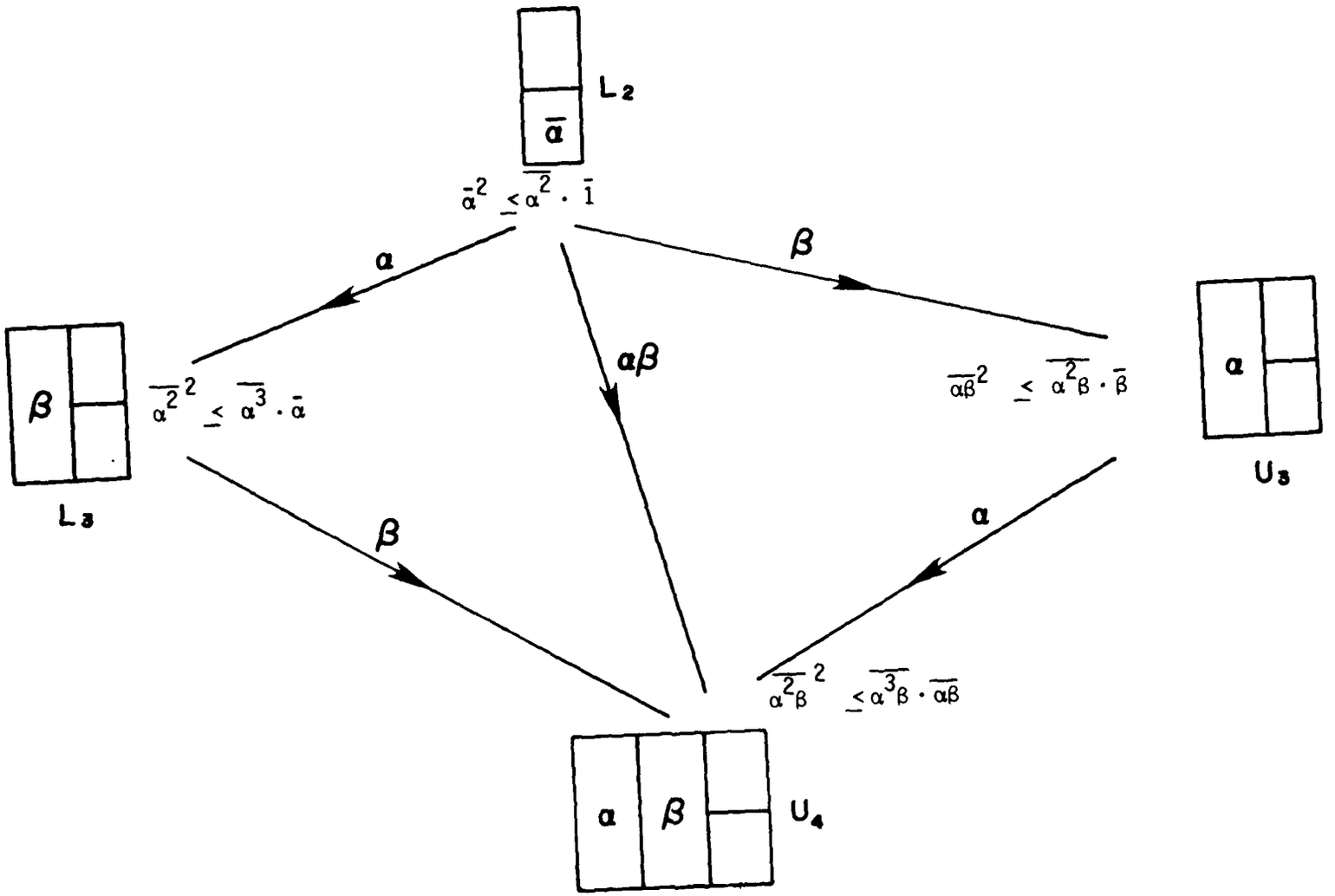

Figure 18. Lowest tree (L_2 to U_4)

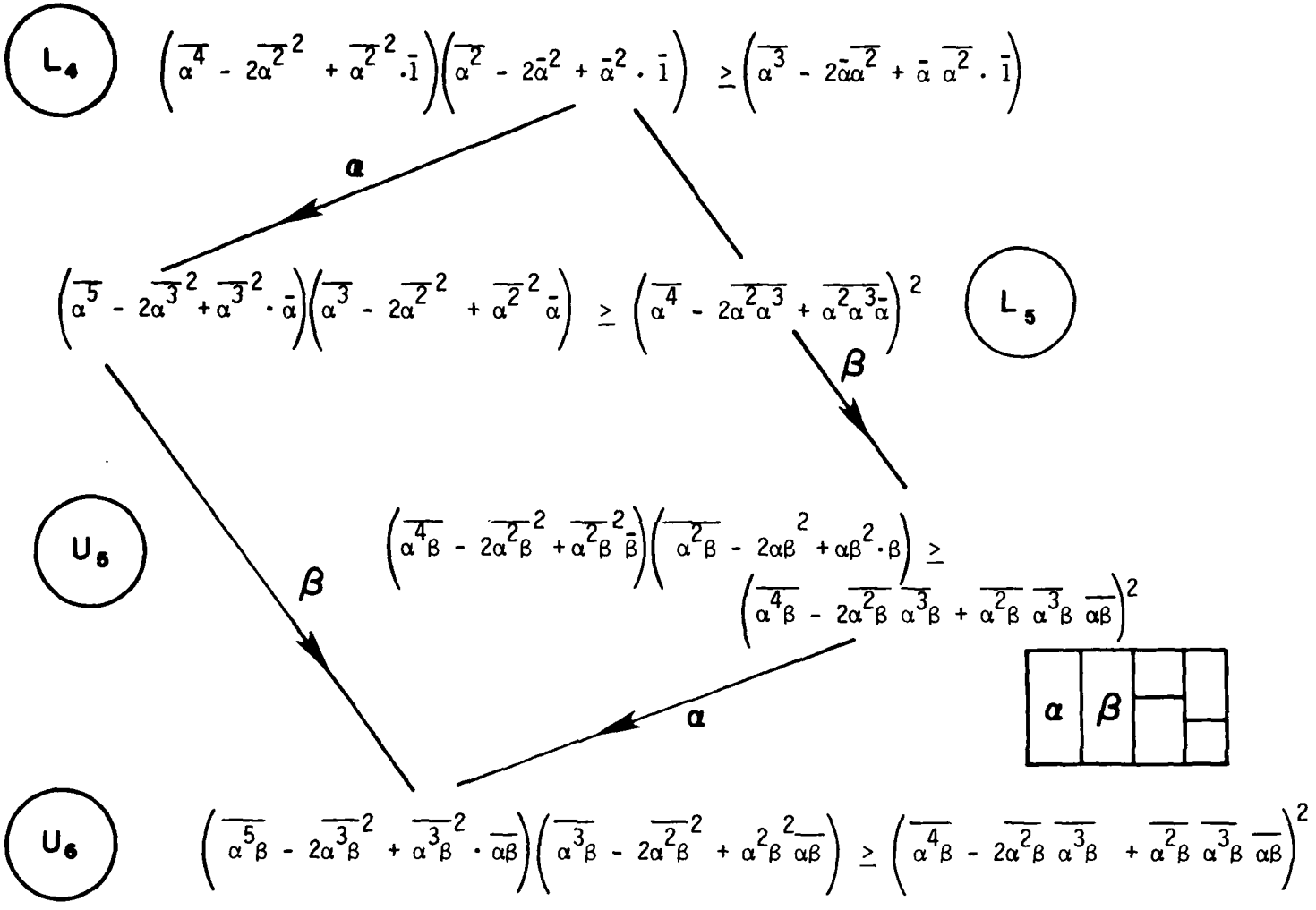

Figure 19. Second tree (L_4 to U_6)

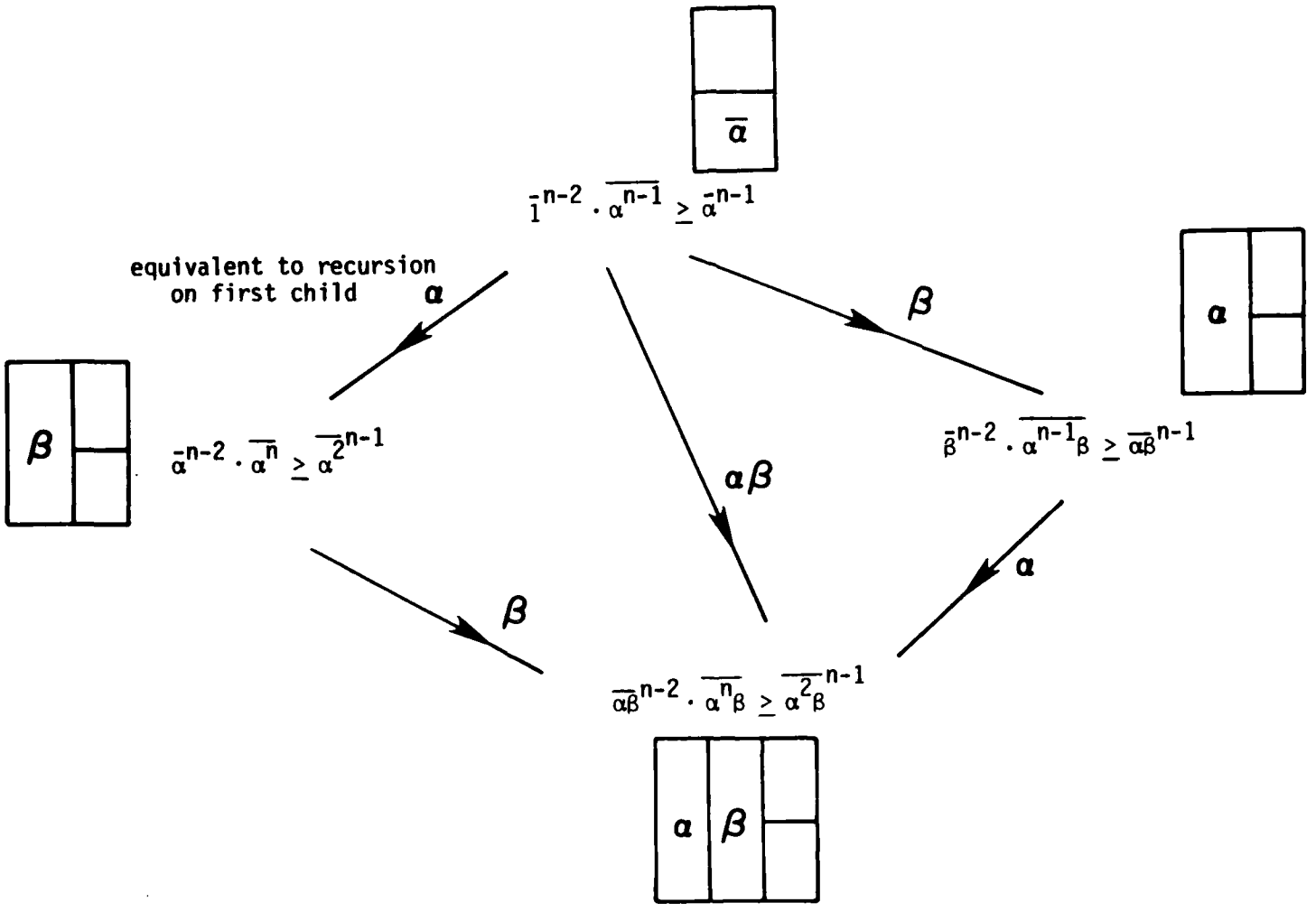

Figure 20. Skip family

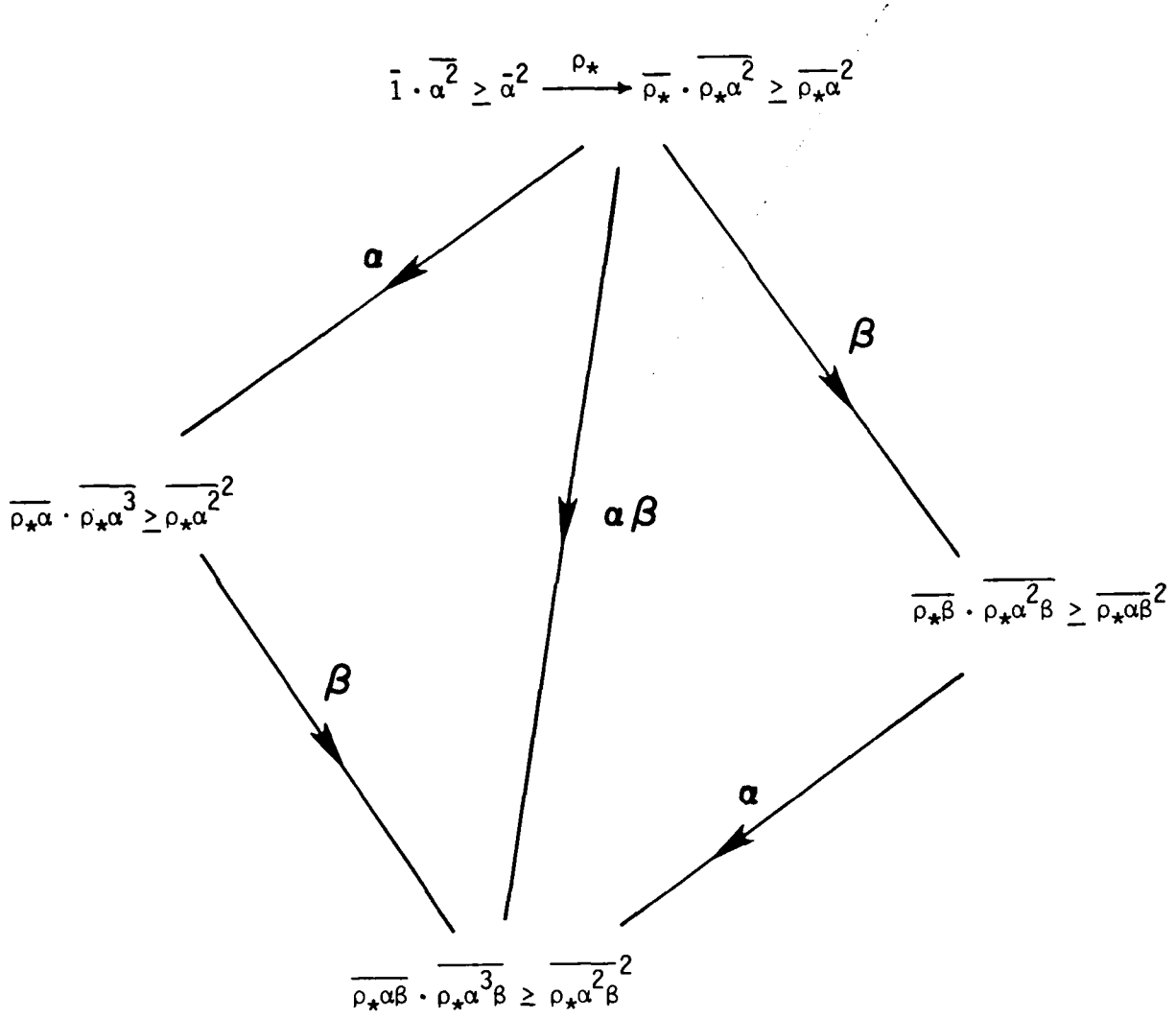

Figure 21. Density family

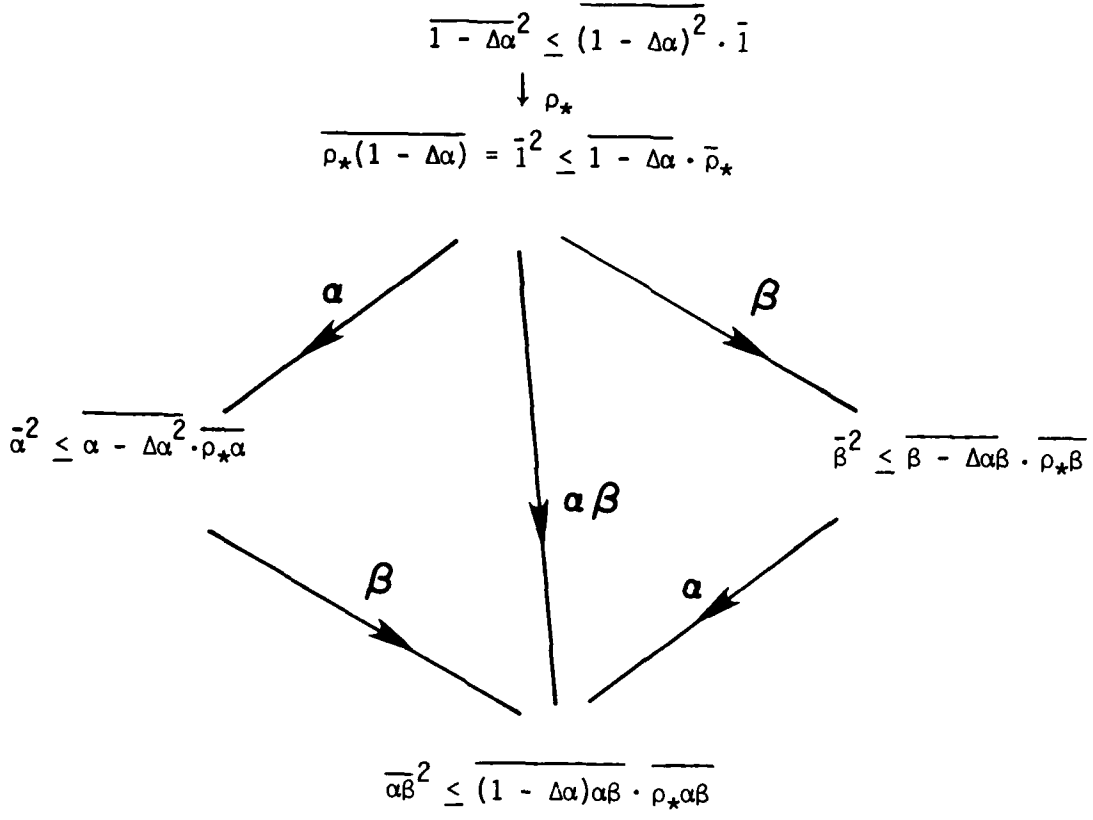

Figure 22. Alternative for bounds on $\overline{\rho_*\alpha}$

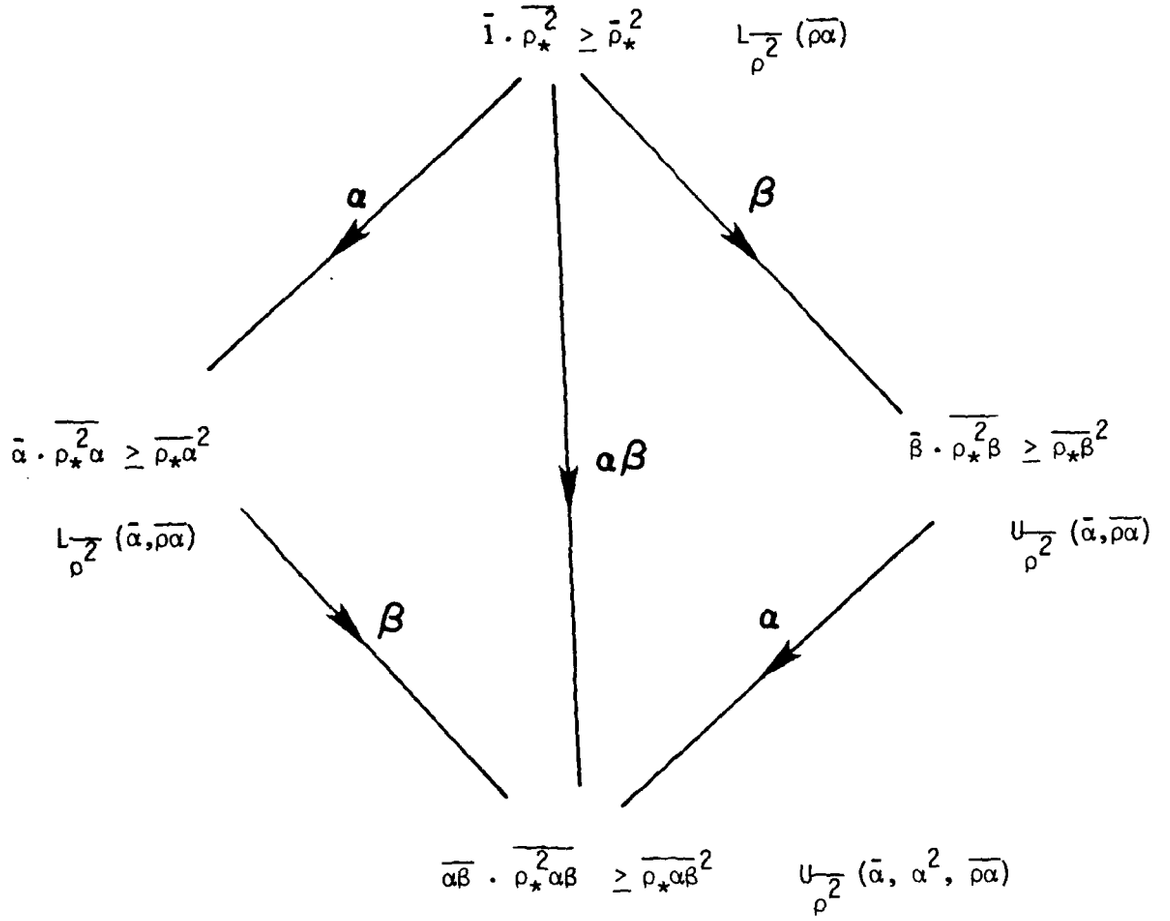

Figure 23. Density correlations

$$\alpha = \frac{A}{1 - \Delta(1 - A)} \quad , \quad \bar{Q}^2 \leq \overline{Q^2} \cdot \bar{1}$$

$$\overline{1 - \Delta(1 - A)}^2 \leq \overline{1 - \Delta(1 - A)^2} \cdot \bar{1}$$

α

$$\bar{A}^2 \leq \overline{A(1 - \Delta[1 - A])} \cdot \bar{\alpha} \quad \text{i.e.:} \quad L_2(\bar{A}, \bar{A}^2)$$

β

$$U\text{-}(\bar{A}, \bar{A}^2): \quad (\overline{1 - \Delta[1 - A]} - \bar{A})^2 \leq \left(\overline{[1 - \Delta(1 - A)]^2} - \overline{A[1 - \Delta(1 - A)]}\right) (1 - \bar{\alpha})$$

Figure 24. Given mole fraction moments, obtain bounds on mass fractions

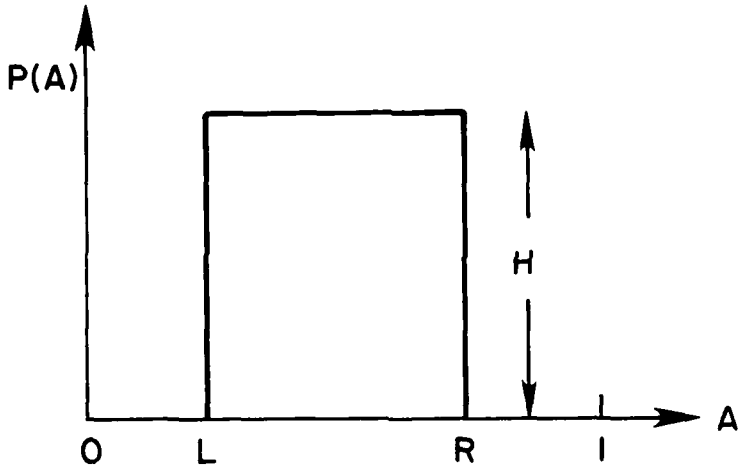

Figure 25. Parameters used to describe the square hat model

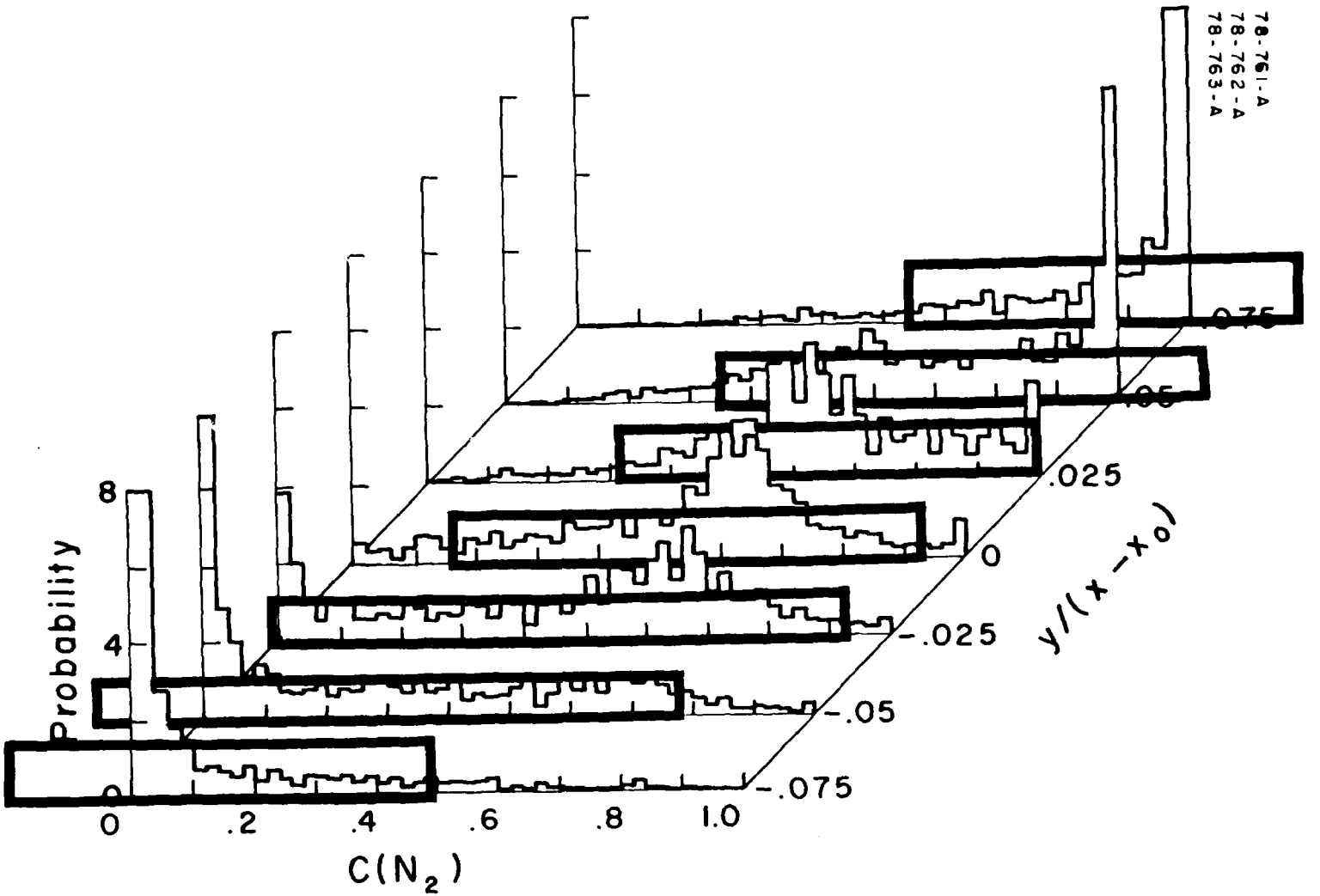

Figure 26. Probability density function; r = 0.38, s = 1.0

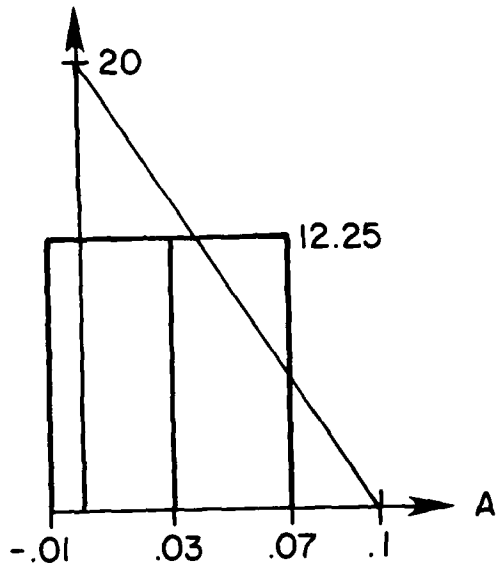

Figure 27. Failure of a square hat to fit a triangular distribution (finite probability of negative molar fraction)

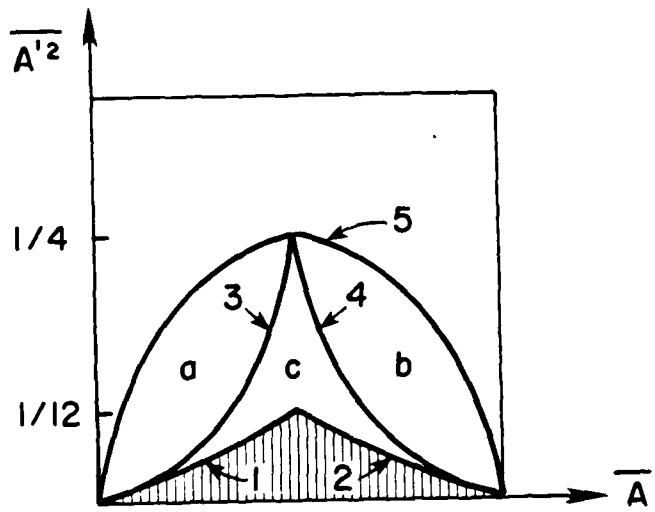

a) L < 0
b) R > 1
c) L < 0 and R > 1

Figure 28. Allowed domain for symmetric models

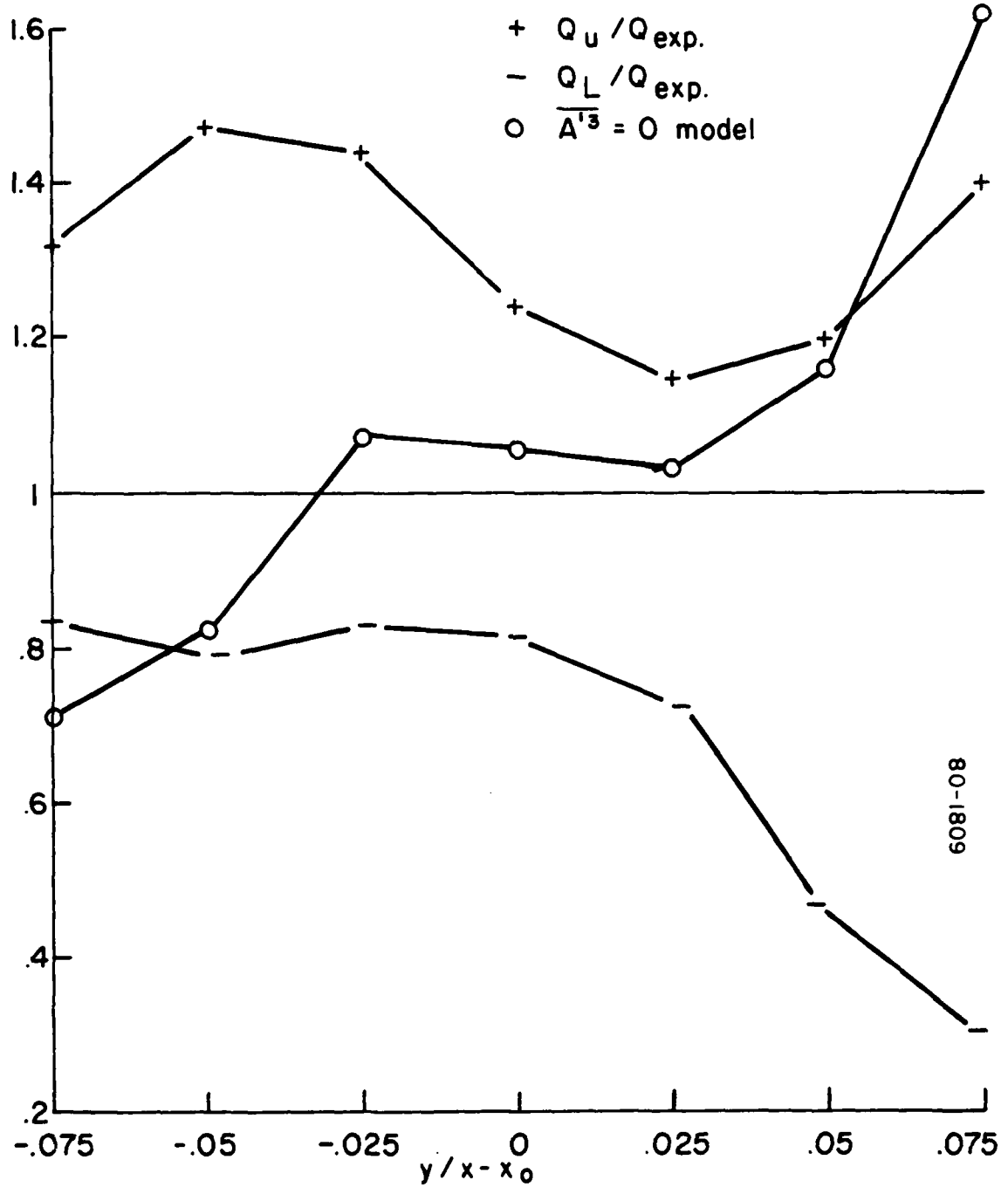

Figure 29. Bounds on Q for (r = 0.38, S = 1, Δ = 0) and $\overline{A'^3} = 0$ model

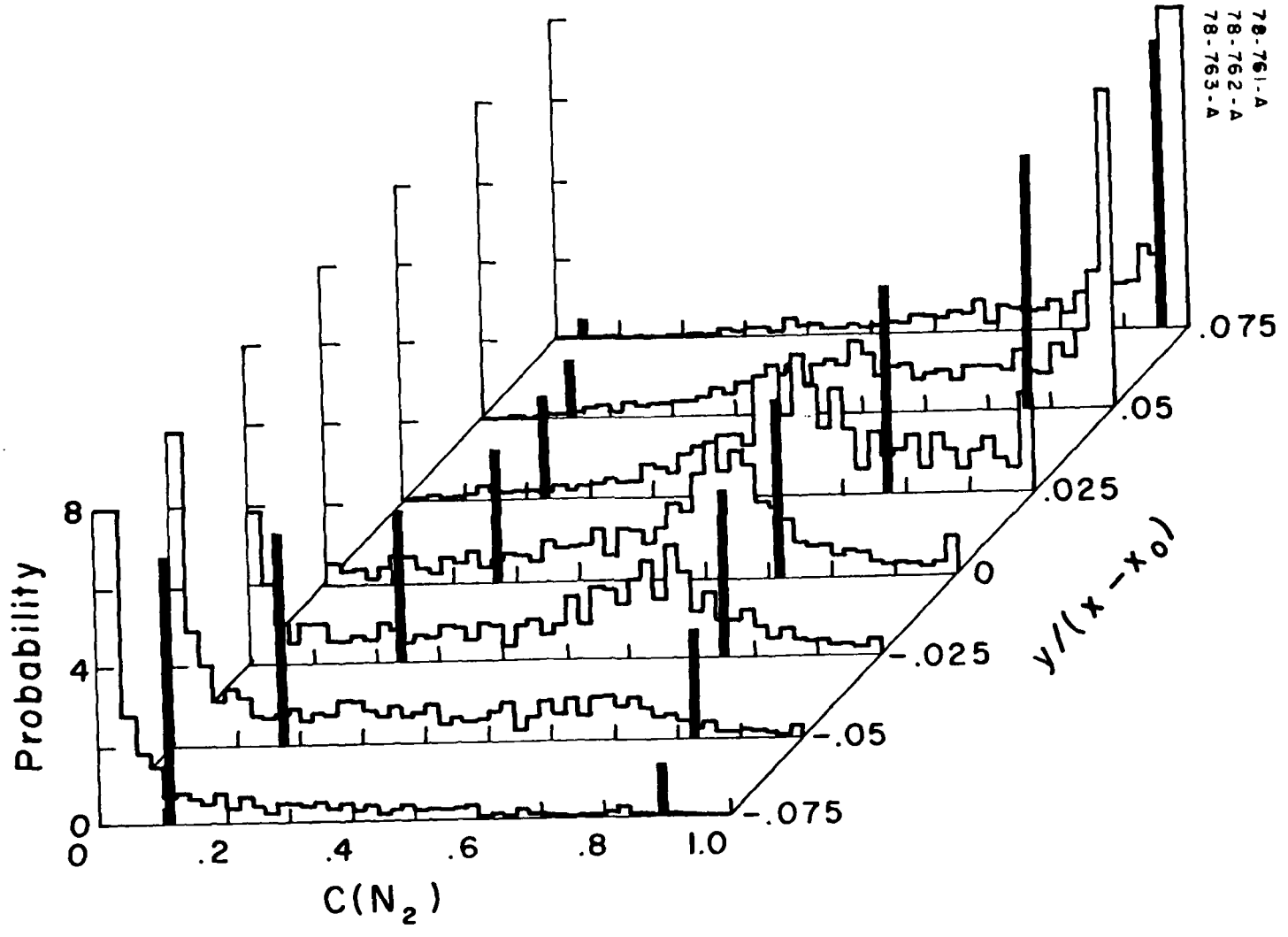

Figure 30. Probability density function; r = 0.38, s = 1.0. The model is $\overline{A^2B^2} = 0$ (or, equivalently, (AB)' = 0)

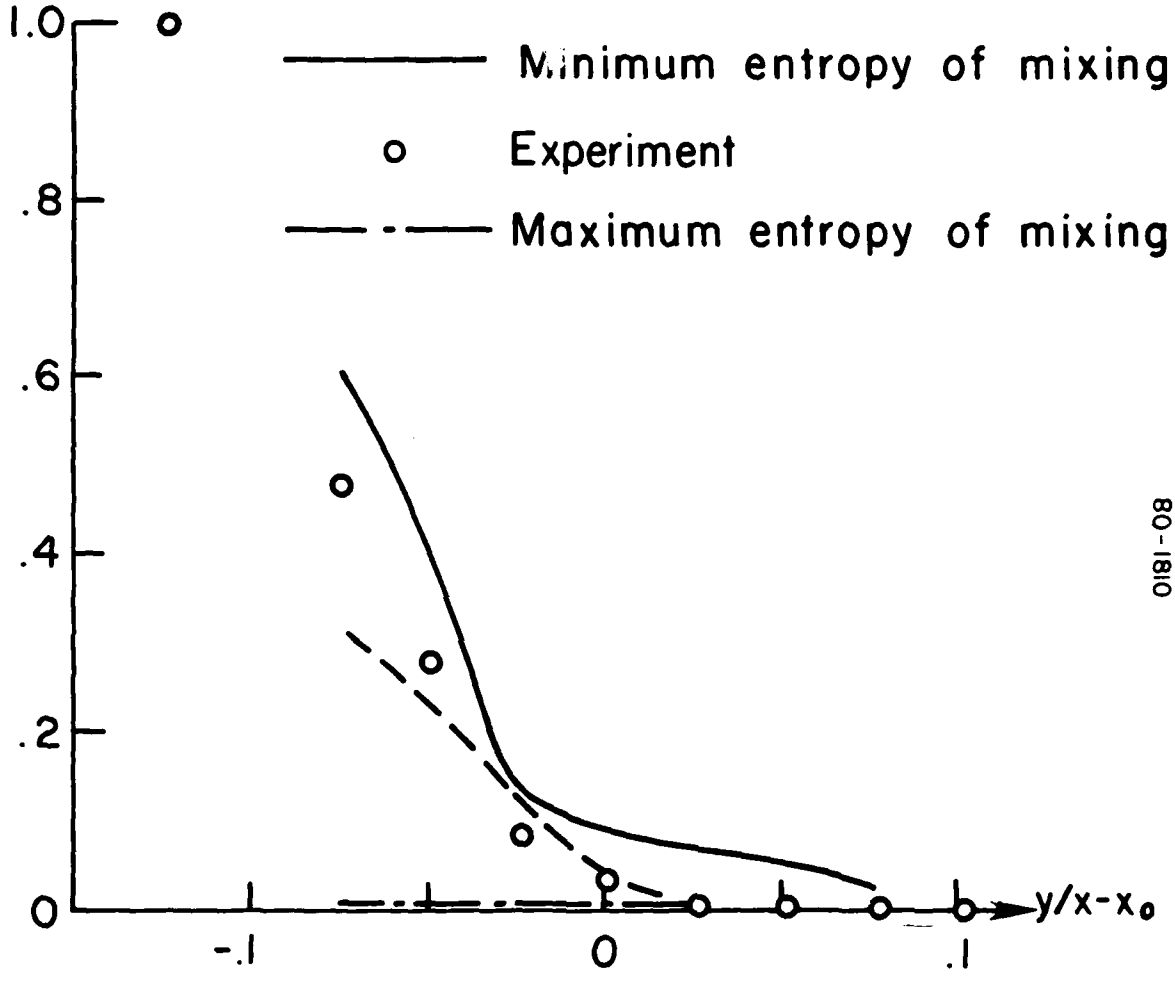

Figure 31. Probability of pure He

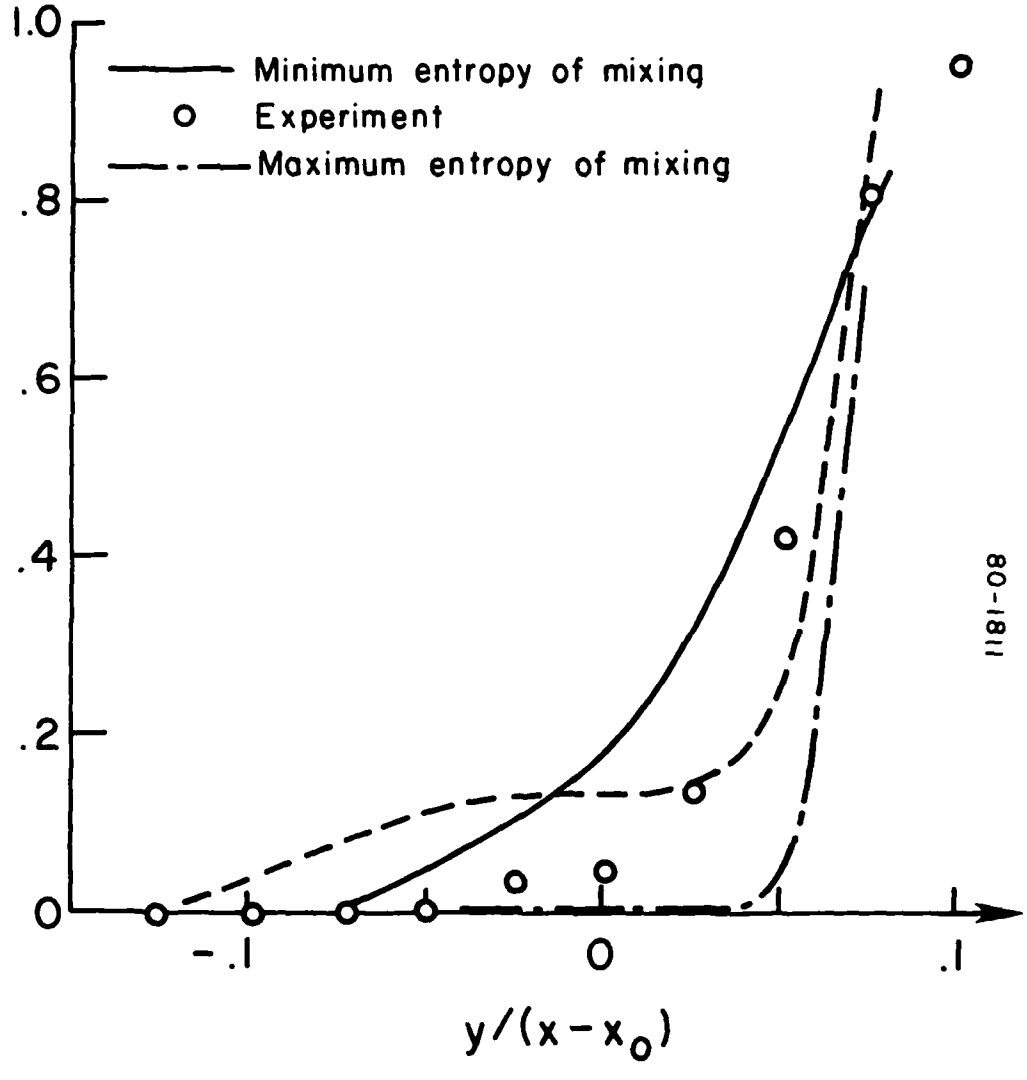

Figure 32. Probability of pure N_2

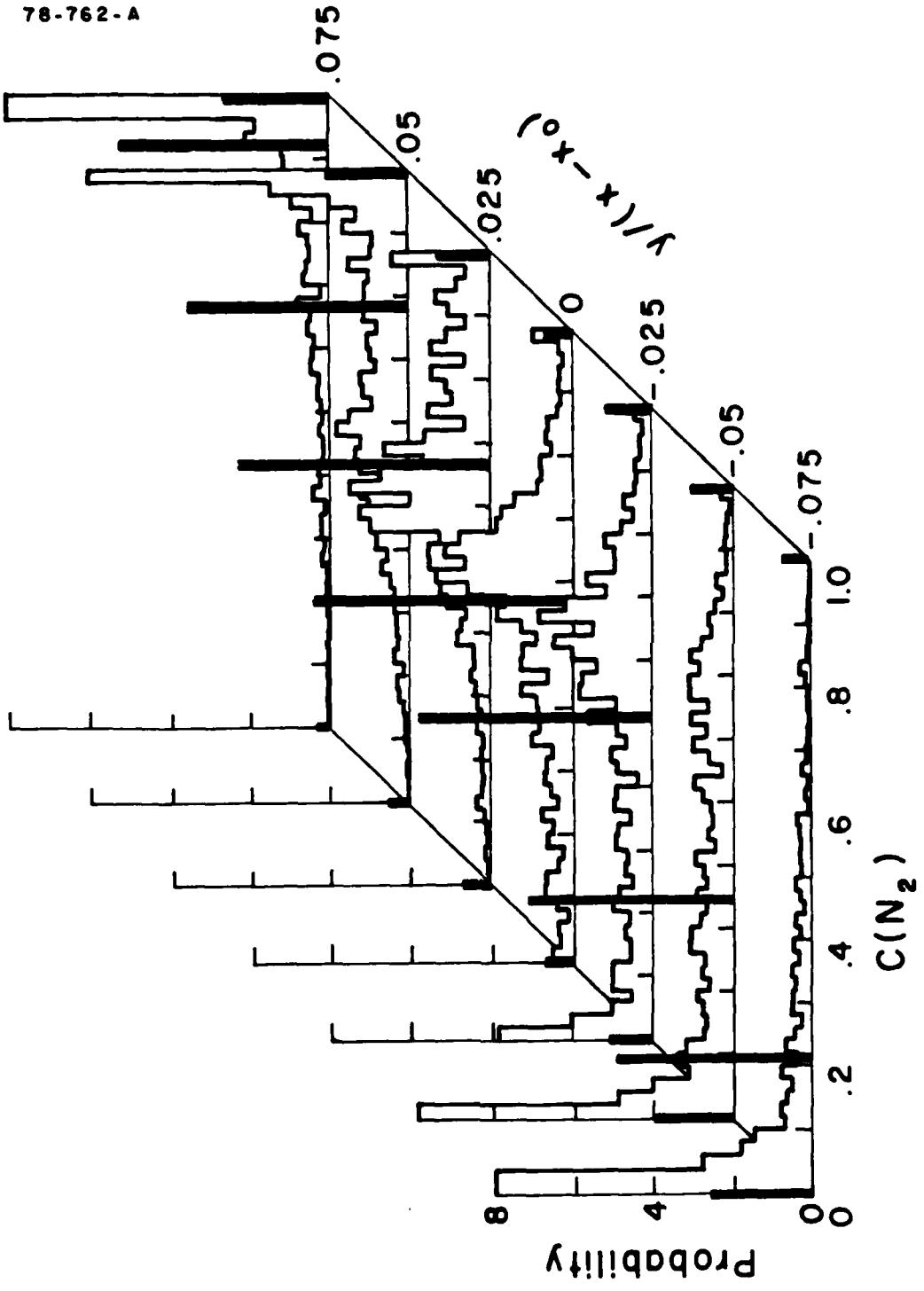

Figure 33. Probability density function; r = 0.38, s = 1.0

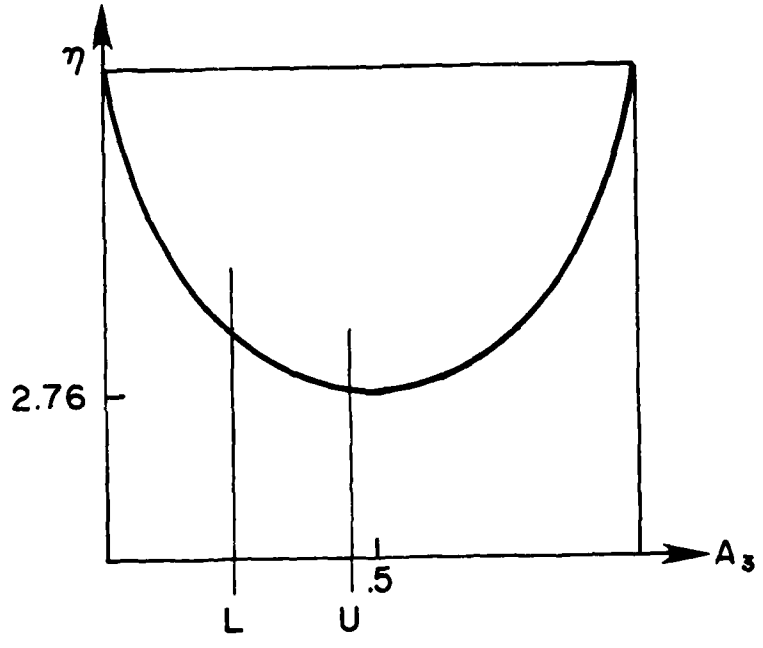

Figure 34. Normalized entropy function for the minimum entropy model

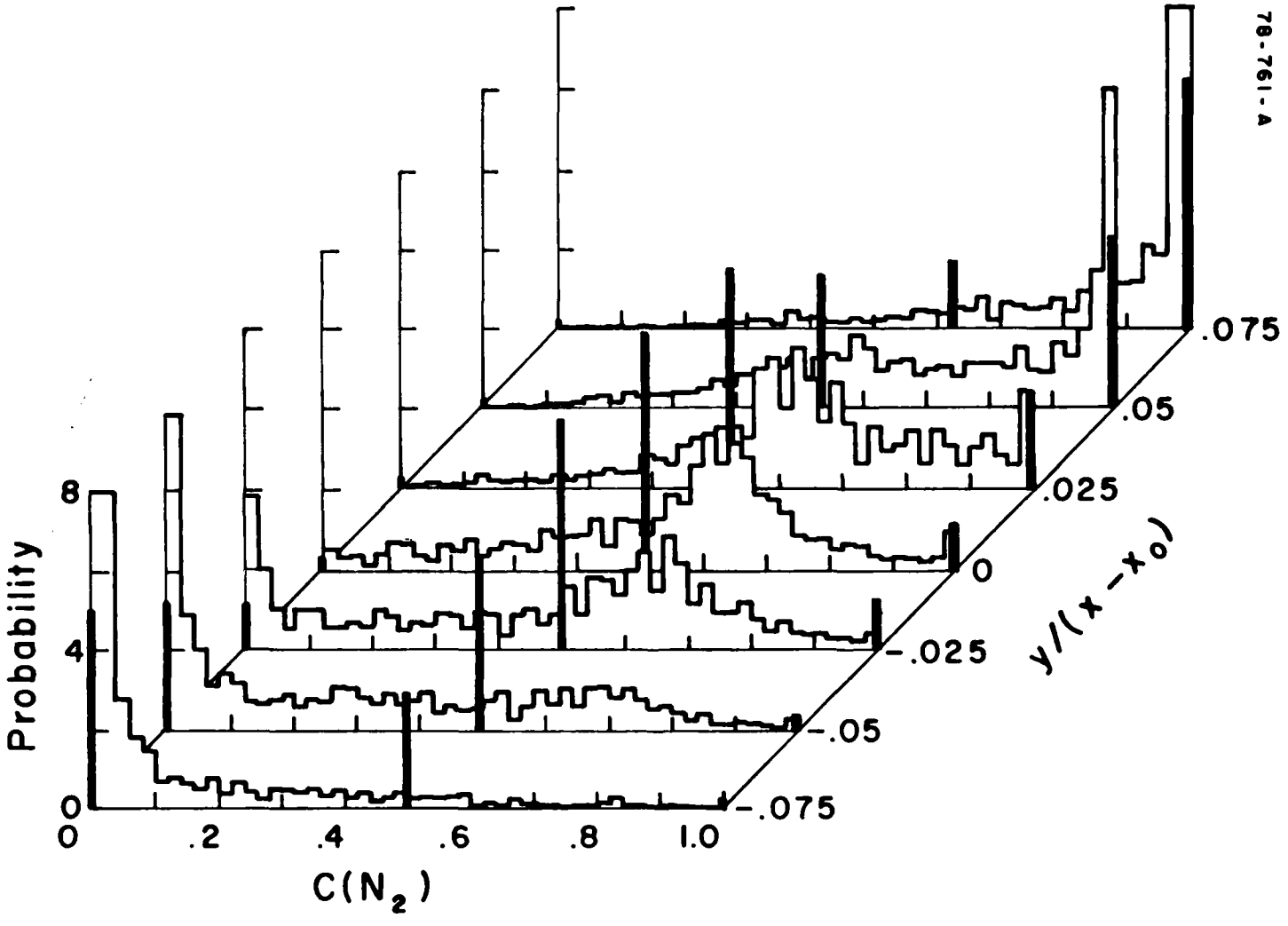

Figure 35. Probability density function; r = 0.38, s = 1.0 (minimum entropy)

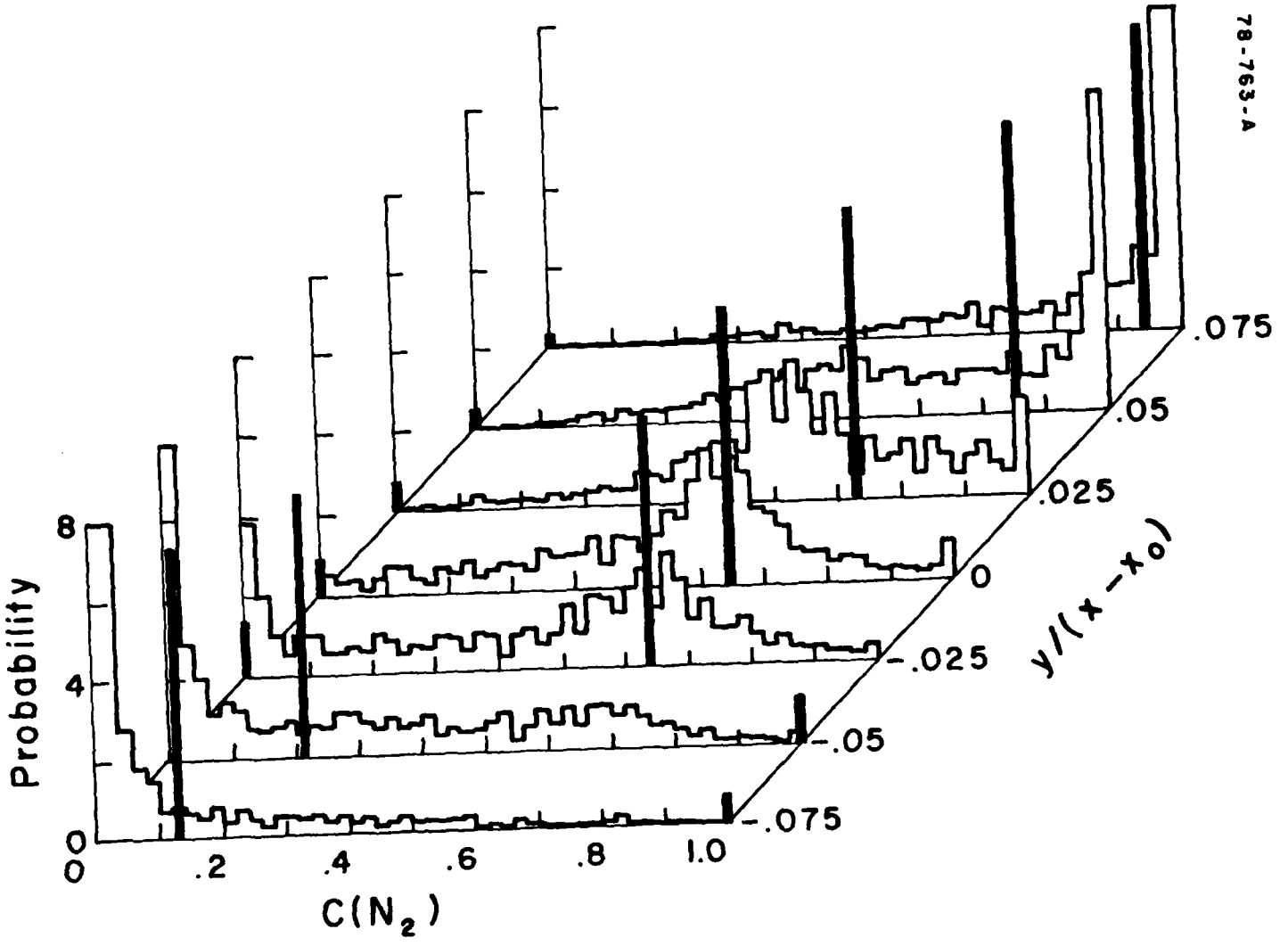

Figure 36. Probability density function; r = 0.38, s = 1.0 (maximum entropy)

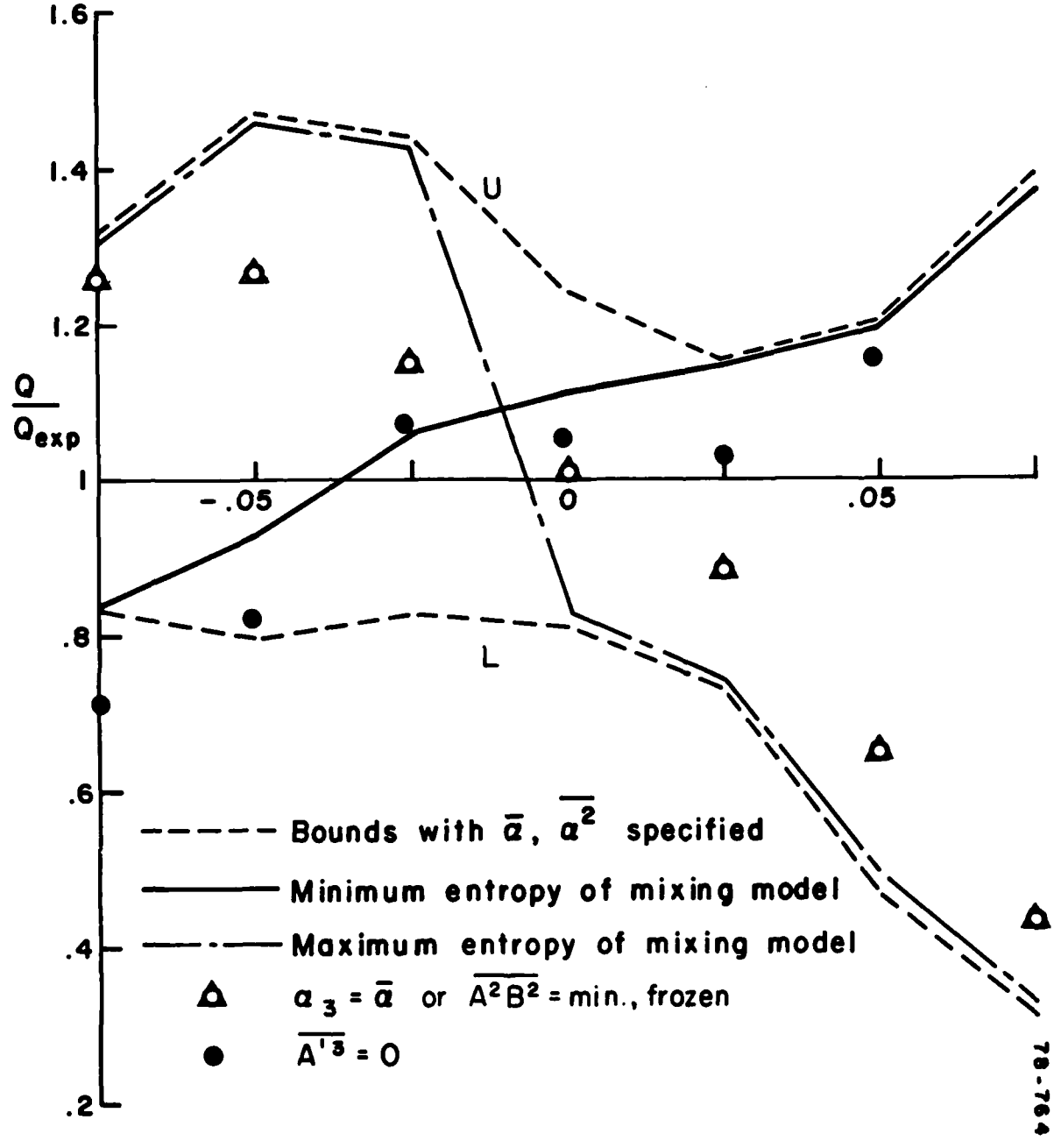

Figure 37. Normalized third moment compared to experiment for $\Delta = 0$

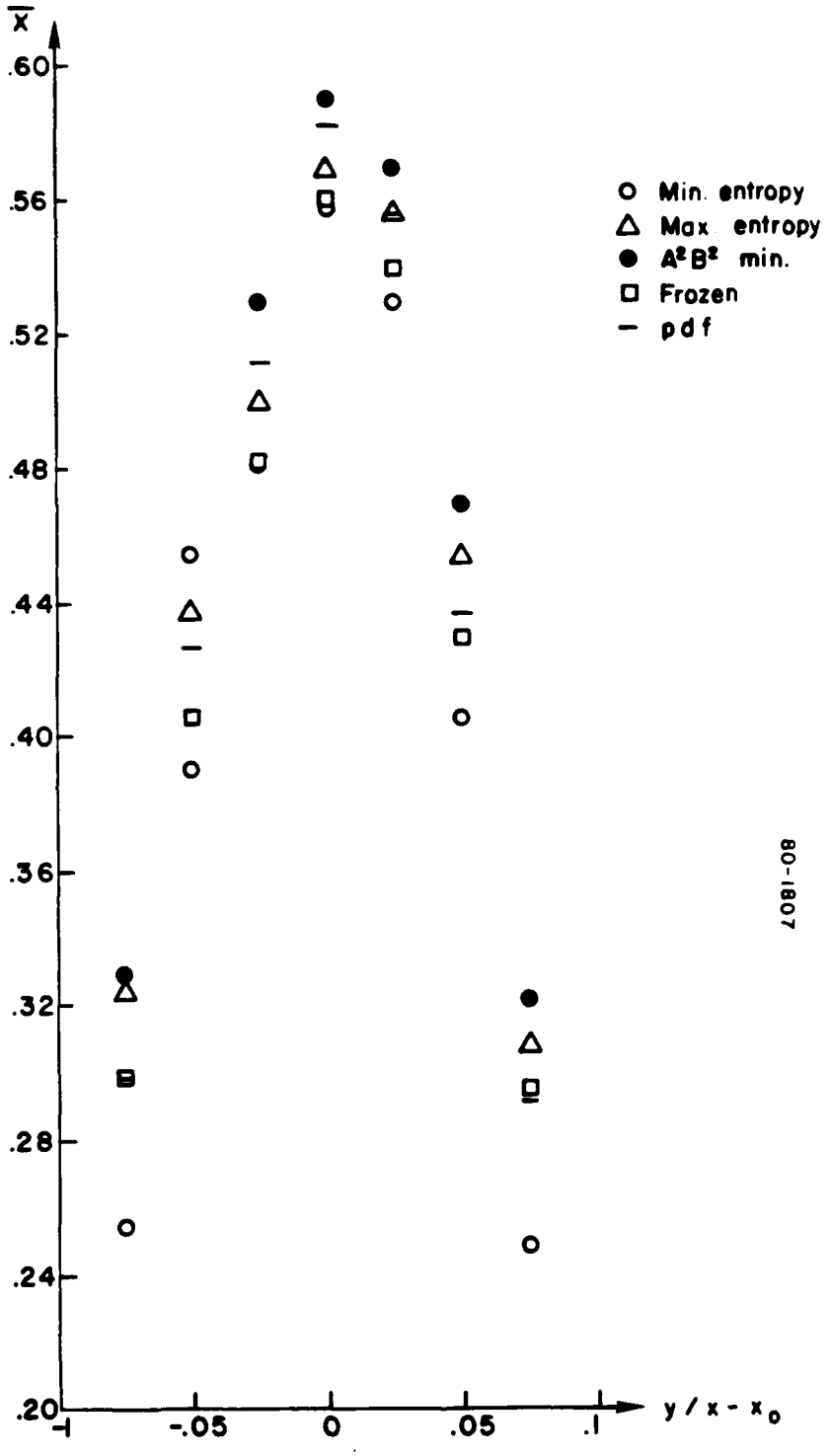

Figure 38. Normalized mean entropy

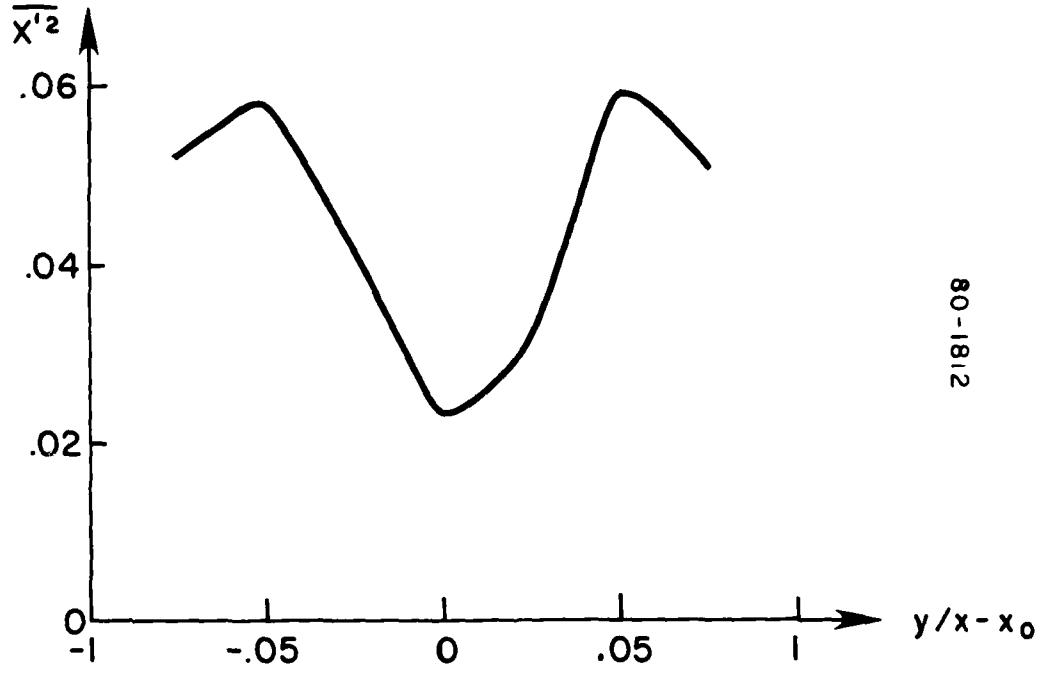

Figure 39. Experimental centered entropy fluctuations

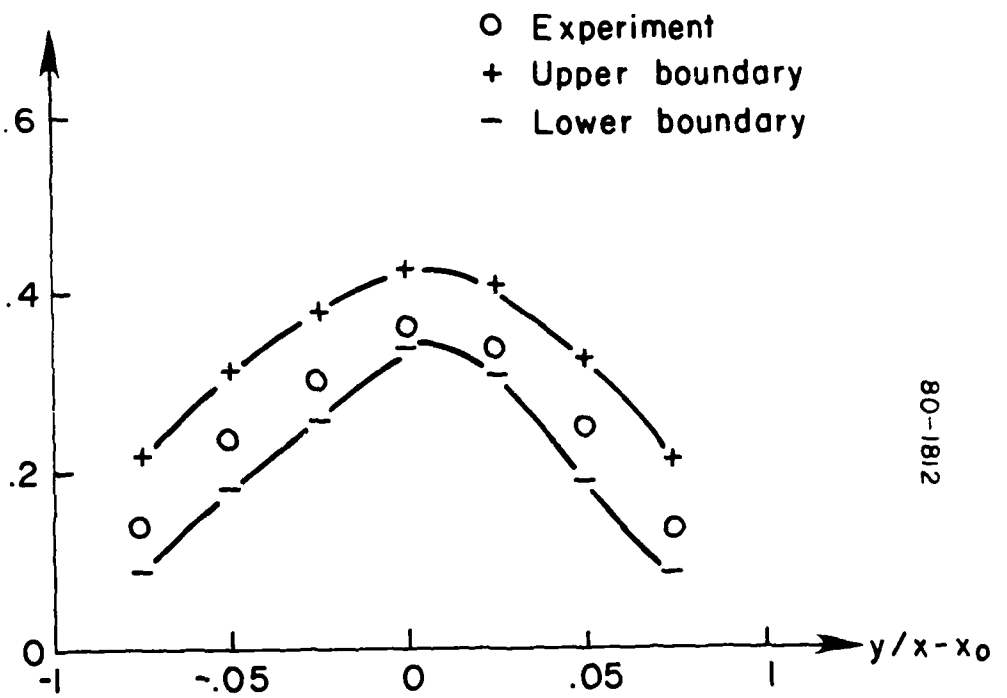

Figure 40. Second moment of the specific entropy

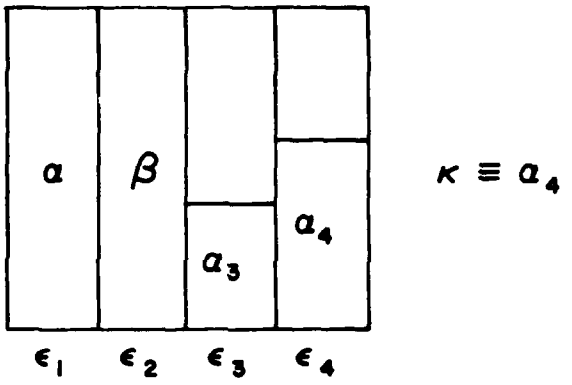

Figure 41. Box model for $\Delta \neq 0$

AD-A102 342 AERONAUTICAL RESEARCH ASSOCIATES OF PRINCETON INC NJ F/G 20/4
STATISTICAL CONSTRAINTS ON SCALAR VARIABLES IN TURBULENT FLOWS.(U)
FEB 81 G SANDRI, P J MANSFIELD, A K VARMA F44620-76-C-0048
UNCLASSIFIED ARAP-346 AFOSR-TR-81-0593 NL

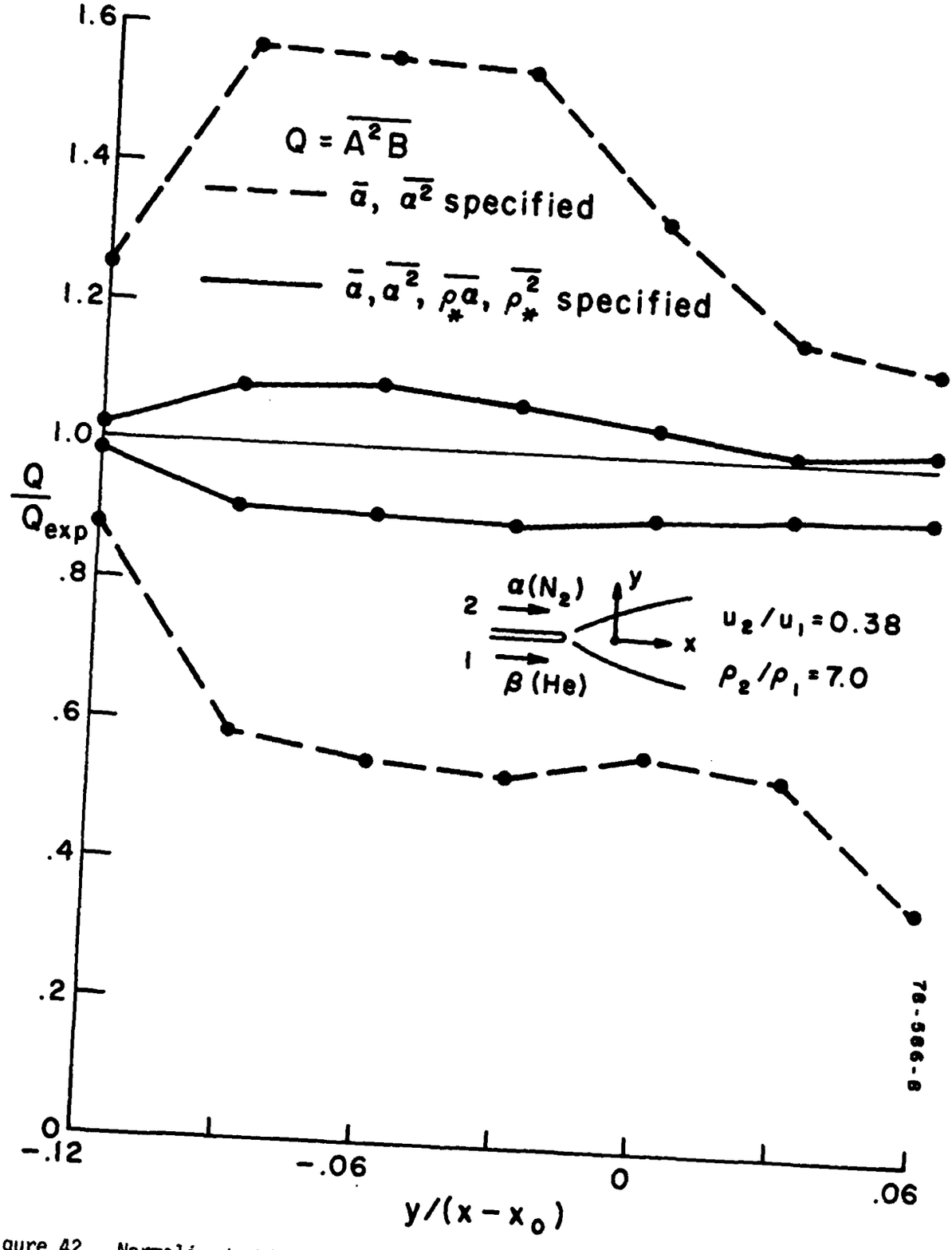

Figure 42. Normalized third moment compared to experiment for $\rho_2/\rho_1 = 7.0$, $u_2/u_1 = 0.38$

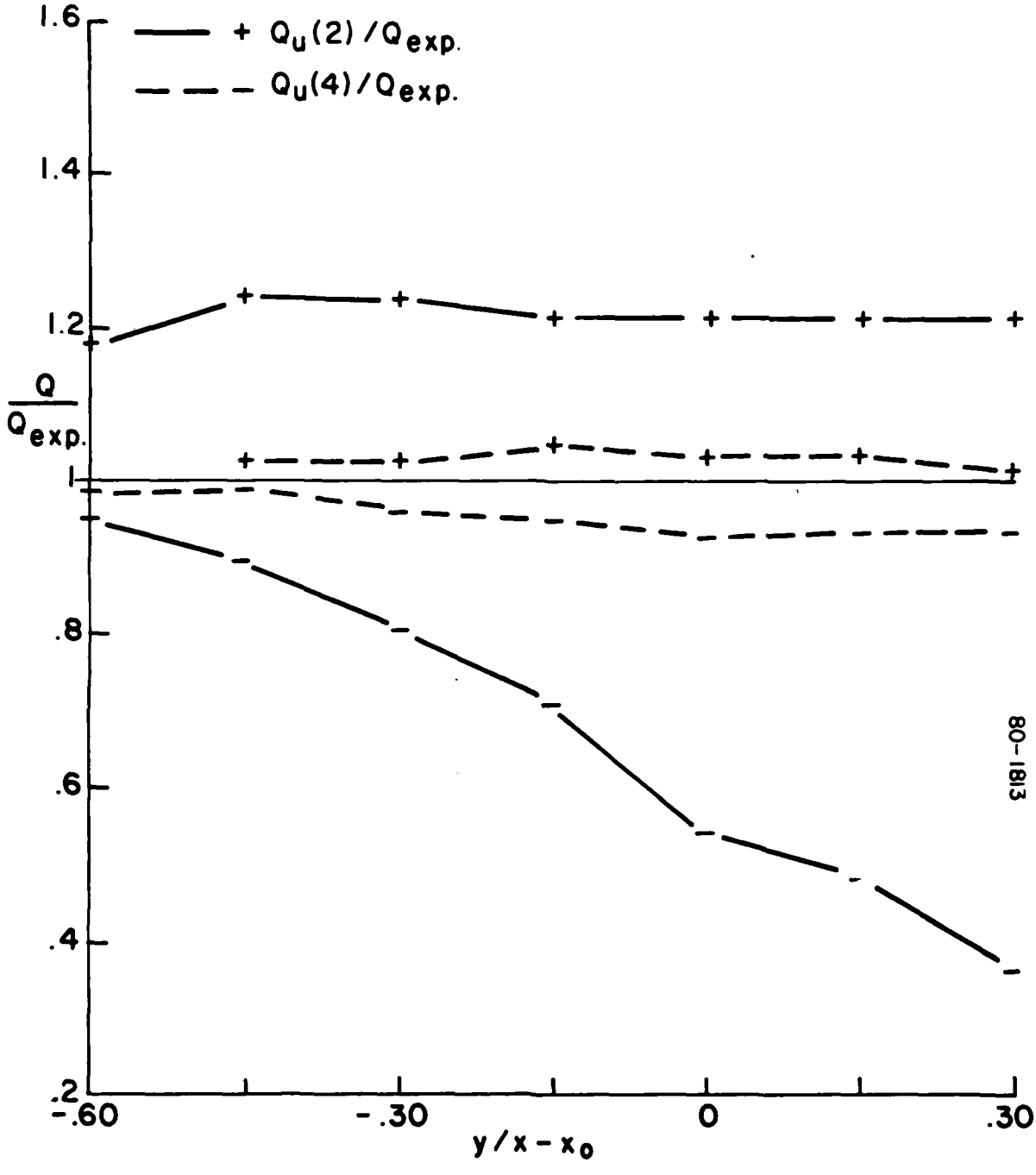

Figure 43. Normalized third moment compared to experiment for $\rho_2/\rho_1 = 7.0$, $u_2/u_1 = 1.0$

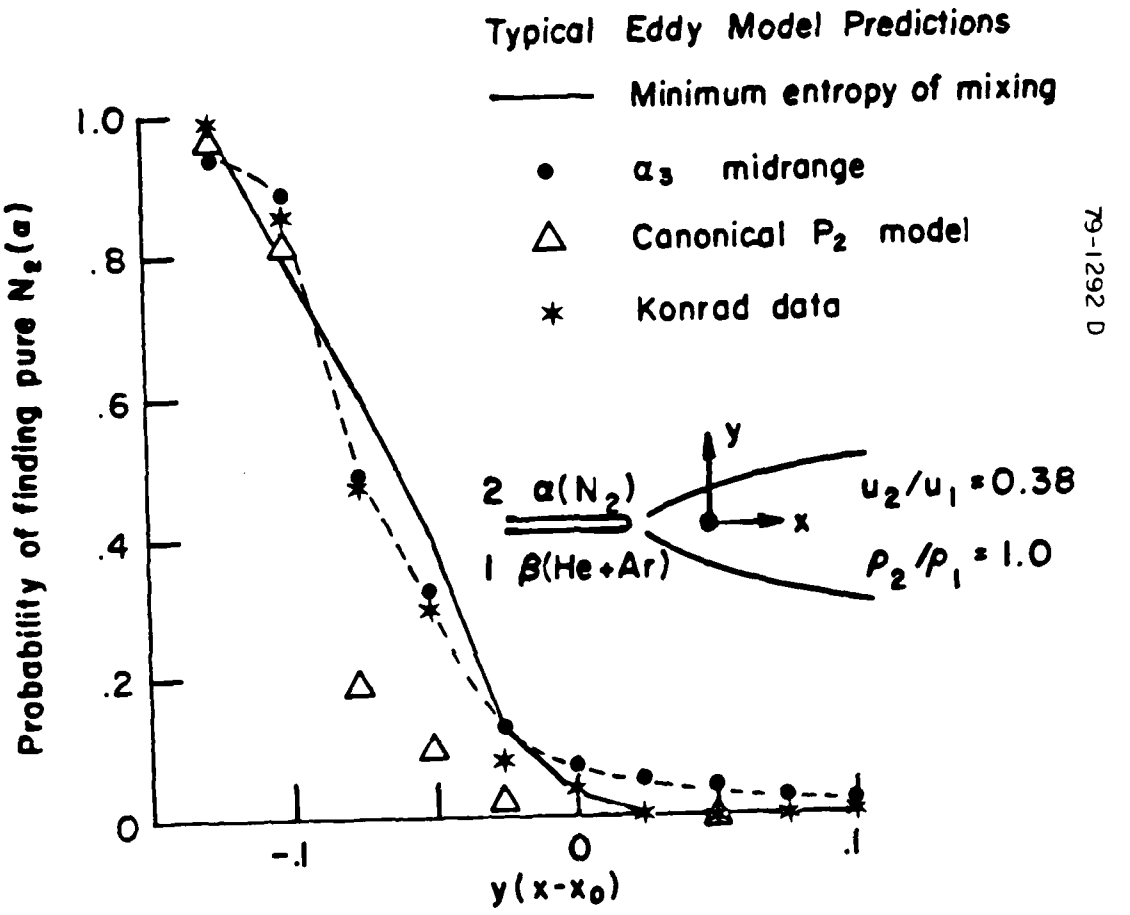

Figure 44. Predictions for pure N_2 compared to experiment

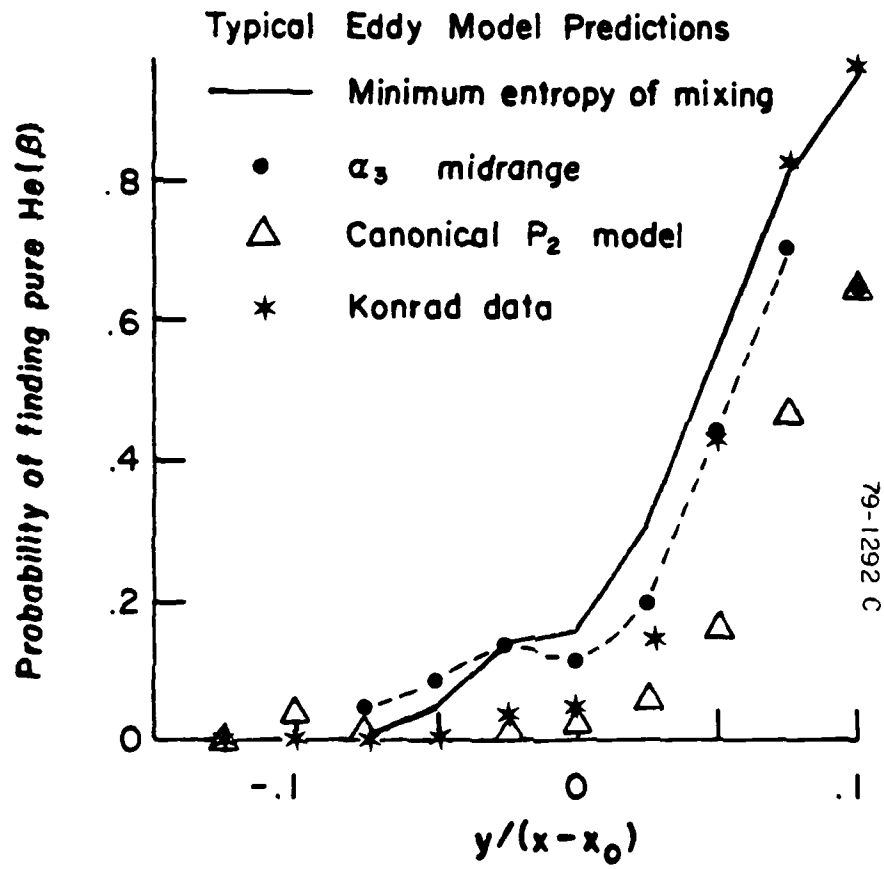

Figure 45. Predictions for pure He compared to experiment

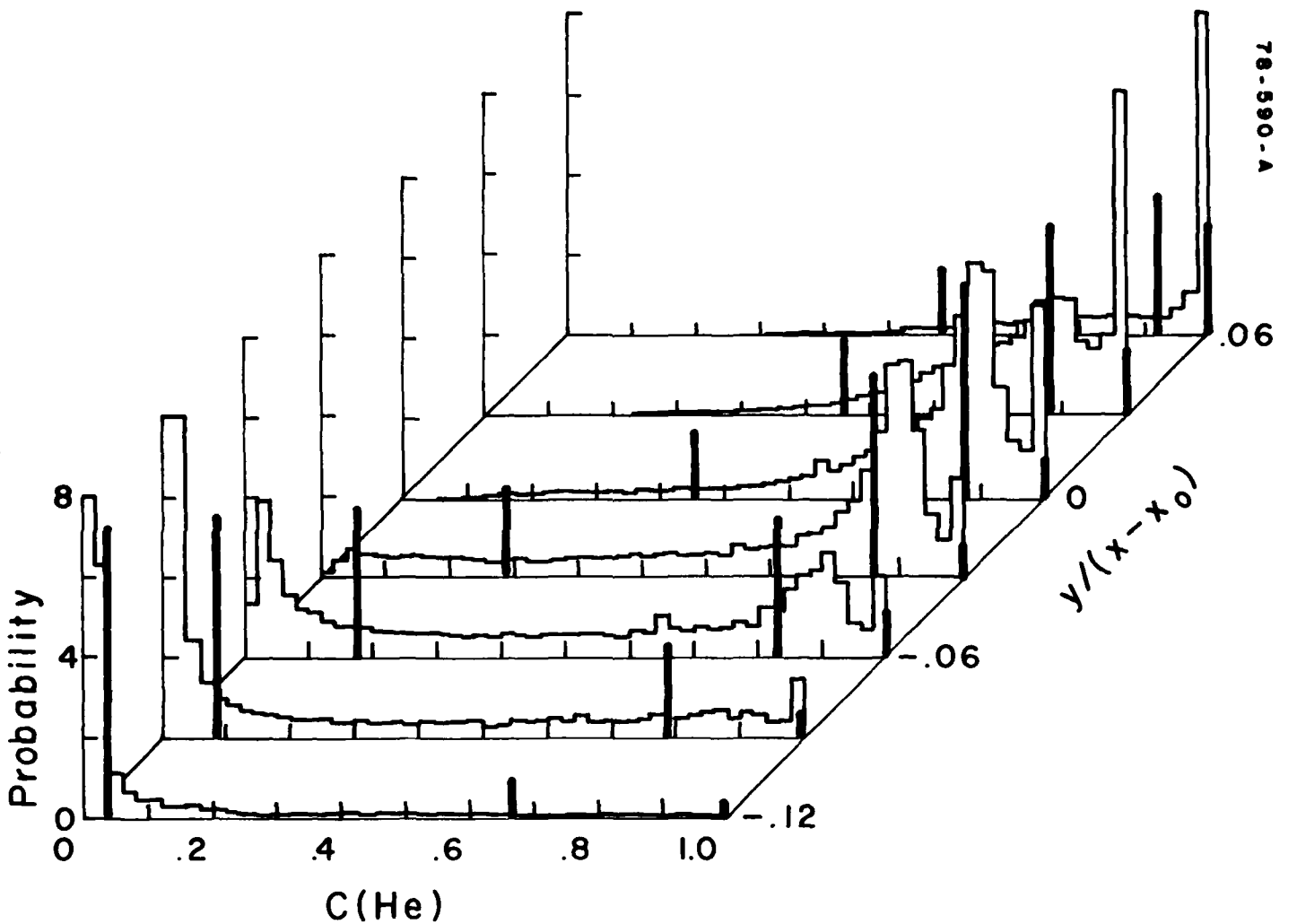

Figure 46. Probability density function; r = 0.38; s = 7.0 (lowest entropy)

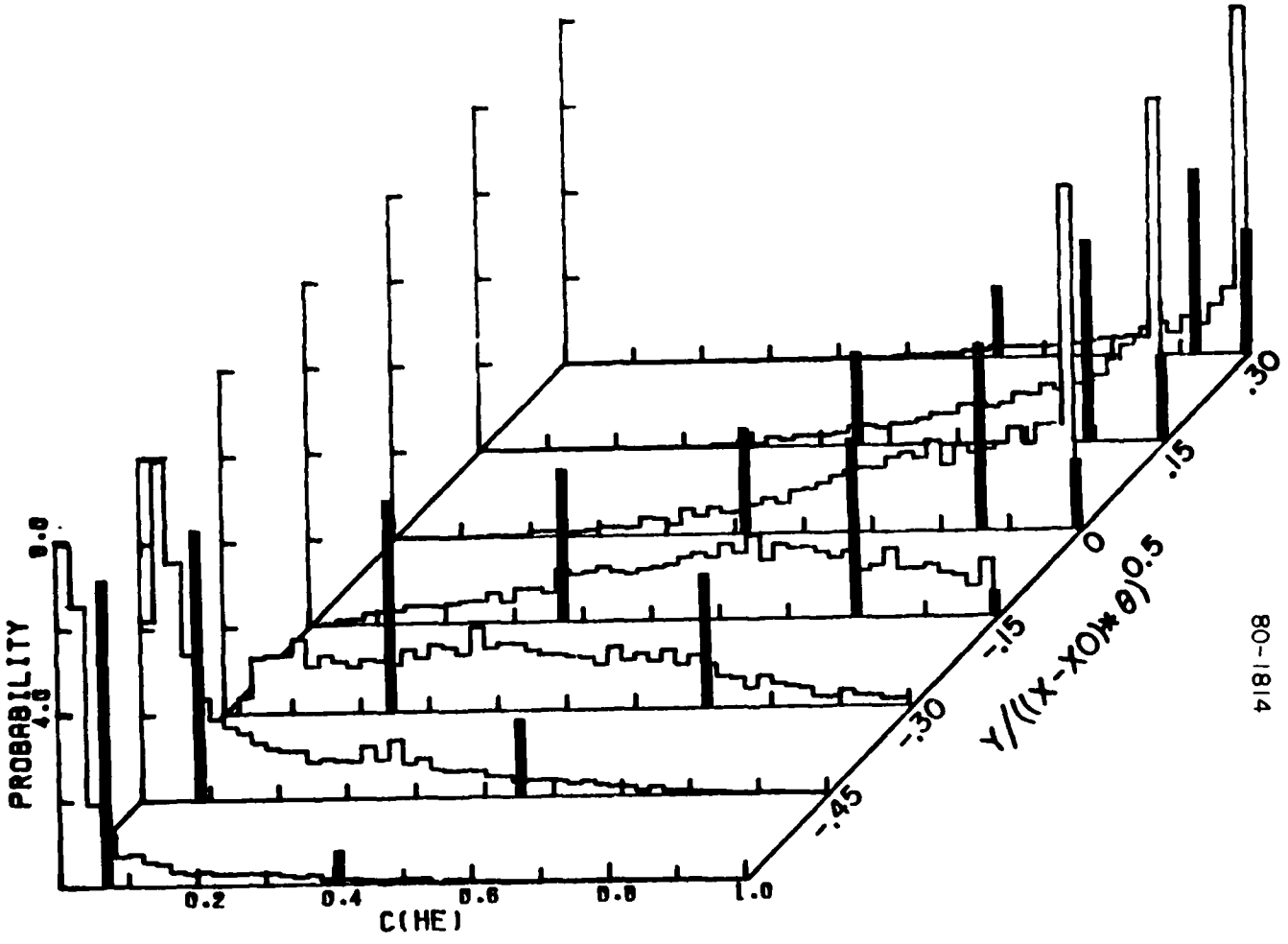

Figure 47. Probability density function; r = 1.0, s = 7.0. Model with four cells and lowest entropy

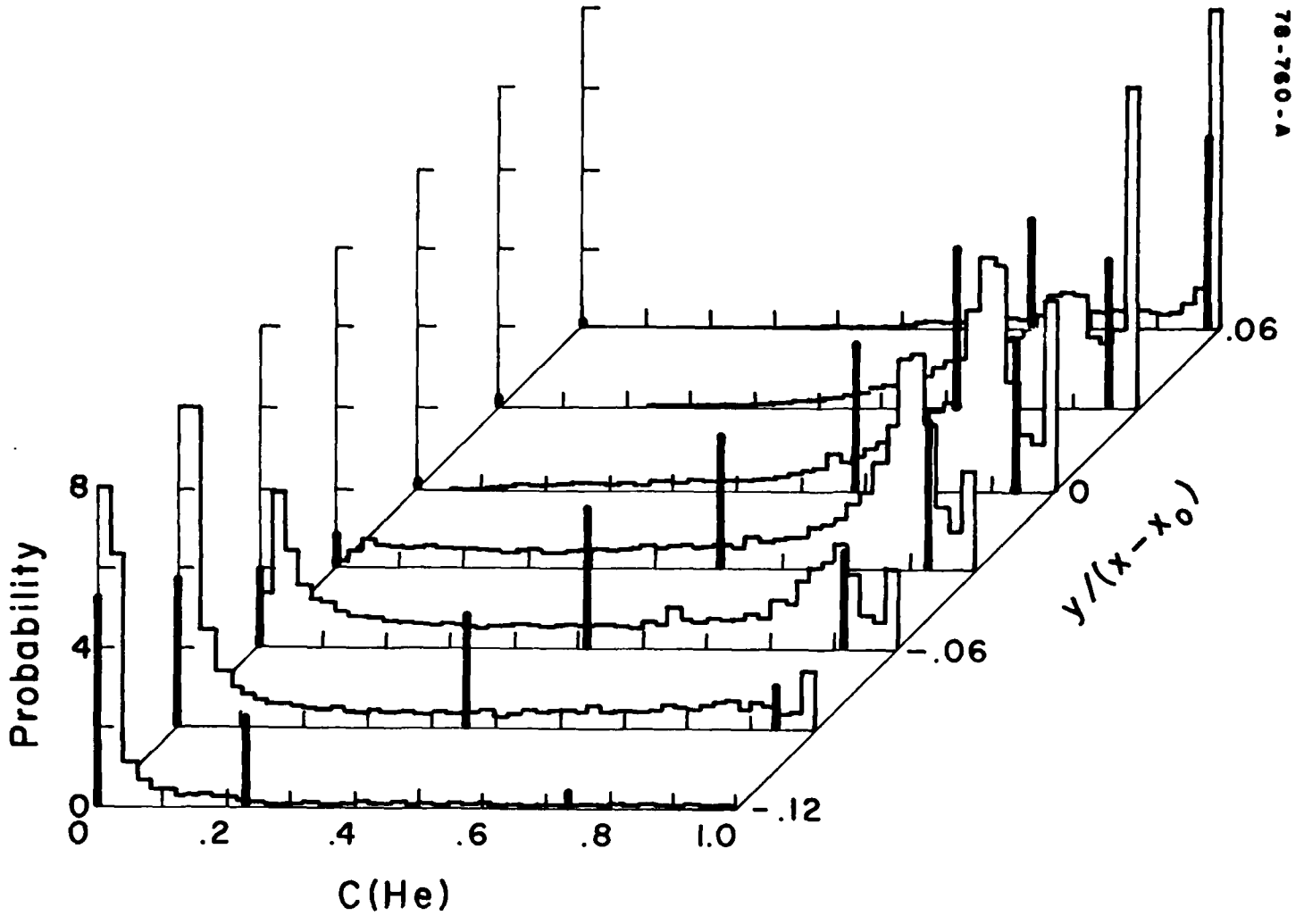

Figure 48. Probability density function; r = 0.38; s = 7.0. Model with four cells and largest entropy. The model shows helium poorness in disagrement with experiment.

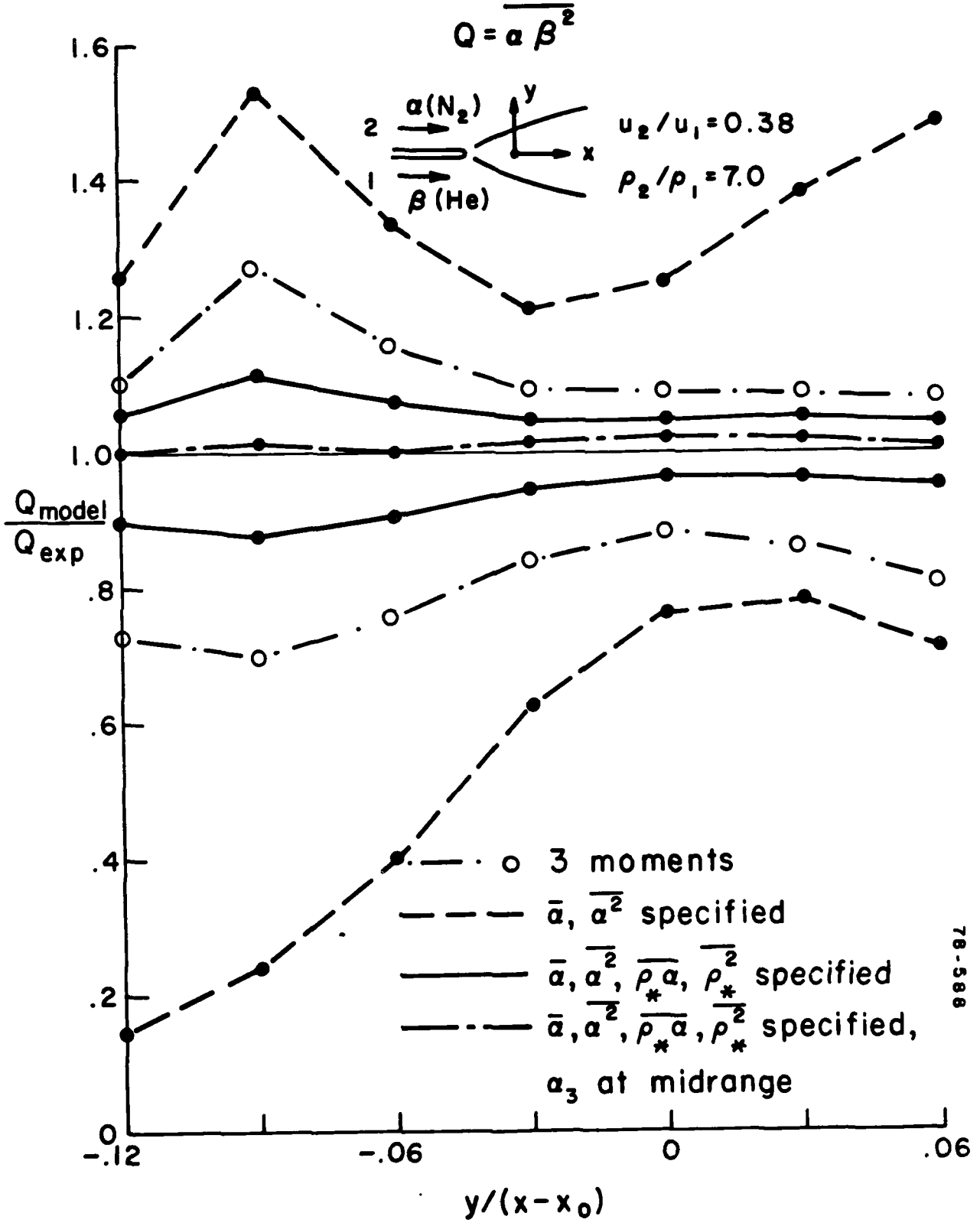

Figure 49. Third moment compared to experiment for $\rho_2/\rho_1 = 7.0$, $u_2/u_1 = 0.38$

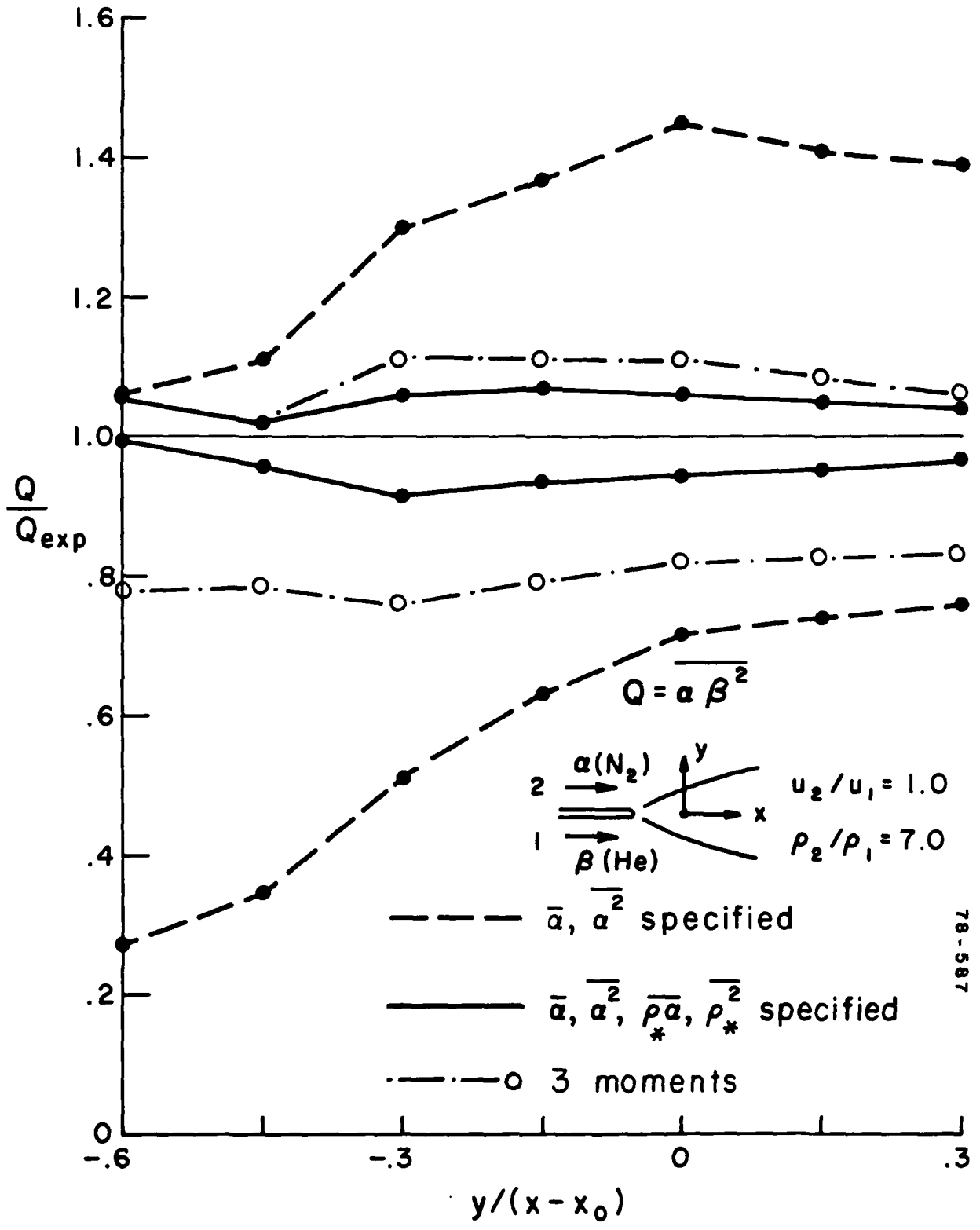

Figure 50. Third moment compared to experiment for $\rho_2/\rho_1 = 7.0$, $_2/_1 = 1.0$

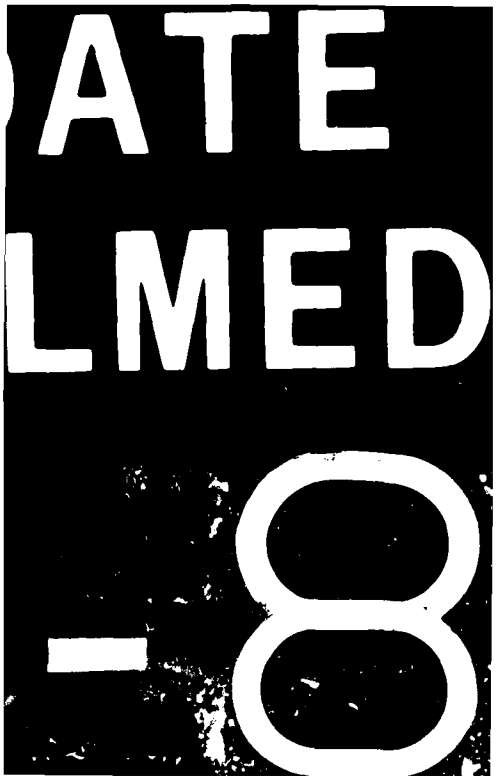
ATE
LMED
-8